TECHNISCHE UNIVERSITÄT MÜNCHEN
Professur Biotechnologie der Naturstoffe

FUNCTIONAL CHARACTERIZATION OF XYLOGLUCAN ENDOTRANSGLUCOSYLASES / HYDROLASES AND AN ESTERASE FROM *Fragaria sp.*

Lucia Dhiantika Witasari

Vollständiger Abdruck der von der Fakultät Wissenschaftszentrum Weihenstephan für Ernährung, Landnutzung und Umwelt der Technischen Universität München zur Erlangung des akademischen Grades eines

Doktors der Naturwissenschaften

genehmigten Dissertation.

Vorsitzender: Prof. Dr. Karl-Heinz Engel
Prüfer der Dissertation: 1. Prof. Dr. Wilfried Schwab
2. Prof. Dr. Brigitte Poppenberger-Sieberer

Die Dissertation wurde am 06.12.2018 bei der Technischen Universität München eingereicht und durch die Fakultät Wissenschaftszentrum Weihenstephan für Ernährung, Landnutzungund Umwelt am 08.04.2019 angenommen.

FOR MY BELOVED FAMILY

My parents

My husband

My daughters

Acknowledgements

Give thanks to Jesus Christ, my Lord for the great life during my PhD study in Germany. For me, getting a Doctorate degree is not only obtaining new knowledges and practical skills related PhD research, but also graduating from real-life examination. Herewith I would like to acknowledge all people who involve and support me during my doctorate study.

I wish to express great appreciation and thanks to Prof. Dr. Wilfried Schwab, my Doktorvater. Thank you for accepting me as your PhD student and offering me an opportunity to pursue my PhD in your laboratory. I would appreciate you for your support and professional guidance during my study. Thank you for providing me a solid teamwork, good working environment and scientific resources to enhance my experimental skills. Especially, thank you for giving me the freedom to pursue alternative projects when I found difficulties for the proposed project.

Thank you for Dr. Fong-Chin Huang and Dr. Thomas Hoffmann for your support and help, especially for providing practical experiences and professional skills. I could come to you anytime to discuss my research problem. Thanks also for reviewing my publication draft.

I would like also to acknowledge the Bina-Team. Chuankui and Fatma, thank you for our friendship. We share not only about research but also life in our office. Katja, thank you for your kindness and help for me, also for sharing your knowledge and skill especially for *in vivo* research and German translation of my summary. Katrin, Doreen, Friedericke thank you for sharing your laboratory experience and useful suggestion. Elisabeth, Nico, Guangxin, and Shuai for your kindly help especially after I returned to Indonesia. Heike Adamski, Mechthild Mayershofer, Kilian Skowranek, Hannelore Meckl, and Dr. Ruth Habegger, thank you for your help for administrative and technical support.

Olena, thank you to be my sister. It was unforgettable memory to share everything with you as new mother. Elsa and Widi, Indonesian students at TUM for our

friendship and your help for my baby. Mas Adam, thank you to be my brother. All of you strengthen me when I was alone and down in Germany.

I am also grateful and thanks to Prof. Dr. Stephen S. Fry, Edinburgh University UK for your support and guidance during my internship to perform *in vitro* assay in your laboratory. Thank you also for Dr. Lenka and Janice for technical support and assistance for my research in Steve lab. For colleague, Rebecca, Cam-Tu, Christina, thank you for our friendship.

Thank you for Prof. Dr. Brigitte Poppenberger-Sieberer and Prof. Dr. Karl-Heinz Engel for participation as members of my examination board. Dr. Wilfried Rozhon, thank you for your advice related localization and microscopy, and also reviewing my publication. Thank you for Prof. Klaus Schwechheimer for access to the fluorescence microscope. Thanks to Prof. Dr. Thomas Brueck for supporting me as mentor for DAAD scholarship.

Thank you for DAAD for the financial support during my PhD study, TUM-GS for the funding for my internship in Edinburgh, Universitas Gadjah Mada for the scholarship for writing my thesis.

To my family, especially my parents, brother and sisters in Indonesia who support me spiritually. Thank you for your prayer.

Table of content

Abbreviation

ATP	adenosine-5'-triphosphate
bp	base pair
BSA	bovine serum albumin
BLAST	Basic Local Alignment Search Tool
cDNA	complementary DNA
CMC	carboxymethyl cellulose
CTAB	cetyltrimethyl ammonium bromide
cv.	cultivar
d	days
DEPC	diethyl pyrocarbonate
DMSO	dimethyl sulfoxide
DNA	deoxyribonucleic acid
DNase	deoxyribonuclease
dATP	deoxyadenosine triphosphate
dNTP	deoxynucleoside triphosphate
DTT	dithiothreitol
E. coli	*Escherichia coli*
EDTA	ethylenediaminetetraacetic acid
FPLC	fast protein liquid chromatography
GST	glutathione-S-transferase
h	hour
HEC	hydroxyethylcellulose
HPLC	high performance liquid chromatography
IPTG	isopropyl-β-$_D$-thiogalactopyranoside
kb	kilo-base pair
kDa	kilodalton
Kcat	Michaelis constant
LB	Luria-Bertani
LC-UV-ESI-MSn	liquid chromatography ultraviolet electrospray ionization mass spectrometry

MES	morpholino ethanesulfonic acid
min	minute
MLG	mixed-linkage β-glucan
MMLV-RT	moloney murine leukemia viruse-reverse transcriptase
MQ water	Milli Q water
mRNA	messenger ribonucleic acid
M.W.	molecular weight
MS	mass spectrometry
MS-Salt	Murashige and Skoog Basal Salt Mix
MXE	MLG:xyloglucan endotransglucosylase
NaOAc	sodium acetate
nt	nucleotides
ODx	optical density at X nm
ORF	open reading frame
PAGE	polyacrylamide gel electrophoresis
PCR	polymerase chain reaction
PMSF	phenylmethylsulfonyl fluoride
PEG 6000	polyethylene glycol 6000
PVP	polyvinylpyrrolidone
qRT-PCR	quantitative real-time PCR
RNA	ribonucleic acid
RNase	ribonuclease
rpm	rotation per minute
RT	reverse transcription
Tm	melting temperature
SDS	sodium dodecyl sulfate
sec	second
TAE	Tris-acetate-EDTA
TE	Tris-EDTA
TLC	thin layer chromatography
Tris	tris(hydroxymethyl)aminomethane
U	unit

UV	ultraviolet
V	voltage
Vmax	maximum reaction rate
WSCA	water-soluble cellulose acetate
X-gal	5-bromo-4-chloro-3-indolyl-β-$_D$-galactopyranoside
XEH	xyloglucan endohydrolase
XET	xyloglucan endotransglucosylase
XTH	xyloglucan endotranglucosylase/hydrolase

ZUSAMMENFASSUNG

Das Weichwerden von Früchten während der Reifung, wie es zum Beispiel bei Erdbeeren der Fall ist, wird u.a. durch eine selektive Modifikation der Zellwandarchitektur vermittelt. Diese Veränderungen der Zellwandstruktur werden einerseits durch die Solubilisierung von Pektinen verursacht und andererseits durch eine Abnahme der Polymergröße des Xyloglucan-Netzwerks. Xyloglucan, eine wesentliche Hemicellulose, hat vermutlich einen großen Einfluss auf die physikalischen Eigenschaften der Zellwand während des Wachstums der Pflanze. Es ist ein Polysaccharid, das ein 1,4-β-verknüpftes Glucan-Rückgrat mit seitlichen 1,6-β-verknüpften Xylosylresten besitzt. Das 1,4-β-verknüpfte Glucan-Rückgrat kann Wasserstoffbrücken zu Cellulose-Mikrofibrillen ausbilden und dadurch zur Stabilität der Zellwand beitragen. Deshalb spielt Xyloglucan eine wichtige Rolle beim durch die Fruchtreifung induzierten Abbau der Zellwand.

Die Entdeckung des Enzyms Xyloglucan Endotransglucosylase/Hydrolase (XTH) in den frühen 1990ern lieferte einen Kandidaten, von dem angenommen wird, dass er ein bestimmender Faktor bei der Zellwandmodifikation im Rahmen der Fruchtreifung ist. XTH Enzyme sind die bekanntesten Beispiele für Transglycanasen, welche Polysaccharid:Polysaccharid Transglycolysierungsreaktionen katalysieren und dabei Substrate wie Xyloglucan, Gemischt-gebundene (1-3,1-4)-β-$_D$-Glucane, Cellulose, Xylane und Mannane miteinander verknüpfen. XTH Enzyme besitzen Xyloglucan Endotransglycosylase (XET) und/oder Xyloglucan Endohydrolase (XEH) Aktivitäten. Entwickeln sie eine XET Aktivität, spalten sie Xyloglucanpolymere endolytisch und verknüpfen die neuentstandenen reduzierenden Enden mit anderen Xyloglucan-Molekülen. Zeigen sie dagegen XEH Aktivität, wird jeweils ein Xyloglucan-Molekül hydrolysiert.

Um den Beitrag der Xyloglucan-Modifizierung zur Erweichung der Erdbeerfrucht während der Reifung zu untersuchen, wurde im Rahmen dieser Doktorarbeit das Genom der diploiden Erdbeersorte *Fragaria vesca ssp. vesca* „Hawaii 4“ durchsucht, um putative *XTH* Gene zu identifizieren. Zusätzlich wurden

Transkriptom-Daten und qPCR Ergebnisse mit einbezogen. Schlussendlich wurden *FvXTH9* (Gen 01986) und *FvXTH6* (Gen 05591) für eine weitere Analyse ausgewählt. Beide Gene zeigten eine hohe Sequenzhomologie, wobei *FvXTH9* das höchste Expressionslevel von allen berücksichtigten *FvXTH* Genen besaß. Beide Gene wurden für eine detaillierte Charakterisierung in den PYES2 Vektor kloniert und in *Saccharomyces cerevisiae* exprimiert.

FvXTH9 und FvXTH6 zeigten XET-Aktivität gegenüber einer Reihe von Akzeptor- und Donor-Substraten. Sie wiesen jedoch auch XEH Aktivität gegenüber Tamarinden-Xyloglucan auf, wobei das Substrat in Oligosaccharide von 10 kDa geschnitten wurde. Interessanterweise zeigte FvXTH9 zudem Gemischt-gebundene Glucan:Xyloglucan Endotransglucosylase (MXE) Aktivität. Beide Enzyme besaßen ein pH Optimum von 6.5. Die optimale Temperatur für FvXTH6 war 30°C. *In vivo* Lokalisationsexperimente in *Nicotiana tabacum* bestätigten, dass beide FvXTH Enzyme im Sekretionsweg der Zelle lokalisiert sind. Eine Überexpression von FvXTH9 und FvXTH6 bewies, dass die behandelten Früchte schneller reiften und eine verringerte Festigkeit gegenüber Früchten zeigten, die mit dem Kontrollvektor pBI121 infiltriert worden waren. Diese Ergebnisse bekräftigen die Annahme, dass FvXTH9 und 6 in die Modifizierung der Zellwand während der Fruchtreifung involviert sein könnten.

Mit dem Ziel weitere Enzyme zu identifizieren, die bei der Reifung der Erdbeerfrucht eine wichtige Rolle spielen, wurden die nativen Proteine aus einem *F.* × *ananassa* Fruchtextrakt isoliert und gereinigt. Durch einen nativen PAGE in Verbindung mit einem direkten Esterase Experiment wurde eine FvGDSL Esterase/Lipase identifiziert, geklont und in *S. cerevisiae* exprimiert. Vorläufige Versuchsergebnisse zeigten, dass dieses Enzym Aktivität gegenüber einer Reihe von Acetatestern aufwies. Als optimaler pH-Wert der Reaktion wurde 6.0 festgelegt. Weitere Untersuchungen sind jedoch notwendig um die Funktion der FvGDSL Esterase/Lipase in Bezug auf die Fruchtreife der Erdbeere zu bestätigen.

SUMMARY

The ripening associated softening of fleshy fruit such as in the strawberry is related to the selective modification of cell wall architecture. During fruit ripening, modifications in cell wall structure are characterized by solubilization of pectic polysaccharides and by a decrease in polymer size of xyloglucan. Xyloglucan, a highly significant hemicellulose may play a crucial role in the determination of the physical properties of the cell wall during growth. Xyloglucan possesses a 1,4-β-glucan backbone with 1,6-α-xylosyl residues along the backbone. Since the 1,4-β-glucan backbone can hydrogen-bond to cellulose microfibrils, xyloglucan contributes to the rigidity of the cell wall when it cross-links adjacent microfibrils and to the loosening of the cell wall when it degrades.

The discovery of the enzyme XTH (xyloglucan endotransglucosylase/hydrolase) in the early 1990s has provided a candidate, which is considered a factor in cell wall modification leading to fruit softening. XTHs are the best-known examples of transglycanases, a class of enzymes that catalyse polysaccharide:polysaccharide transglycosylation reactions involving substrates such as xyloglucan, mixed-linkage (1-3, 1-4)-β-D-glucan (MLG), cellulose, xylans and mannans. XTHs exhibit xyloglucan endotransglycosylase (XET) and/or xyloglucan endohydrolase (XEH) activities. XET catalyzes endolytic cleavage of xyloglucan polymers and re-joins the newly generated reducing ends to other xyloglucan molecules whereas XEH activity results in hydrolysis of one xyloglucan molecule.

To determine the contribution of xyloglucan modification to strawberry fruit softening during ripening we searched the genome sequence of the diploid strawberry *F. vesca* ssp. vesca accession Hawaii 4 for putative *XTH* genes. Based on transcriptome data and qPCR analysis, gene 01986 (*FvXTH9*) showed the highest expression level of all FvXTHs and was selected with the closely related gene 05591 (*FvXTH6*) for further analysis. To investigate it role in fruit ripening in more detail, the coding sequence of FvXTH9 and *FvXTH6* were cloned into the vector PYES2 and expressed in *Saccharomyces cerevisiae*.

FvXTH9 and FvXTH6 displayed different activities of xyloglucan endotransglucosylase (XET) towards various acceptor and donor substrates. The enzymes had also xyloglucan endohydrolase (XEH) activity by cutting the tamarind xyloglucan, which resulted in 10 kDa oligosaccharides. Interestingly, FvXTH9 showed activity of mixed-linkage glucan:xyloglucan endotransglucosylase (MXE). The pH optimum of both FvXTH9 and FvXTH6 was 6.5. The optimum temperature was 30°C for FvXTH6. Prediction of the sub-cellular localization suggested localization to the secretory pathway, which was confirmed by *in vivo* localization studies in *Nicotiana tabacum*. Overexpression study showed that *F.* × *ananassa* fruits infiltrated with FvXTH9 and FvXTH6 ripened faster and showed decreased firmness compare to the empty vector control pBI121. Thus, FvXTH9 and FvXTH6 might promote transgenic strawberry fruit ripening through involvement in the modification of cell wall components.

To investigate further enzymes related to the strawberry fruit ripening, native proteins from *F.* × *ananassa* fruit extract were isolated and purified. A FvGDSL esterase/lipase was found in native PAGE using a direct esterase assay. Therefore, this enzyme was cloned and expressed in *S. cerevisiae*. Preliminary assays showed that this enzyme had esterase activity toward a range of acetate esters. The optimum pH for the esterase activity of FvGDSL esterase/lipase was pH 6.0. Further research need to be performed to investigate FvGDSL esterase/lipase functions related to the strawberry plant ripening.

1. INTRODUCTION

1.1. Strawberry plant

1.1.1. Description

The strawberry plant (*Fragaria* sp.) is an excellent crop to be used in genetic and physiological studies because their plants require only a small space to grow and have a short generation time, as compared with other Rosaceae families, such as apples or peaches. Strawberry is considered a non-climacteric fruit, as the ripening process is independent of an increased ethylene respiration and biosynthesis (Hancock 1999; Giovannoni, 2004). The true fruit of strawberry are the achenes that dot the surface of an enlarged receptacle. Achene is the product of an individual carpel and contains a single seed. The flavorful and fleshy tissue is the receptacle, a modified stem tip (Darrow 1966; Hancock 1999).

The woodland strawberry, *F. vesca* is a perennial with a small genome size (240 MB; 2n=2x=14), and the complete DNA sequence has already been published (http://www.strawberrygenome.org/) (Shulaev *et al.,* 2011). *F. vesca* has a short seed to fruit cycle (3.5 months), high seed production (160 per primary berry), and inbred lines are available. The woodland strawberry is capable of asexual clonal propagation via runners, stolons or branch crowns. Some lines are amenable to *Agrobacterium*-mediated transformation (Folta and Dhingra 2007; Oosumi *et al.,* 2006; Qin *et al.,* 2008; Slovin and Michael 2011; Slovin *et al.,* 2009).

The cultivated octoploid strawberry *Fragaria* × *ananassa* (2n=8x=56) harbors eight sets of chromosomes, derived from probably four different diploid relatives (one of them is *Fragaria vesca*). The floral structure, sepal and petal numbers, floral organ arrangement, floral organ morphology and coloring, and early fruit development of *F.* × *ananassa* are basically the same as *F. vesca.* The differences are the stamen number and fruit size. While *F.* × *ananassa* has on average 25 stamens per flower, *F. vesca* has 20 stamens per flower. The high-level of colinearity between the genomes of octoploid and diploid *Fragaria*

suggests that genomic information from diploid *F. vesca* is transferable to the octoploid (Rousseau-Gueutin *et al.,* 2008).

1.1.2. Fruit ripening and firmness

The strawberry fruit consists of a number of small dry achenes embedded on the surface of a large fleshy receptacle (Figure 1; Hancock, 1999). The ripening of garden strawberry fruit can be divided into seven stages: small green, big green, green-white, white, turning, ripe and over-ripe (Zhang *et al.,* 2011). At the beginning, cell division occurs during the first 10 d, and a combination of cell division and cell expansion occurs between 10 and 15 d after anthesis, which leads to a progressive enlargement of the receptacle (Zhang *et al.,* 2011, Aharoni, 2002). Berry enlargement is dependent on auxin secreted from developing fertilized achenes (Nitsch, 1950). The level of chlorophylls decreases during the enlargement process and then the fruits turn from green to white (Zhang *et al.,* 2011). Meanwhile, accumulations of water and sugars occurs (Knee *et al.,* 1977). The cell walls of fleshy fruits change structures and compositions during ripening (Lefever *et al.,* 2004). Subsequently, between 25 to 30 d after anthesis, the receptacles are becoming red and soft when anthocyanins such as pelargonidin 3-glucoside and cyanidin 3-glucoside begin to accumulate in the fruit (Rosli *et al.,* 2004; Zhang *et al.,* 2011). The reduction in firmness observed in mature fruit and during ripening is due to solubilization and depolymerization of cell wall components by cell wall modifying enzyme such as cellulases and pectin-methylesterases (Rosli *et al.,* 2004). Depend on the genotype and the temperature; the strawberry fruit is fully ripe between 30 to 40 d after anthesis (Zhang *et al.,* 2011).

a.

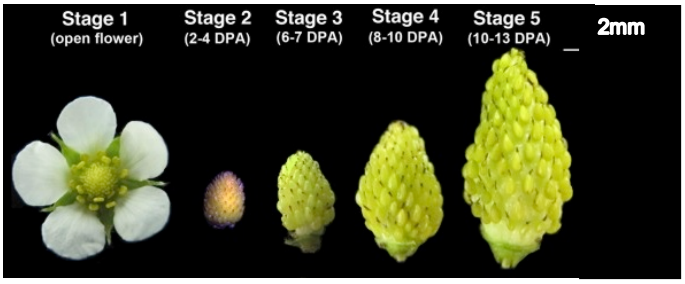

b.

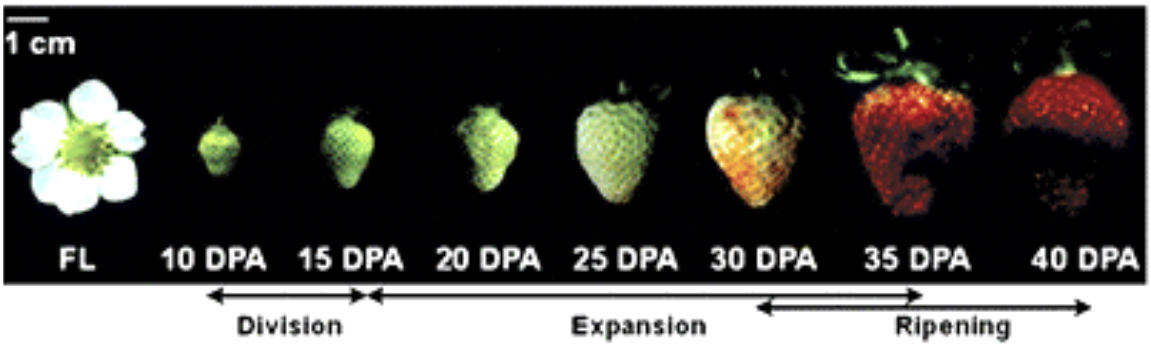

Figure 1. Strawberry fruit development

(a) *F. vesca* early fruit development from open flower to stage 5 (10-13 days after anthesis (DPA)) (Kang *et al.,* 2013). (b) *F.* × *ananassa* var. Troyonoka fruit development from flower (FL) to over-ripe fruit (40 DPA) (Zhang *et al.,* 2011)

1.2. Plant cell walls

Plant cell walls can be classified into two types: primary and secondary based on structural and biochemical differences and the developmental stage of the cells that generate them (Taiz and Zeiger, 2010). Primary walls are deposited during cell growth, and need to be mechanically strong, stable and sufficiently extensible to permit cell expansion and cell division. Primary cell walls consist of polysaccharides that can be generally classified as cellulose, hemicelluloses, and pectins (Figure 2). Cellulose is generated at the plasma membrane in the form of paracrystalline microfibrils. Hemicellulose and pectins belonging to matrix polysaccharides are synthesized within Golgi cisternae (Reiter, 2002). The cell

wall thickens and strengthens by formation of the secondary cell wall. Secondary cell walls are deposited after the cessation of cell growth and confer mechanical stability upon specialized cell types such as xylem elements and sclerenchyma cells. In addition to containing cellulose and hemicellulose, the secondary wall contains lignin. Lignin is highly cross-linked to enhance mechanical support for the plants to grow upward.

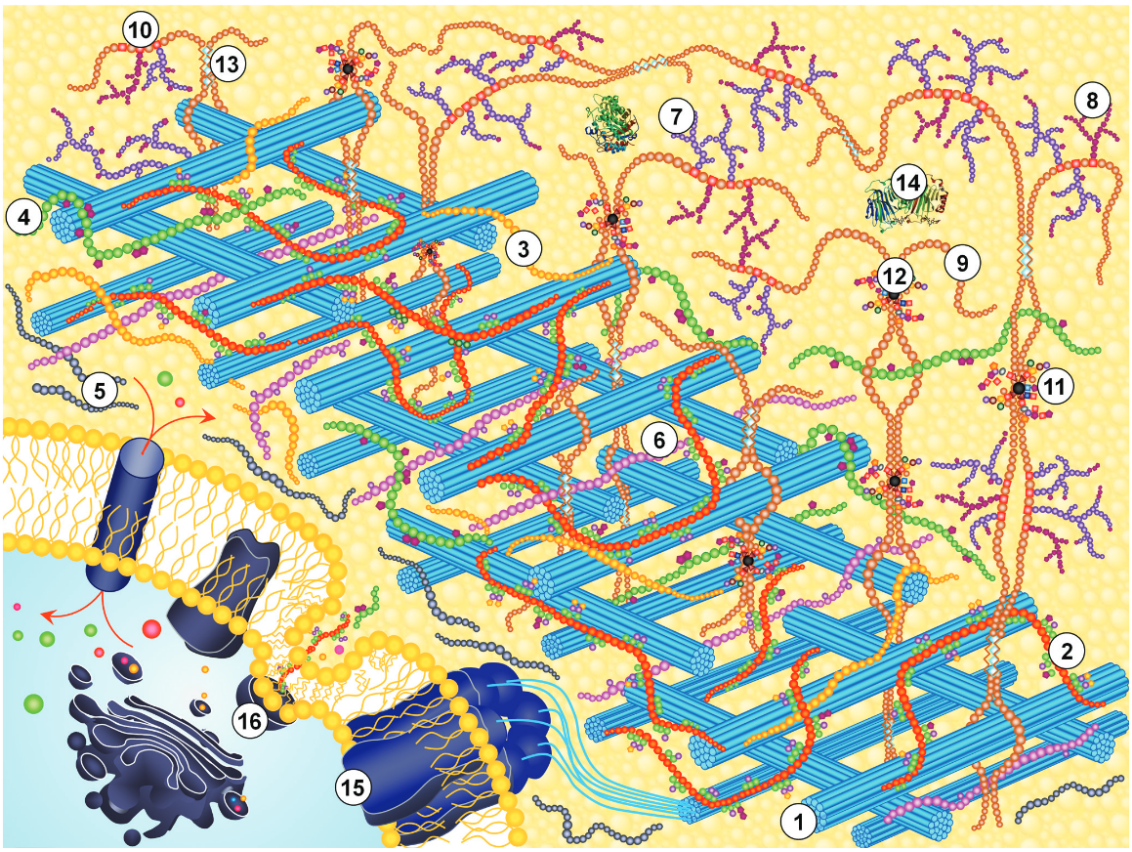

(adopted from Frankova and Fry, 2013)

Figure 2. Model of the polysaccharide framework in a plant cell wall.

1, cellulose; 2-6, hemicellulose; 2, xyloglucan; 3, mixed-linkage glucan; 4, xylan and related heteroxylans; 5, allose; 6, mannan and related heteromannans; 7-11, pectins; 7, galactan; 8, arabinan; 9, homogalacturonan; 10, rhamnogalacturonan I; 11, rhamnogalacturonan II; 12, boron bridge; 13, 'egg-box' with calcium bridges; 14-16, non-polysaccharide components; 14, enzymes and structural proteins; 15, cellulose synthase complex; 16, transport vesicles.

1.2.1. Cellulose

Cellulose is the most abundant polysaccharide in nature. The primary structure of cellulose is a linear homopolymer of β-1,4-linked–glucose residues. The linear structure can be extended to molecules containing several thousand glucose units, in a cellulose polymer chain. Many properties of cellulose depend on its chain length or degree of polymerization, the number of glucose units that form one polymer molecule.

1.2.2. Hemicelluloses

Hemicelluloses are polymers with a backbone of β-glucose (β-Glc), β-xylose (β-Xyl) or β-mannose (β-Man) or β-Man and β-Glc and usually possessing short side chains (Frankova and Fry, 2013). Hemicelluloses encompass xyloglucans, glucuronoarabinoxylans, (gluco)mannans and mixed-linkage glucans (MLG). Xyloglucans consist of a heavily substituted β-1,4-glucan backbone. Glucuronoarabinoxylans contain a substituted β-1,4-linked xylan backbone and (gluco)mannans have a variably substituted backbone that includes β-1,4-linked mannose (glucose and mannose) residues. MLG is an unsubstituted backbone of glucosyl residues containing both β-1,3- and β-1,4-linkages (Lerouxel *et al.,* 2006).

The most important biological role of hemicelluloses is their contribution to strengthening the cell wall by interaction with cellulose. Hemicelluloses share an ability to hydrogen-bond to cellulose and differ in the alkali concentration required for extraction. Low alkali concentrations may extract xylans with many side chains and higher concentrations are required for xylans with fewer side chains. The highest concentration is needed for MLG and xyloglucans. Complete extraction of xyloglucans requires 6 M NaOH at 37 °C (Edelmann and Fry, 1992).

1.2.3. Pectins

Pectins form part of the primary cell wall and most of the middle lamella between adjacent cells. Pectins are water-soluble, highly hydrophilic polysaccharides that form gels in solution. Pectins are galacturonic acid-rich polysaccharides

comprised of distinct domains of homogalacturonan (HG), rhamnogalacturonan-I (RG-I) and rhamnogalacturonan-II (RG-II) (O'Neill *et al.,* 1990; Visser and Voragen, 1996). Homogalacturonan is a linear chain of (1→4)-linked α-$_D$-galactopyranosyluronic acid (GalpA) residues in which some of the carboxyl groups are methyl esterified and also partially O-acetylated at C-3 or C-2 (Ridley *et al.,* 2001). Rhamnogalacturonan-I (RG-I) contains a backbone of the repeating disaccharide [→4)-α-$_D$-GalpA-(1→2)-α-$_L$-Rhap-(1→]. The substituted galacturonan referred to as rhamnogalacturonan II (RG-II) has a backbone of linear 1,4-linked α-$_D$-GalpA residues (O'Neill *et al.,* 1990).

1.3. Xyloglucan

Xyloglucan can be found in the middle lamella, primary walls, and gelatinous wall layer of higher plants. Xyloglucan possesses a backbone of β-(1→4)-Glc with 1,6-α-xylosyl residues along the backbone. Generally, the backbone consists of a cellotetraose (G4G4G4G) repeat with the first three Glc residues carrying an α-Xyl residue, whereas the Glc residue number four is unsubstituted. In dicotyledons, major species-specific differences appear in the additional galactosyl and fucosyl-galactosyl residues attached to the xylose residues (Hayashi, 1989). Some of the Xyl residues carry an additional β-Gal residue (β-Gal-(1→2)-α-Xyl), and the β-Gal itself often carries α-Fuc (α-Fuc-(1→2)-β-Gal-(1→2)-α-Xyl) (Fry *et al.,* 1993).

Abbreviated names are available for xyloglucan-derived oligosaccharides (Fry *et al.,* 1993, Pena *et al.,* 2008). Each (1→4)-linked β-$_D$-glucosyl residue (and unbranched Glc residues) along the xyloglucan backbone is given a one-letter code according to its substituents (Table 1). Generally, all residues are pyranoses except arabinose, which may be pyranose (Ara*p*) or furanose (Ara*f*) (Frankova and Fry, 2012). Reduced xyloglucan oligosaccharides are given the suffix "ol".

Table 1. Nomenclature of xyloglucan oligosaccharides.

Code	Structure
A	α-D-Xyl-(1→6)-[α-L-Ara*f*-(1→2)]-β-D-Glc*
B	α-D-Xyl-(1→6)-[β-D-Xyl-(1→2)]-β-D-Glc*
C	α-D-Xyl-(1→6)-[α-L-Ara*f*-(1→3)-β-D-Xyl-(1→2)]-β-D-Glc*
D	α-L-Ara*p*-(1→2)-α-D-Xyl-(1→6)-β-D-Glc*
E	α-L-Fuc-(1→2)-α-L-Ara*p*-(1→2)-α-D-Xyl-(1→6)-β-D-Glc*
F	α-L-Fuc-(1→2)-β-D-Gal-(1→2)-α-D-Xyl-(1→6)-β-D-Glc*
G	β-D-Glc* with no side-chain attached
Gol	Glucitol (the former reducing terminus after reduction with $NaBH_4$)
J	α-L-Gal-(1→2)-β-D-Gal-(1→2)-α-D-Xyl-(1→6)-β-D-Glc*
L	β-D-Gal-(1→2)-α-D-Xyl-(1→6)-β-D-Glc*
M	α-L-Ara*p*-(1→2)-[β-D-Gal-(1→4)]-α-D-Xyl-(1→6)-β-D-Glc*
N	α-L-Ara*p*-(1→2)-[β-D-Gal-(1→6)-β-D-Gal-(1→4)]-α-D-Xyl-(1→6)-β-D-Glc*
P	β-D-GalA-(1→2)-[β-D-Gal-(1→4)]-α-D-Xyl-(1→6)-β-D-Glc*
Q	β-D-Gal-(1→4)-β-D-GalA-(1→2)-[β-D-Gal-(1→4)]-α-D-Xyl-(1→6)-β-D-Glc*
S	α-L-Ara*f*-(1→2)-α-D-Xyl-(1→6)-β-D-Glc*
T	β-L-Ara*f*-(1→3)-α-L-Ara*f*-(1→2)-α-D-Xyl-(1→6)-β-D-Glc*
U	β-D-Xyl-(1→2)-α-D-Xyl-(1→6)-β-D-Glc*
V	α-D-Xyl-(1→4)-α-D-Xyl-(1→6)-β-D-Glc* (present work)
X	α-D-Xyl-(1→6)-β-D-Glc* (=isoprimeverose)

* The β-D-Glc in each structure is part of the (1→4)-β-glucan backbone of the xyloglucan.

(adopted from Frankova and Fry, 2012)

The name of the oligosaccharide contains these code letters listed in sequence from non-reducing to reducing terminus of the backbone. In dicot, frequently observed xyloglucans include XXXG, XXLG, XXFG, and XLFG (Table 2; Frankova and Fry, 2013).

Table 2. Abbreviated nomenclature of xyloglucan oligosacchaides.

Structure*	Abbreviation	Structure	Abbreviation
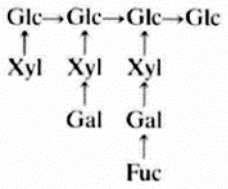	XLFG	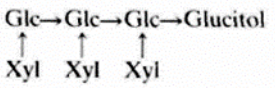	XXXGol
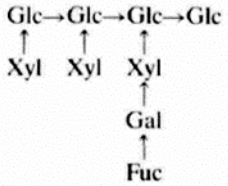	XXFG	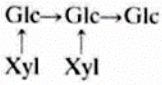	XXG
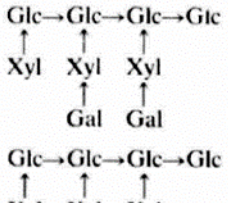	XLLG	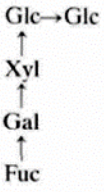	FG
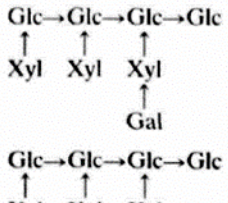	XXLG	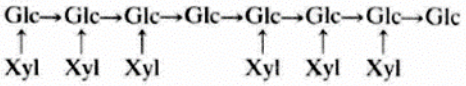	XXXGXXXG
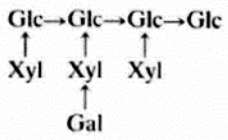	XLXG	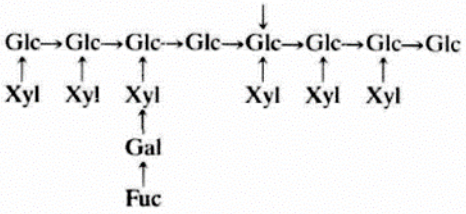	XXFGAXXG

* Sugar residues and their linkages are represented as follows: Ara α-$_L$-arabinofuranosyl-(1→2)-, Fuc α-$_L$-fucopyranosyl-(1→2)-, Gal β-$_D$-galactopyranosyl-(1→2)-, Glc β-$_D$-glucopyranosyl-(1→4)-, Xyl α-$_D$-xylopyranosyl-(1→6)-.

(adopted from Fry *et al.,* 1993)

1.4. Mix linkage glucan (MLG)

Mixed-linkage (1→3, 1→4)-β-$_D$-glucan (MLG) is a hemicellulose of poalean primary cell walls, e.g. grasses, cereals and reeds (Trethewey *et al.,* 2005). MLG has been found also in Equisetum species (Fry *et al.,* 2008, Sorensen *et al.,* 2008). In cell walls, MLG is hydrogen bonded to the cellulose (Carpita *et al.,* 2001)

and may tether microfibrils (Labavitch and Ray 1978, Wada and Ray 1978, Fry, 1989). The polysaccharide typically takes the form:

…G3G4G4G3G4G4G4G3G4G4G3G4G4G3G…,

reading from non-reducing to reducing terminus, where 'G' is β-$_D$-glucopyranose, and '3' and '4' indicate (1→3) and (1→4) bonds, respectively. The underlined domains are effectively cellotriose and (minor) cellotetraose units, interlinked by (1→3) bonds (Meikle *et al.,* 1994).

Characterization of MLG can be simply done by digestion with lichenase, which cleaves the (1→4) bond in the sequence …G3G4G…, producing oligosaccharides always with a (1→3) bond at the reducing end (Meikle *et al.,* 1994; Grishutin *et al.,* 2006; Li *et al.,* 2006). The major oligosaccharide released by lichenase digestion of poalean MLG is G4G3G, and few amounts of G4G4G3G. Cellulase digests MLG mainly at the (1→4) bond in the sequence …G4G3G…, yielding oligosaccharides with a (1→3) bond at the non-reducing terminus.

1.5. Diversity of the xyloglucan endotransglycosylase/hydrolase (XTH) gene family and phylogenetic tree of XTH genes

XTH enzymes belong to the glycoside hydrolase (GH) family 16, a member of clan B in the Carbohydrate-Active enZYmes (CAZY) classification (Cantarel *et al.,* 2009). Other family member of GH16 include 1,3-1,4 β-glucanases (lichenases), keratan-sulfate-endogalactosidases, κ-carrageenases, β-agarases, and 1,3-β-glucanases (laminarinases). These family members display a diversity of substrate specificities which cleave β-1,3 or β-1,4 bonds in various glucans and galactans (Eklöf and Brumer, 2010). Within GH16, the XTH gene products are closely related to bacterial β-1,3-1,4-glucan hydrolases and fungal CRH (Congo Red Hypersensitive) gene products (Cabib *et al.,* 2008). XTH genes encode a large multi-protein family. Among dicots, there are 33 in *Arabidopsis thaliana* (Yokoyama and Nishitani, 2001), 41 in poplar (Geisler-Lee *et al.,* 2006) and 25 in tomato (*Lycopersicon esculentum* cv T5) (Saladié *et al.,* 2006). In

monocots, there are 29 in rice (*Oryza sativa*) (Yokoyama *et al.,* 2004) and 22 in barley (*Hordeum vulgare*) (Strohmeier *et al.,* 2004). Nine have been found in the lycopodiophyte Selaginella (Van Sandt *et al.,* 2007) and 32 in the Physcomitrella (Yokoyama *et al.,* 2010).

The molecular phylogeny originally divided the XTH gene products into three major groups: I, II, and III (Campbell and Braam, 1999). This classification has undergone continual revision as a consequence of numerous plant genome sequencing projects (http://www. phytozome.org/). A comparison of two plant genomes of *Oryza sativa* (a monocot) and *Arabidopsis thaliana* (a dicot), indicated that groups I and II had become indistinguishable (Yokoyama *et al.,* 2004). There are a number of statistically robust clades within the composite group I/II, although there is no evidence that these clades harbour significantly different activities (Eklöf and Brumer, 2010). Moreover, members of groups I and II have been found to exhibit only xyloglucan endotransglycosylase (XET) activity (Maris *et al.,* 2011; Nishitani and Tominaga, 1992; Rose *et al.,* 2002). A strict XET enzyme of group I/II is PttXET16A (Johansson *et al.,* 2004). Group III can be divided in two groups: III-A and III-B (Baumann *et al.,* 2007), supported by sequence analysis and catalytic activity. TmNXG1 from nasturtium (*Tropaeolum majus*) and VaXGH from azuki bean (*Vigna angularis*) of group III-A, are thus far the only XTH gene products with demonstrable hydrolytic (xyloglucan endohydrolase, XEH) activity (Edwards *et al.,* 1986; Fanutti *et al.,* 1993, 1996; Tabuchi *et al.,* 2001; Baumann *et al.,* 2007). XTH genes in group III-B: AtXTH27 (Campbell and Braam, 1999), SlXTH5 (Saladie *et al.,* 2006), and HvXTH8 (Kaewthai *et al.,* 2010), show exclusively XET activity, thus validating a functional distinction between the A and B clades. A small outlying group, close to the root and comprising At-XTH1 to At-XTH3, At-XTH11, and Pt-XTH15, is possibly ancestral, clade between group I/II and group III (Baumann *et al.,* 2007). A new phylogenetic tree has been proposed based on the sequences of proteins encoded by XTHs of various plants, including *Arabidopsis thaliana, Oryza sativa, Solanum lycopersicum, Tropaeolum majus, Populus tremula x Populus tremuloides, Populus trichocarpa, Litchi chinensis, Vitis labrusca x Vitis vinifera, and Carica papaya* (Baumann *et al.,* 2007).

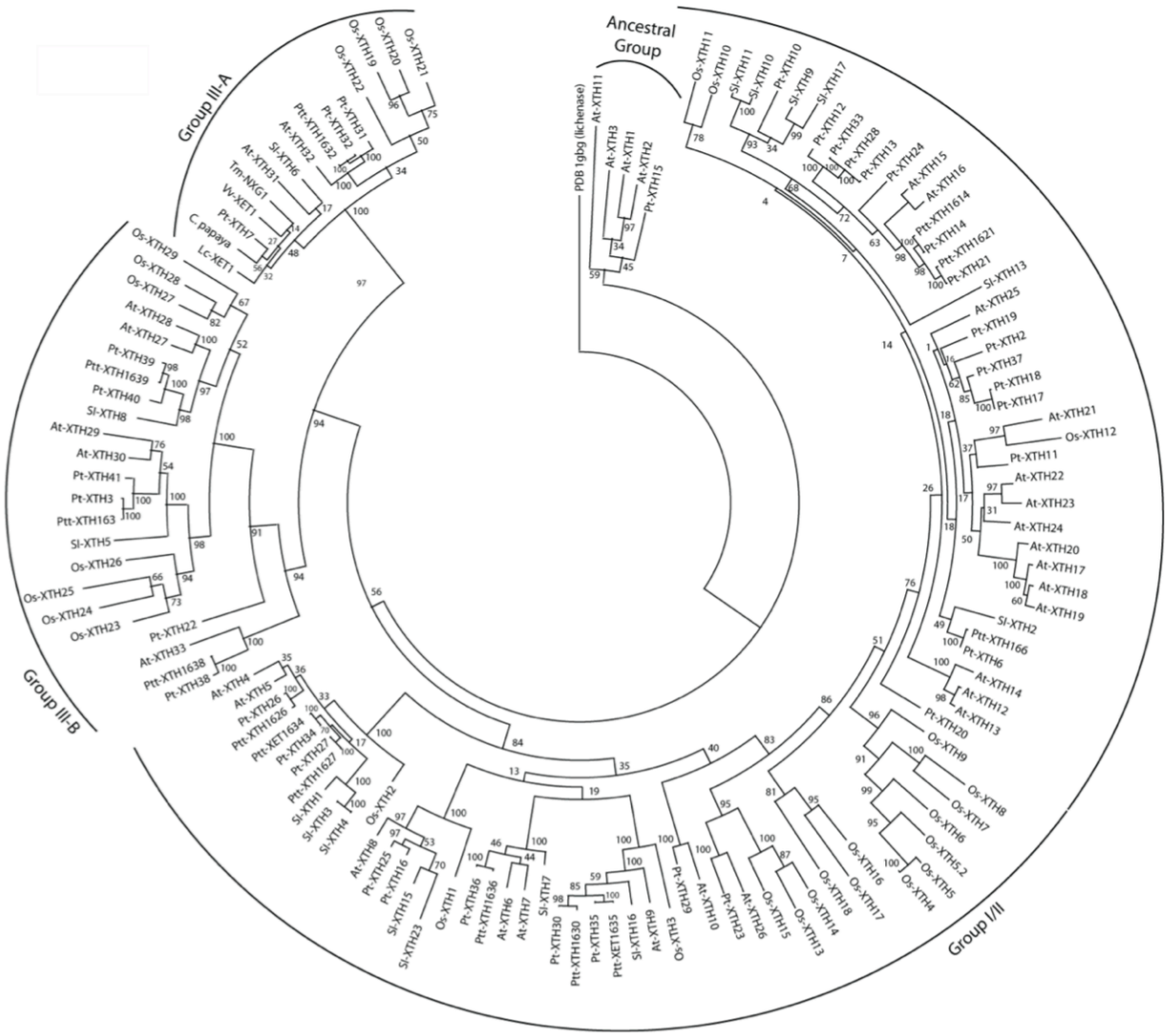

(Adopted from Baumann *et al.,* 2007)

Figure 3. The phylogenetic tree of XTHs

The tree is based on 130 full-length XTH gene products and *Bacillus licheniformis* Lichenase with PDB identifier 1GBG and GenPept accession number CAA40547; Bootstrap values from 100 maximum likelihood resamplings are indicated.

1.6. Substrate and function of XTH gene products

XTHs exhibit one or both of the following enzymatic activities: (i) xyloglucan endotransglucosylase (XET; EC 2.4.1.207), which catalyzes the cleavage and rejoining the xyloglucan backbone by transglycosylation (Figure 4), and (ii)

xyloglucan endohydrolase (XEH; EC 3.2.1.151), which simply catalyzes hydrolysis of xyloglucan.

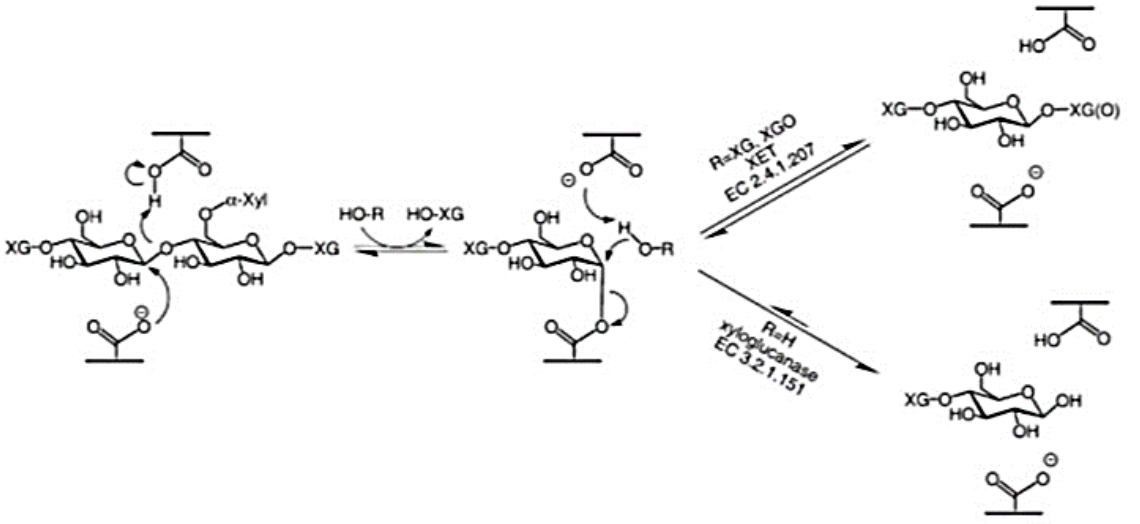

(Adopted from Baumann *et al.,* 2007)

Figure 4. The chemical mechanism of hydrolysis and transglycosylation.

XET catalyzes, in a first step, an endolytic cleavage of a cross-linking xyloglucan polymer that permits cellulose microfibrils to separate and the cell to expand. In the second reaction step, XET transfers the newly generated end to another sugar polymer, thereby restoring stable cell wall structure (Smith and Fry, 1991; Xu *et al.,* 1995; Purugganan *et al.,* 1997; Campbell and Braam, 1999). During XET action, one polysaccharide chain (the donor-substrate) is cleaved, and a portion of it is then grafted on to an acceptor-substrate, which can be either another xyloglucan chain or a xyloglucan oligosaccharide (XGO) (Figure 4).

When XXXG is added to segments, xyloglucan endotransglucosylase bound to the internal regions of xyloglucan in the cell walls could cleave the xyloglucan and transfer the newly generated reducing end to the non-reducing end of XXXG. If endogenous xyloglucan exists as a tether between cellulose microfibrils, such a reaction involving XXXG could result in the cleavage of the tether. If endogenous xyloglucans were endotransglycosylated with a large amount of XXXG, their molecular sizes in the wall would decrease. When whole xyloglucan is added to segments, on the other hand, xyloglucan endotransglucosylase could catch the

internal region of exogenous whole xyloglucan, cleave it, and transfer this newly generated reducing end to the non-reducing end of the endogenous one. Thus, the xyloglucan in the wall becomes a larger molecule through endotransglycosylation. XET contributes to growth promotion in two ways. (1) In the absence of oligosaccharides it causes a polysaccharide-to-polysaccharide transglycosylation, reversibly loosening the cell wall and permitting molecular creep. (2) In the presence of suitable oligosaccharides it causes a polysaccharide-to-oligosaccharide transglycosylation, effectively cleaving the polymer and resulting in a more permanent wall-loosening (Fry *et al.,* 2012).

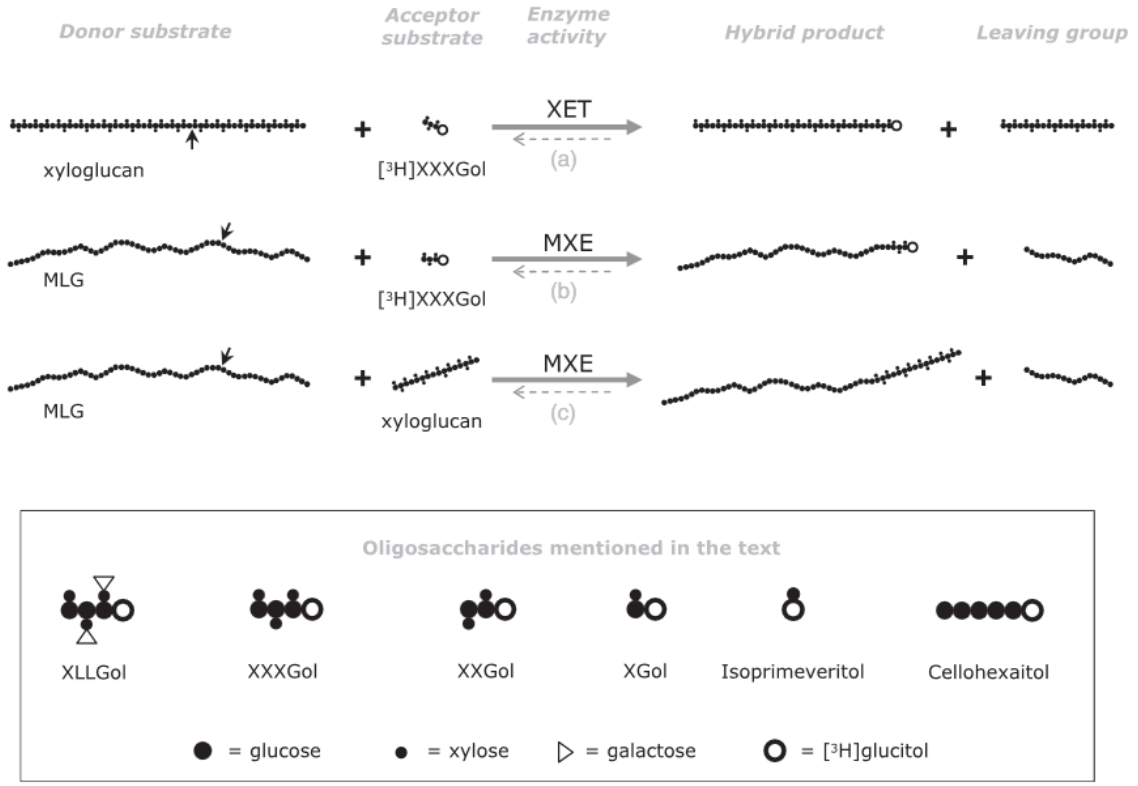

(Adopted from Fry *et al.,* 2008)

Figure 5. Enzymic reactions and oligosaccharide structures.

Xyloglucan endotransglucosylase (XET) activity cleaves xyloglucan (donor-substrate; ↑ = bond cleaved) and grafts a portion on to an acceptor-substrate, which can be a xyloglucan oligosaccharide e.g. [^{3}H]XXXGol; reaction (a). MLG:xyloglucan endotransglucosylase (MXE), cleaves mixed-linkage (1⟶3, 1⟶4)-β-$_{D}$-glucan (MLG) (donor substrate; ↓ = bond cleaved) and grafts a portion on to an acceptor-substrate, which can be a xyloglucan oligosaccharide, reaction (b) or a high molecular-weight xyloglucan chain, reaction (c).

An enzyme activity was detected in *Equisetum* with the formation of MLG →xyloglucan bonds as the preferred reaction, well exceeding the classic XET reaction rate (Figure 5; Fry *et al.,* 2008).

1.7. Substrate recognition and binding of XETs and XEHs

The conserved sequence of the catalytic motif in XTHs is 83(H/W/R)-(D/N)-**E**-(I/L/F/V)-**D**-(F/I/L/M)-**E**-(F/L)-(L/M)-G92 (boldface shows catalytic residues, numbering is based on *Ptt*XET16-34) (Figure 6).

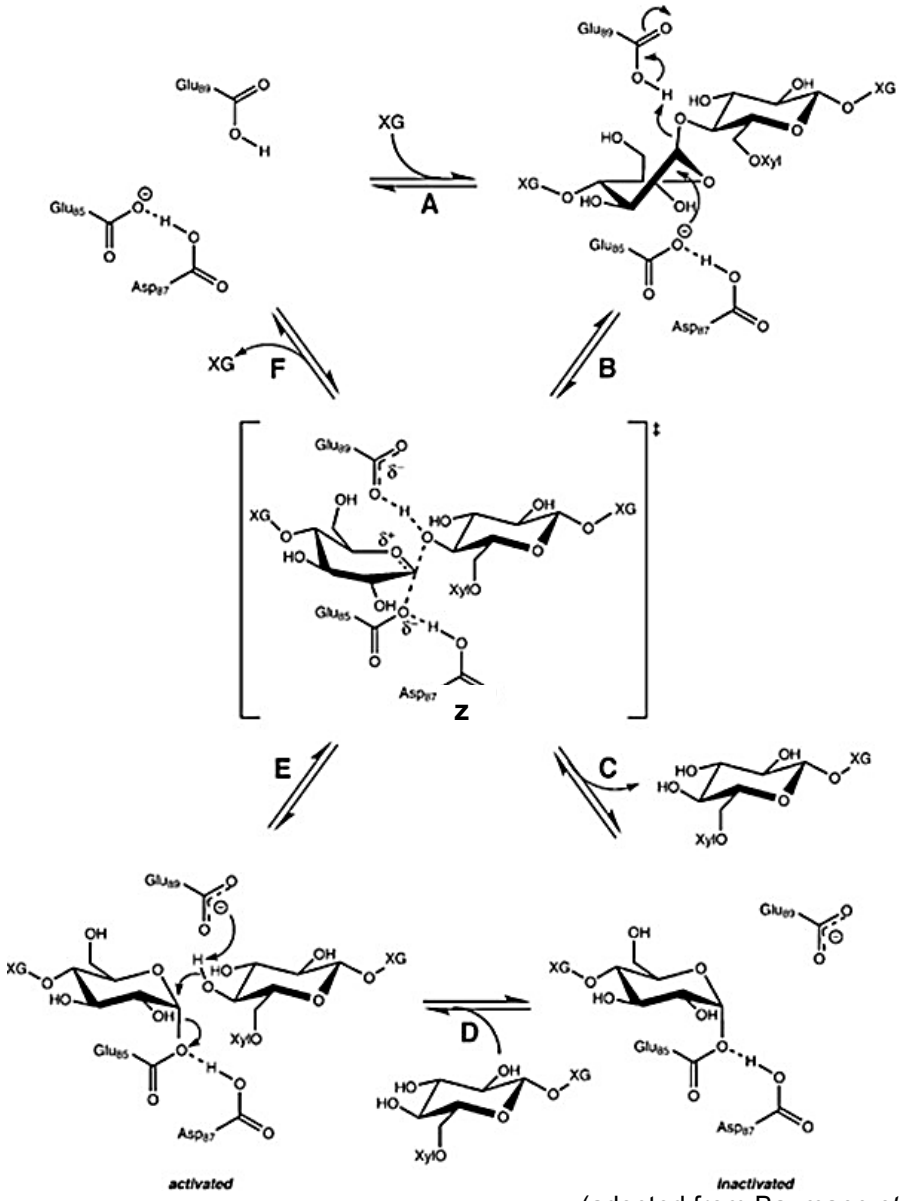

(adopted from Baumann *et al.,* 2007)

Figure 6. Schematic representation of XET-catalyzed transglycosylation.

Glu-85 is positioned by a tight hydrogen bond to Asp-87. The Asp-87 modulates the ionization state of Glu-85. Glu-85 acts as a “nucleophile” that attacks the anomeric carbon of the xyloglucan glucose backbone to produce the glycosyl-enzyme intermediate (an oxocarbenium ion-like transition state). Glu-89 protonates the departing xyloglucan chain and activates the incoming acceptor substrate. (Planas, 2000; Eklöf and Brumer, 2010; Kawethai, 2011).

A xyloglucan polysaccharide (XG) binds to the active site cleft with the glucopyranose ring potentially adopting a twist-boat conformation (Figure 6A; Davies *et al.,* 2003). E85, the proposed nucleophile, is positioned by a tight hydrogen bond to D87. (Figure 6B) Catalysis proceeds through an oxocarbenium ion-like transition state (z), with departure of the leaving group facilitated by proton donation from E89. (Figure 6C) The nascent nonreducing end diffuses away from the hydrolytically stable covalent glycosyl-enzyme intermediate (Figure 6D). An acceptor sugar chain enters the catalytic cleft and activates the catalytic machinery for transglycosylation (Figure 6E and F). E89 now acts as a Bronsted base to activate the attacking hydroxyl group, with catalysis proceeding through the transition state (z), leading to transglycosylation and product release (Figure 6F).

1.8. XTHs role in the different processes of plant development

XTH activities and levels of XTH expression increase during a number of developmental processes that involve net cell wall degradation. This includes fruit ripening (Redgwell and Fry 1993; Cutillasiturralde *et al.,* 1994; Maclachlan and Brady 1994, Arrowsmith and de Silva 1995; Schröder *et al.,* 1998; Rose and Bennett 1999), mobilization of seed reserves (Farkaš *et al.,* 1992; Fanutti *et al.,* 1993), and formation of root aerenchyma (Saab and Sachs 1996), mesophyll air spaces (Antosiewicz *et al.,* 1997), abscission zones (Xu *et al.,* 1995), and vascular tissue (Medford *et al.,* 1991; Xu *et al.,* 1995; Antosiewicz *et al.,* 1997; Oh *et al.,* 1998; Vissenberg *et al.,* 2000). It is suggested that, besides their apparent involvement in cell expansion, XTHs may have an important function catalyzing xyloglucan depolymerization and/or solubilization during cell wall disassembly (Rose *et al.,* 2012).

XTHs could also play essential roles in a variety of growth and differentiation processes, including primary root elongation (Osato *et al.,* 2006), hypocotyl growth (Wu *et al.,* 2005), vein differentiation (Matsui *et al.,* 2005), flower opening (Harada *et al.,* 2011), fruit ripening (Saladié *et al.,* 2006; Miedes and Lorences, 2009), petal abscission (Singh *et al.,* 2011), and wood formation (Nishikubo *et al.,* 2011).

1.9. GDSL Esterase/Lipase

GDSL esterases and lipases are hydrolytic enzymes with multifunctional properties such as broad substrate specificity and regiospecificity. They have potential for use in the hydrolysis and synthesis of important ester compounds of pharmaceutical, cosmetics, food, biochemical, and biological interests (Akoh *et al.,* 2004). GDSL is a new subfamily of hydrolytic / lipolytic enzymes. In contrast to most lipases that contain a GxSxG motif, GDSL lipases exhibit a GDSL motif GxSxxxxG, in which the active site Ser is located near the N-terminus (Brick *et al.,* 1995; Upton *et al.,* 1995)

1.9.1. GDSL esterase/lipase conserved sequence and activity

Enzymes that belong to the GDSL family of esterases/lipases share five blocks of highly conserved homology of blocks I, II, III, and V, which are important for their classification. These consensus motifs are specific to different phylogenetic clades and/or subclades from conjoint tree that differed in biological functions. Unlike other lipases, GDSL hydrolases have broadly diverse enzymatic activities, including esterase, thioesterase, arylesterase, lysophospholipase and protease activity in the same enzyme (Molgaard *et al.,* 2000; Lee *et al.,* 1997; Akoh *et al.,* 2004). The flexible substrate-binding pocket in the active site, which facilitates the binding of different substrates can explain this multienzymatic activity. Considering that many motifs can be functionally important and play a role in enzyme specificity and biochemical activity, the long loop regions extending from the protein core in the plant GDSL esterases/ lipases might be involved in the diversification of molecular multifunctionality, as this was found in bacterial species (Lo *et al.,* 2003; Mathews *et al.,* 2007).

The GDSL family is further classified as SGNH hydrolase because of the presence of the strictly conserved residues Ser-Gly-Asn-His in the conserved blocks I, II, III, and V (Brick *et al.,* 1995; Upton *et al.,* 1995; Akoh *et al.,* 2004). Each of the four residues plays a key role in the catalytic function of the enzyme. The catalytic Ser in block I serves as the nucleophile and a proton donor to the oxyanion hole. The Gly residue in block II and the Asn in block III serve as two other proton donors to the oxyanion hole. His residue in block V acts as a base to make active site Ser more nucleophilic by deprotonating the hydroxyl group. Another feature in block V is the presence of Asp located at the third amino acid preceding His (i.e., DxxH serves as the third member of the catalytic triad). Members of the SGNH-hydrolase superfamily facilitate the hydrolysis of a broad range of substrates, including polysaccharides, lysophospholipids, and other ester containing compounds (Lo *et al.,* 2003; Molgaard *et al.,* 2000), giving SGNH hydrolase great potential in both basic research and industrial applications.

All the structures of the GDSL esterase/lipase that have been described to date belong to the α/β hydrolase fold superfamily of proteins. The main difference in folding from classical α/β hydrolase fold is a distinct location of the residues involved in active site formation, which direct to a different analogous orientation of the catalytic triad with regard to the central parallel β-sheet (Molgaard *et al.,* 2000; Lo *et al.,* 2003).

1.9.2. Mechanism action of GDSL esterase/lipase

GDSL esterase/lipase belongs to the family II of carboxylesterases. The primary reaction catalyzed by this enzyme is hydrolysis. The ability to hydrolyze ester bond to an acid and alcohol metabolite is a two-steps process. The first step is nucleophilic attack of catalytic serine –OH on the carbonyl carbon of the ester bond. This step releases an alcohol metabolite and an acylated enzyme due to a covalent linkage formed between the acid moiety of substrate and Ser (S) residue at the catalytic site. The step is stabilized through hydrogen bonding to His (H), which in turn is stabilized by the carboxylic group of the acidic member of the catalytic triad. In the second step, the His (H) residue of the catalytic triad shows

affinity toward water molecules and it also helps the enzyme to return to its active state with the release of an acid moiety (Sood *et al.,* 2016; Montella *et al.,* 2012)

1.9.3. Member of GDSL esterase/lipase

Selected members of GDSL esterase/lipase class include *Aeromonas hydrophilia* lipases/acyltransferase, *Vibrio parahemolyticus* hemolysin/phospholipase, *Xenorhabdus luminescens* lipase, *Arabidopsis thaliana* proline-rich protein, *Brassica napus* proline-rich protein, *Vibrio mimicus* arylesterase, *Escherichia coli* thioesterase/protease I /lysophospholipase L, *Streptomyces rimosus* lipase, and *Streptomyces scabies suberin* esterase (Akoh *et al.,* 2004). Representative members of the SGNH family include *Escherichia coli* thioesterase/protease I/lysophospholipase L and thioesterase/protease I, TEP-I (Lo *et al.,* 2003; Tyukhtenko *et al.,* 2003).

The GDSL esterases/lipases have been also found in plant species. In the plant kingdom, more than 1100 members represent the novel family of the GDSL esterases/lipases from twelve different fully sequenced plant genomes. It was reported that GDSL family from *Arabidopsis thaliana* consists of 108 members (Ling, 2008), and *Vitis vinifera, Sorghum bicolour*, *Populus trichocarpa, and Physcomitrella patens* contain 96, 130, 126 and 57 members, respectively (Volokita *et al.,* 2010). Search across multiple databases revealed 114 members from *Oryza sativa*, 53 members from *Zea mays*, 90 members from *Selaginella moellendorffii*, 88 members from *Medicago truncatula*, 102 members from *Chlamydomonas reinhardtii,* 59 members from *Ostreococcus tauri*, and 75 members from *Phaeodactylum tricornutum* (Youens-Clark *et al.,* 2010; Ouyang *et al.,* 2007).

1.9.4. Role of GDSL lipases in plant metabolism

GDSL-lipases are expressed in epidermal cells of the peel, close to the cuticular membranes (Lemaire-Chamley *et al.,* 2005; Reina *et al.,* 2007; Mintz-Oron *et al.,* 2008; Matas *et al.,* 2010; Yeats *et al.,* 2010), and the expression of an Arabidopsis GDSL-lipase is upregulated by WIN1/SHN1, a transcription factor

that regulates cutin deposition (Kannangara *et al.,* 2007; Shi *et al.,* 2011). In addition, GDSL-lipases are synthesized as preproteins containing signal peptides predicted to facilitate extracellular exportation. This extracellular location was confirmed for most characterized GDSL-lipases in latex (Abdelkafi *et al.,* 2009), in nectar (Kram *et al.,* 2008), in the secretome of plant cells (Oh *et al.,* 2005; Naranjo *et al.,* 2006; Hong *et al.,* 2008; Kusumawati *et al.,* 2008), and in sporollenin, a cutin-like polymer of the pollen coat (Updegraff *et al.,* 2009).

GDSL esterases/lipases might play an important role in the regulation of plant development and morphogenesis. A lipolytic enzyme Arab-1 in Arabidopsis was isolated, sequenced, and translated and when expressed in *E. coli*, the gene product showed lipolytic activity (Brick *et al.,* 1995). Another GDSL enzyme from post-germinated sunflower (*Helianthus annuus* L.) seeds was isolated, purified, and had fatty acylester hydrolase activity (Beisson *et al.,* 1997). Three *Neocallimastix patriciarum* esterases involved in the degradation of complex polysaccharides were found to belong to the GDSL-family (Dalrymple *et al.,* 1997). They show acetylxylan esterase activity able to remove O-acetyl groups from xylose residues in xylan and xylo-oligomers. Deacetylation of xylans with this enzyme may have application in food by increasing the biodegradability of xylans and render cellulose more accessible, or it may enhance the breakdown or hydrolysis of acetylxylan by other enzymes. The acetylxylan esterase may participate in the degradation of plant cell walls in association with xylanases, cellulases, and mannanases.

Plant GDSL-lipase activity has been widely associated with seed germination (Clauss *et al.,* 2008), pollen hydration (Updegraff *et al.,* 2009), pathogen defense (Oh *et al.,* 2005; Kwon *et al.,* 2009; Lee *et al.,* 2009), and the abiotic stress response (Hong *et al.,* 2008; Zhou *et al.,* 2009). Enod8 is a member of the GDSL lipase/esterase family that was isolated from *Medicago sativa* root nodules (Pringle *et al.,* 2004). In *Brassica napus*, BnLIP2 encodes a GDSL lipase; its expression was induced during germination and maintained in mature seedlings, suggesting functions in both germination and morphogenesis (Ling *et al.,* 2006). GDSL lipases perform also critical roles in the biotic and abiotic stress responses

of plants. GLIP1 is an Arabidopsis GDSL lipase that possesses anti-microbial activity and regulates pathogen resistance to *Alternaria brassicicola* in association with ethylene signaling (Oh *et al.,* 2005). In hot pepper, CaGLIP1 encodes a GDSL lipase that has been shown to modulate pathogen and wound stress resistance (Kim *et al.,* 2008; Hong *et al.,* 2008). In contrast to the pathogen resistance provided by Arabidopsis GLIP1, virus-induced gene silencing of CaGLIP1 conferred resistance to *Xanthomonas campestris* pv. vesicatoria. Recombinant GLIP2 proteins possessed lipase and anti-microbial activities, inhibiting germination of fungal spores (Lee *et al.,* 2009).

1.10. AIM OF THE STUDY

The general objective of the present investigation was to perform a detailed characterization of xyloglucan endotransglucosylases/hydrolases (FvXTH9 and FvXTH6) and esterase (FvGDSL esterase/lipase) enzymes from *Fragaria vesca.*

The specific goals were:

Expression, purification and characterization of FvXTH9 and FvXTH6 and FvGDSL esterase/lipase

In vitro enzymatic characterization including donor/acceptor substrate preference and enzyme kinetics of FvXTH9 and FvXTH6 heterologously produced in the yeast *Saccharomyces cerevisiae.*

In vivo localization of FvXTH9 and FvXTH6 in *Nicotiana tabacum* leaves

In vivo assay for the role of FvXTH9 and FvXTH6 during fruit ripening by transient expression in *F.* × *ananassa* fruit.

2. MATERIAL AND METHOD

2.1. Materials

2.1.1. Plant materials

Octoploid strawberry plants (*Fragaria* × *ananassa* cv. Elsanta) and diploid (*Fragaria vesca* Hawaii 4) were obtained from a producer (Kraege Beerenpflanzen, Telgte, Germany). *F. vesca* was used for mRNA isolation and cloning purposes whereas *F.* × *ananassa* was used for transient expression studies. For genetic and molecular analyses, fruits were injected 14 days after pollination and harvested 8–14 days after agroinfiltration. Plants of strawberry were grown under greenhouse conditions (16h/8h, light/dark period) in Dünast, Freising, Germany.

Nicotiana tabacum was used for localization. Plant was grown under greenhouse condition at 25°C and a 16 h photoperiod under 120 µmol m^{-2} sec^{-1} irradiance provided by Osram Fluora lamps (München, Germany) in Freising, Germany.

2.1.2. Chemicals

Chemicals and solvents were obtained from Sigma-Aldrich (Taufkirchen, Germany), Carl Roth (Karlsruhe, Germany), VWR International (Darmstadt, Germany) and J. T. Baker (Austin, TX, USA), unless otherwise noted.

2.1.2.1. Polysaccharides

Tamarind seed xyloglucan was a generous gift from Dr K. Yamatoya, Dainippon Pharmaceutical Co.; carboxymethyl cellulose (CMC) (Na^+ salt, low viscosity) and barley mixed-linkage β-glucan MLG were from Sigma-Aldrich; hydroxyethylcellulose (HEC) was from Fluka; and cellulose acetate was from Sigma-Aldrich.

2.1.2.2. Oligosaccharides

Non-radioactive XXXGol was from Megazyme (Bray, Ireland). Specific cello-oligosaccharides were from Sigma. Tritiated XLLGol, XXXGol, XXGol, XGol, isoprimeveritol, and cellohexaitol were prepared by NaB^3H_4 reduction of the corresponding reducing oligosaccharides (Hetherington and Fry, 1993).

2.1.3. Bacterial and yeast strains

Table 3. Bacteria / yeast strain and genotypes

Bacteria / yeast strain	Genotype
E. coli JM 109 (Promega)	*end*A1, *rec*A1, *gyr*A96, *thi, hsd*R17 (r_k^-, m_k^+),*rel*A1,*sup*E44, Δ(*lac-pro*AB),[F´ *tra*D36, *pro*AB, *laq*I^qZΔM15]
E. coli NEβ 10 (New England Biolabs)	Δ(ara-leu) 7697 araD139 fhuA ΔlacX74 galK16 galE15 e14- ϕ80dlacZΔM15 recA1 relA1 endA1 nupG rpsL (StrR) rph spoT1 Δ(mrr-hsdRMS-mcrBC)
E. coli BL21 (DE3) pLysS (Novagen)	F^- *ompT hsdS*$_B$ (r_B^- m_B^-) *gal dcm* (DE3)
Agrobacterium tumefaciens AGL0 (Lazo *et al.*, 1991)	C58 Rif^r
Agrobacterium tumefaciens GV3101 (Van Larebeke *et al.,* 1974)	C58C1 Rif^r
Saccharomyces cerevisiae INVSc-1 (Invitrogen)	MATa his3Δ1 leu2 trp1-289 ura3-52 /MATα his3Δ1 leu2 trp1-289 ura3-52

2.1.4. Enzymes

Table 4. List of enzymes

Enzyme name	Concentration	Manufacture
DnaseI	1U/µl	Thermo Scientific
Moloney Murine Leukimia Virus (M-MLV) Reverse Transcriptase	200 U/µl	Promega
Recombinant RNasin® Ribonuclease Inhibitor	40U/µl	Promega

Tag ® DNA-Polymerase	5 U/µl	New England Biolabs
Phusion® DNA-Polymerase	2 U/µl	Thermo Scientific
Restriction endonuclease BamH I	20 U/µl	Fermentas
Restriction endonuclease Sac I	20 U/µl	Fermentas
Restriction endonuclease Nco I	20 U/µl	Fermentas
Restriction endonuclease Not I	20 U/µl	Fermentas
Restriction endonuclease EcoRV	20 U/µl	Fermentas
T4 DNA ligase	3 U/µls	Promega

2.1.5. Markers

Table 5. List of markers

Marker	Manufacture
GeneRuler™ 1kb DNA Ladder	Fermentas
GeneRuler™ DNA Ladder Mix	Fermentas
PageRuler Plus Prestained Protein Ladder	Thermo Scientific

2.1.6. Antibiotics

Table 6. Final concentration and solvent of antibiotics

Antibiotics	Final concentration	Solvent	Manufacture
Ampicillin	100 µg/ml	Water	Sigma
Chloramphenicol	34 µg/ml	Ethanol	Sigma
Kanamycin	25 µg/ml	Water	Sigma
Rifampicin	25 µg/ml	Methanol	Fluka

2.1.7. Vectors

2.1.7.1. Vectors and sequencing primers

Table 7. Vectors with appropriate antibiotics and sequencing primers

Vector name	Antibiotics	Sequencing primers
pGEM-T (Promega)	Ampicillin	T7, SP6
pGEX-4T-2 (GE Healthcare)	Ampicillin	pGEX-F, pGEX-R
PYES2 (Invitrogen)	Ampicillin	PYES2F, PYES2R
pBI121	Kanamycin	M13F, M13R
pGWR8	Kanamycin	T7, T3

2.1.7.1.1. pGEM-T

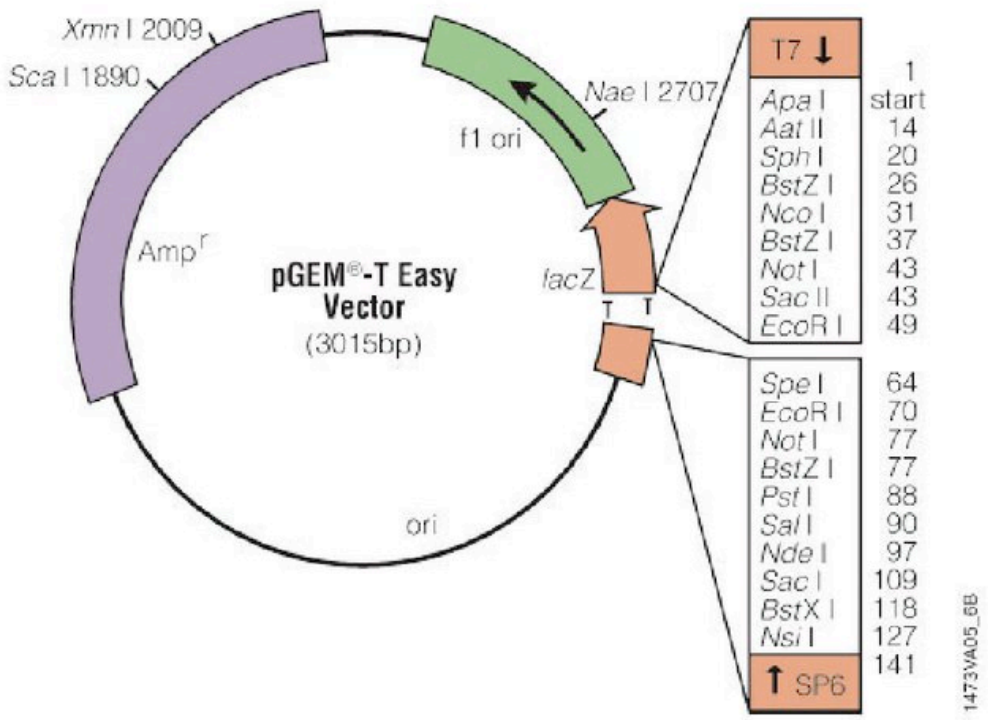

2.1.7.1.2. pGEX-4T-2

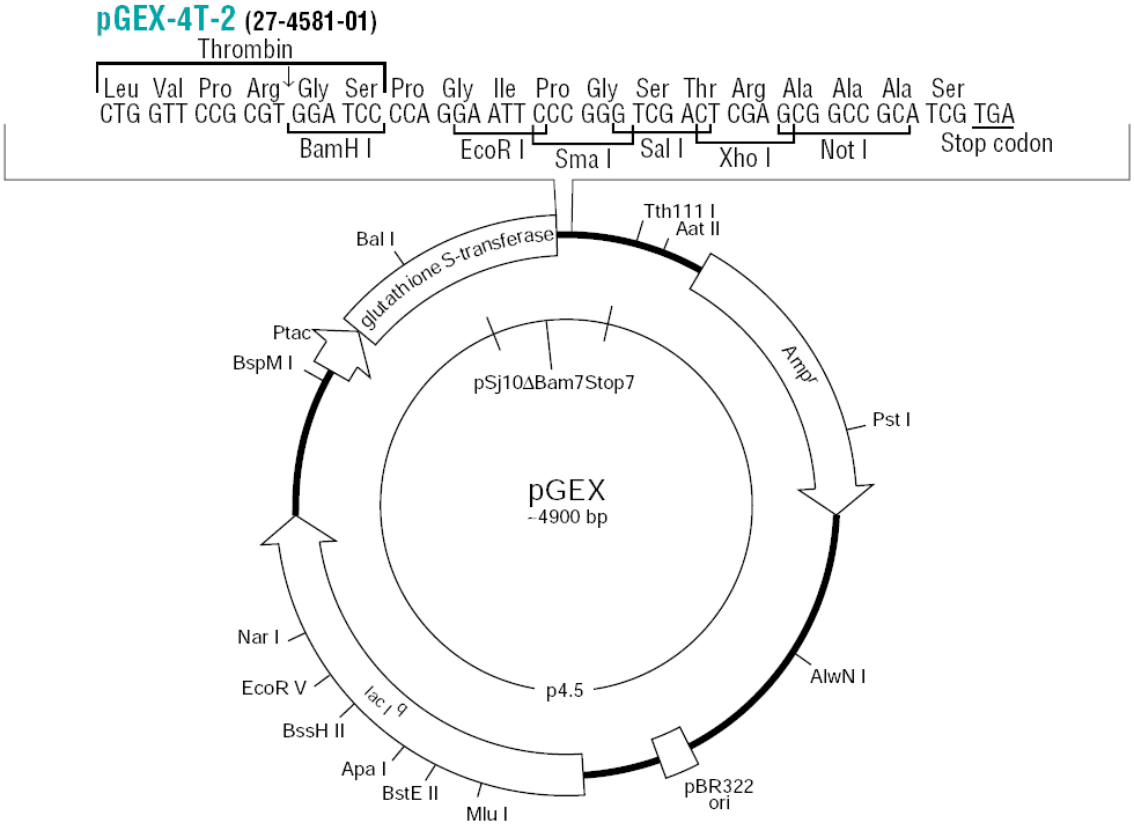

2.1.7.1.3. PYES2

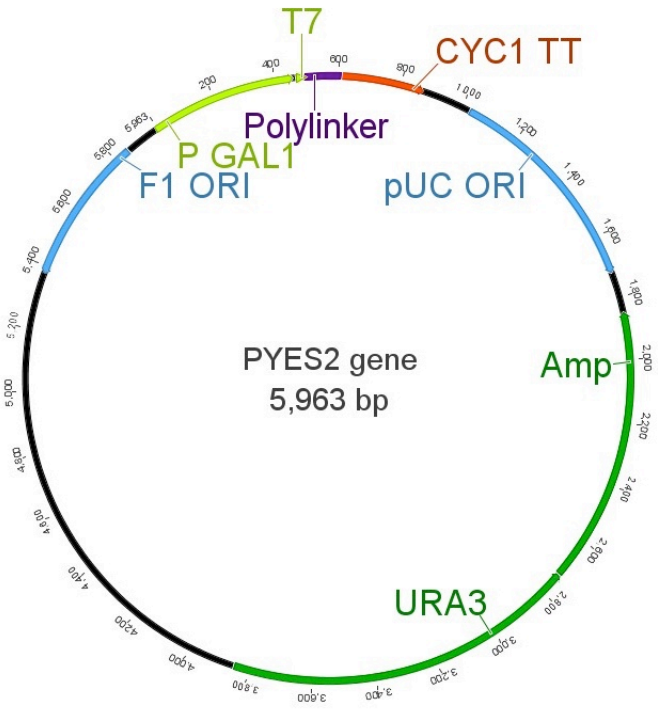

2.1.7.1.4. pBI121

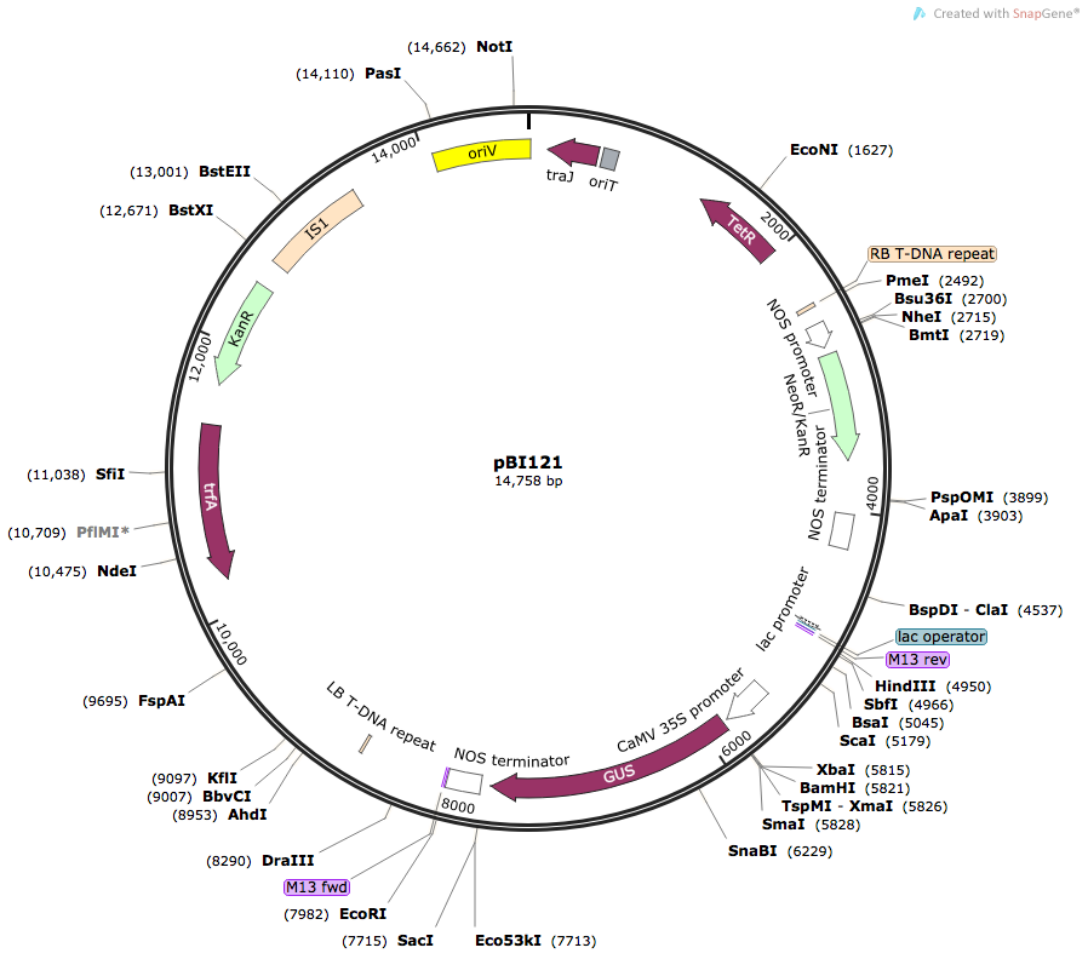

2.1.7.1.5. pGWR8

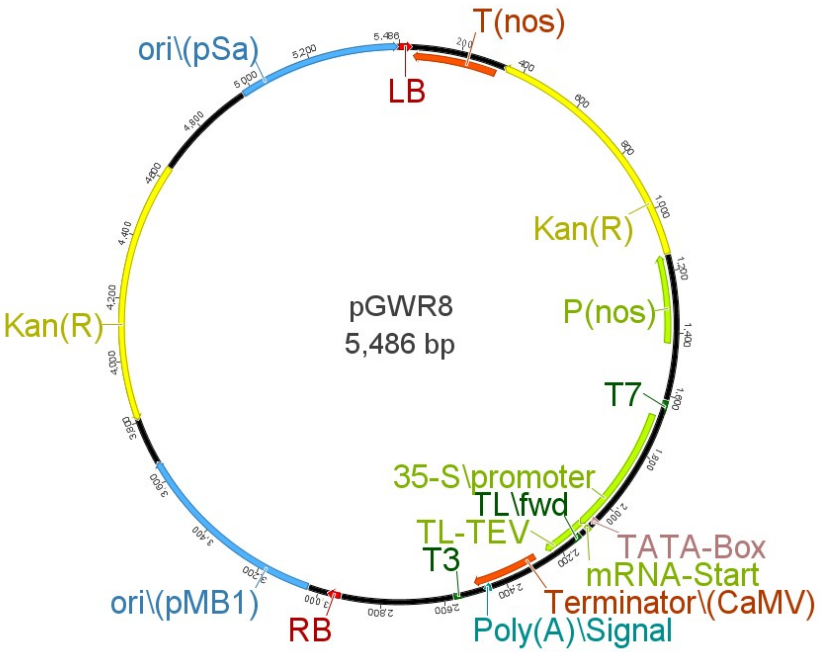

2.1.8. Primers

All primers were ordered from Eurofins MWG Synthesis GmbH (Ebersberg, Germany).

Table 8. Primers used for *FvXTH6* cloning

Primer Name	Vector	Description	Sequence (5'→ 3')
FP_FvXTH6	-		CCAGGATCCATGTATCCCTCTTTGAGG
RP_FvXTH6	-		ATAGTCGACGAGGCCGGCGACAC
FP_FvXTH6_PYES2	PYES2		CGGAATTCAACACAATGTCTCCCTCTTTG
RP_FvXTH6HIS_PYES2	PYES2		TAAAGCGGCCGCTTAATGATGATGATGATGATGGAGGCCGGCGACAC
FP_FvXTH6_pBI121	pBI121	BamHI	TAGAGGATCCATGTATCCCTCTTTG
RP_FvXTH6_pBI121	pBI121	SacI	ATTCGAGCTCTTAGAGGCCGGCGAC
FP_FvXTH6_pGWR8	pGWR8	NcoI	CATGACATGTATCCCTCTTTGAGGAG
RP_FvXTH6_pGWR8	pGWR8	NotI	TATAGCGGCCGCTGAGGCCGGCGAC
FP_FvXTH6_qPCR	-		GAGGCAGGGCCATCCAGCTC
RP_FvXTH6_qPCR	-		TCCGGCAGAGTCACCGGGAA
IS-RT_F	-		ACCGTTGATTCGCACAATTGGTCATCG
IS-RT_R	-		TACTGCGGGTCGGCAATCGGACG

Table 9. Primers used for *FvXTH9* cloning

Primer Name	Vector	Description	Sequence (5'→ 3')
FP_FvXTH9	-		ATGGCTTCTGCCTCTTTGTTTTTGAGTGTC
RP_FvXTH9	-		CTAGTGACGGTGGTGCACACACTCGAC
FP_FvXTH9_PYES2	PYES2		CGGGGTACCAACACAATGTCTTCTGCCTCTTTG
RP_FvXTH9_PYES2	PYES2		TAAAGCGGCCGCTTAGTGACGGTGGTGCAC
RP_FvXTH9HIS_PYES2	PYES2		TAAAGCGGCCGCTTAATGATGATGATGATGATGGTGACGGTGGTGC
FP_FvXTH9_pBI121	pBI121	BamHI	TAGAGGATCCATGGCTTCTGCCTC
RP_FvXTH9_pBI121	pBI121	SacI	ATTCGAGCTCCTAGTGACGGTGGTGC
FP_FvXTH9_pGWR8	pGWR8	EcoRV	ACCGGATATCATGGCTTCTGCCTCTTTG
RP_FvXTH9_pGWR8	pGWR8	NotI	TATAGCGGCCGCTGTGACGGTGGTG
FP_FvXTH9_qPCR	-		CGCTGACGACTGGGCCACAC
RP_FvXTH9_qPCR	-		GCCGGGCACTCACAGGCATT
IS-RT_F	-		ACCGTTGATTCGCACAATTGGTCATCG
IS-RT_R	-		TACTGCGGGTCGGCAATCGGACG

Table 10. Primers used for *FvGDSL* esterase/lipase cloning

Primer Name	Vector	Description	Sequence (5'→ 3')
FP_GDSL 27964	-		ATGCTGGGAATGGAGATTTGGAAG
RP_GDSL 27964	-		GCTCCTATGACAAGCCTGAGTAATG G
FP_GDSL_ PYES2	PYES2		CGGGGTACCAACACAATGTCTGGA ATGGAG
RP_GDSL_ PYES2_HIS	PYES2		TAAGCGGCCGCTTAATGATGATGAT GATGATGGCTCCTATGAC
FP_GDSL_ qPCR	-		ACCGGAGGATCAACAATTAGAAGG CCGA
RP_GDSL_ qPCR	-		ATTTGGAAGTCTGCTTCTCTCATAG GGA
IS-RT_F	-		ACCGTTGATTCGCACAATTGGTCAT CG
IS-RT_R	-		TACTGCGGGTCGGCAATCGGACG

2.1.9. Media

2.1.9.1. <u>LB medium/plates</u>

10 g/l tryptone

5 g/l yeast extract

10 g/l NaCl

15 g/l agar 1.5% (for plates)

Adjust pH to 7.0 with NaOH

2.1.9.2. <u>LB plates / Ampicillin /IPTG/X-gal</u>

500 mL LB medium containing 1.5% agar

0.5 mL ampicillin (100 mg/ml)

0.4 mL X-Gal (50 mg/mL stock in N-N'-dimethyl formamide)

2.5 mL IPTG (0.1 mM stock in water)

2.1.9.3. YPD (Yeast extract Peptone Dextrose) medium

1% yeast extract

2% peptone

2% dextrose ($_D$-glucose)

2.1.9.4. SOC medium

20 g/l tryptone

5 g/l yeast extract

0.584 g/l NaCl

0.186 g/l KCl

2.03 g/l $MgCl_2$ x $6H_2O$

1.204 g/l $MgSO_4$

3.603 g/l $_D$-glucose

Adjust pH to 7 with NaOH

2.1.9.5. SC-U medium/plates (synthetic minimal defined medium for yeast)

0.67% yeast nitrogen base (without amino acids)

2% carbon source ($_D$-glucose or $_D$-galactose)

amino acids: 0.01% (arginine, cysteine, leucine, lysine, threonine, tryptophan), 0.005% (aspartic acid, histidine, isoleucine, methionine, phenylalanine, proline, serine, tyrosine, valine)

0.01% (adenine, uracil)

2% agar (for plates) up to 900 ml distilled water: add 100 ml of filter-sterilized 20% $_D$-glucose or $_D$-galactose after autoclaving

20% $_D$-glucose or $_D$-galactose: 100 g of $_D$-glucose or $_D$-galactose in 400 ml distilled water. Add distilled water to 500 ml and sterilize through a 0.22 µm filter after dissolving

2.1.9.6. MMA medium

4.3 g/l MS-salt (Sigma)

1.952 g/l MES (10 mM)

20 g/l sucrose

Adjust pH to 5.6 with KOH

2.1.9.7. AB Medium

1 g/l NH_4Cl

0.3 g/l $MgSO_4 \times 7H_2O$

0.15 g/l KCl

0.01 g/l $CaCl_2 \times 2H_2O$

0.0025 g/l $FeSO_4 \times 7H_2O$

0.27 g/l KH_2PO_4

10 g/l $_D$-glucose

3.90 g/l MES

Adjust with KOH to pH 5.6; autoclave and add acetosyringone to 100 µM

2.1.10. Buffer and solution

2.1.10.1. DNA Extraction buffer

2.0% CTAB (w/v)

1.4 M NaCl 20 mM EDTA (pH 8.0)

100 mM Tris-HCl (pH 8.0)

Add 0.2% β-mercaptoethanol to the buffer before use and then heat to 60°C for pre-warmed buffer

2.1.10.2. TE buffer

1 mM EDTA (pH 8.0)

10 mM Tris-HCl (pH 8.0)

2.1.10.3. RNA extraction buffer

3% CTAB (w/v)

3% PVP, K30 (Roth)

25 mM EDTA (pH 8.0)

2 M NaCl

100 mM Tris-HCl (pH 8.0)

Add 40 µl/ml β-mercaptoethanol to the buffer before use and then heat to 65°C for pre-warmed buffer

2.1.10.4. GST wash/bind buffer (pH 7.3)

4.3 mM Na_2HPO_4

1.47 mM KH_2PO_4

0.137 M NaCl

2.7 mM KCl

GST elution buffer (prepare fresh buffer)

10 mM L-glutathione reduced (Roth)

50 mM Tris-HCl (pH 8.0)

2.1.10.5. SDS-PAGE

12% Tris-glycine SDS-PAGE gel (Anamed, Groß-Bieberau, Germany)

4× Roti® Protein Loading buffer (Roth)

2.1.10.6. 1× Electrode (Running) buffer

25 mM Tris

192 mM glycine

0.1% SDS

2.1.10.7. Staining solution

0.33 g Coomassie Brilliant Blue G250

120 ml methanol

24 ml acetic acid

120 ml H_2O

2.1.10.8. Destaining solution

20% ethanol

10% acetic acid

2.1.10.9. 10× DNA loading dye

0.21% Orange G

0.1 M EDTA (pH 8.0)

50% glycerol

2.1.10.10. 50× TAE buffer

242 g/l Tris

57.1 ml/l acetic acid

100 ml/l 0.5 M EDTA (pH 8.0)

2.1.10.11. Glycerol for cell stocks

65% glycerol (v/v)

0.1 M $MgSO_4$

25 mM Tris pH 8.0 with HCl

2.1.10.12. Chemically competent cells

Trituration buffer (prepared fresh and filter-sterilized buffer):

100 mM $CaCl_2$ x $2H_2O$

70 mM $MgCl_2$ x $6H_2O$

40 mM NaOAc

Adjust pH to 5.5 with HCl

2.1.11. Commercial kits

Table 11. List of commercial kits

Kit name	Manufacture
NucleoSpin ® Extract II	Macherey-Negel, Düren, Germany
Wizard® Plus SV Minipreps DNA Purification System	Promega
S. c. EasyComp. Transformation Kit	Invitrogen
Fast SYBR® Green Master Mix	Applied Biosystems, Foster City, CA, USA
pGEM®-T Easy vector Kit	Promega

2.1.12. Equipment

General laboratory equipment is alphabetically listed in Table 12.

Table 12. General laboratory equipment

Unit	Device
Agarose gel electrophoresis	MIDI (Carl Roth GmbH & Co. KG, Karsruhe, Germany) MAXI (NeoLab, Heidelberg, Germany)

Autoclave	Systec V 95 (Systec, Wettenberg, Germany)
Balances	SCALTEC SPB61 (SCALTEC Instruments GmbH, Heiligenstadt, Germany) TP 214 (Denver Instrument, Bohemia, US-NY) Scout Pro SPU4001 (Ophaus, Pine Brook, US-NJ) Sartorius X634 Sartorius AG, Göttingen, Germany
Bio-imaging system G:BoX for gel visualization	Syngene, Cambridge, UK
Blotting chamber	Semy Dry Blotter (Biostep GmbH, Jahnsdorf, Germany)
Centrifuges	Sigma K415, Sigma 1-14, Sigma 2K15 (Sigma, Osterode am Harz, Germany) Eppendorf 5415R, MiniSpin (Eppendorf AG, Hamburg, Germany)
Clean bench	Hera Safe (Heraeus Holding GmbH, Hanau, Germany)
Elisa reader	Clario star, BMG Labtech, Oertenberg, Germany
Freeze dryer	Savant ModulyoD (Thermo Fisher Scientific Inc., Waltham, US-MA)
Incubator	Forma Steri-Cycle CO2 (Thermo Fisher Scientific Inc., Waltham, US-MA)
NanoDrop ND-1000	peQLab Biotechnologie GmbH, Erlangen, Germany
pH-Meter	CG 820 (Schott Geräte GmbH, Mainz, Germany)
Spectrophotometer	Nicolet evolution 100 (Thermo Fisher

	Scientific Inc., Waltham, US-MA)
StepOnePlus™RT-PCR System	Applied Biosystems®, Foster City, US-CA
Scintillation counter	Tri-Carb2800TR (PerkinElmer Life and Analytical Sciences, Shelton, US-CT)
SDS-PAGE electrophoresis	Biorad
Shaking incubator	GFL, Burgwedel, Germany
Texture Analyzer	TA-XT2i (Stable Micro Systems, Godalming, Surrey, UK)
Thermocycler (PCR)	Primus 96 advanced (PeqlabBiotechnologie, Erlangen, Germany) SensoQuestlabcycler (SensoQuest GmbH, Göttingen, Germany)
Thermomixer	Eppendorf, Hamburg, Germany
Ultra Turrax	T18 basic (IKA® Works Inc. Wilmington, NC, USA)
Ultrasonic bath	RK103H (Bandelin Electronic, Berlin, Germany
Ultrasonic Homogenizer	BandelinSonopuls UW2200 (Bandelin Electronic)
Vortexer	VWR, Darmstadt, Germany
Water bath	Julabo, Seelbach, Germany

2.1.13. Software

The following software was used:

1. GENEIOUS Pro 5.5.6 (http://www.geneious.com/)
2. R 3.2.2 (R Core Team, 2015, http://www.r-project.org/)
3. R Studio (http://www.rstudio.com/)
4. StepOneTM Software 2.1 (Applied Biosystems, Foster City,US-CA)
5. BioEdit - BLAST (http://www.ncbi.nlm.nih.gov/BLAST/)
6. Vector NTI (Invitrogen, Carlsbad, USA)

7. GeneDoc - MegAlign Version 4.0 (DNA STAR)
8. SigmaPlot 12.0 (Systat Software)
9. Mendeley (https://www.mendeley.com/)
10. FluoView

2.2. Apparatus

2.2.1. FPLC (Fast protein liquid chromatography)

ÄKTA purifier System (GE Healthcare, Biosciences AB, Uppsala, Sweden) with the following equipment:

Pump	P-900 (with four pump heads in two pump modules)
Monitor	UPC-900 (including the combined measurement of UV absorption, pH and conductivity)
Monitor	UV-900 (with variable wavelength in the range 190-700 nm)
Valve	INV-907 (with rotary 7-port valve)
Mixer	M-925 (single chamber mixer)
Fraction collector	Frac-950
Software	UNICORN (version 5.20)

2.2.1.1. Program for purification of His-tag protein

Column 5 ml HisTrap FF Column (GE Healthcare)	
Solution	B1: Elution buffer B2: MQ water A1: Wash/bind buffer A2: 20% ethanol
Column equilibration	
Flow rate	2.00 ml /min
Running solution	5 column volumes of MQ water B2 5 column volumes of binding buffer A1
Monitor at 280 nm	Baseline should be stable after washing.
Column loading	
Flow rate	0.5 ml /min

Loading protein	10 ml protein extracts
Running solution	Along with MQ water B2
Column washing	
Flow rate	0.5 ml /min
Running solution	5-10 column volumes of binding buffer A1 until OD280 is stable (to reach the baseline).
Protein elution	
Flow rate	0.5 ml /min
Running solution	10 column volumes of elution buffer B1
Collected fractions	2 ml each fraction
Column washing	
Flow rate	5.00 ml /min
Gradient	50% of elution buffer B1 for 10 ml
	100% of elution buffer B1 for 10 ml
Running solution	5 column volumes of MQ water B2
	5 column volumes of 20% ethanol A2
Storage of HisTrap column	at 4 °C after washing with 20% ethanol

2.2.2. Liquid chromatography ultraviolet electro-spray ionization mass spectrometry (LC-UV-ESI-MS^n)

HPLC	Agilent 1100 Series (Agilent Technologies Inc., Santa Clara, California, USA)
Pump	Agilent 1100 Quaternary Pump
Autosampler	Agilent Autosampler
Injection volume	5 µL
Separation column	Luna 3 µm C18 (2) 100 Å 150 x 2.0 mm (Phenomenex Aschaffenburg, Germany) (Part Number: 00F-4251-B0)
Precolumn	Security Guard Cartridges C18 4 x 2 mm (Penomenex)

Column temperature	25 °C
Solvents	A: Water plus 0.1% formic acid
	B: Methanol plus 0.1% formic acid
Flow Rate	0.2 ml/min
Gradient	0-30 min: 0-50% B
	30-35 min: 50-100% B
	35-50 min: 100% B
	50-55 min: 100-0% B
	55-65 min: 0% B
UV-Detector	Agilent 1100 variable wavelength detector
Wavelength	340nm

2.2.3. Mass Spectrometer Bruker Daltonics esquire 3000^{plus} (Bruker, Bremen, Germany)

Spray gas	Nitrogen (30.0 psi)
Dry gas	Nitrogen (330 °C, 9 l/min)
Scan range	*m/z* 100 to 800
Polarity	positive/negative
ICC target	20,000 or 200 ms
Target mass (SPS)	*m/z* 400
Capillary voltage	- 4000 V
End pate offset	- 500 V
MS/MS	Auto-tandem MS
Collision gas	Helium 5.0 (3.56 $\times 10^{-6}$ mbar)
Collision voltage	1.0 V
Data analysis	Bruker Daltonics Esquire 5.1 with Data Analysis 3.1 and Quant Analysis 1.5 package (Bruker Daltonics, Bremen, Germany)

Agilent 6300 series ion trap LC/MS system software (version 6.2) with Data Analysis and Quant Analysis

2.3. Method

2.3.1. Molecular biology method

2.3.1.1. mRNA isolation

Total RNA was prepared as described by Liao *et al.* (2004). Frozen plant material (2 g) was ground to a fine powder in liquid nitrogen. The powder was added to 20 ml of pre-warmed RNA extraction buffer (3% CTAB, 3% PVP (MW 40.000), 25 mM EDTA, 2 M NaCl, 100 mM Tris-HCl (pH 8.0), 40 µl/ml β-mercaptoethanol) and incubated at 65 °C for 10 min. The mixture was inverted three times during the incubation. Afterwards, an equal volume of chloroform/isoamyl alcohol (CI; 24:1, v/v) was added and inverted gently for 10 min. Then centrifugation at 16,700 *g* for 10 min at 10°C was performed, and the supernatant was transferred into a new falcon tube. Chloroform/isoamyl alcohol extraction was repeated twice. The collected supernatants from two extractions were mixed with 1/3 volume of 8 M lithium chloride and stored at 4 °C overnight. The total RNA was precipitated by centrifugation at 16,700 *g* for 30 min at 4 °C. The pellet was mixed with 500 µl of 0.5% SDS and an equal volume of CI (24:1) then centrifuged at 16,700 *g* for 10 min at 4 °C. The supernatant containing RNA was transferred to a new Eppendorf tube containing twice volume of 100% ethanol and then stored at -20°C for 2 h. The total RNA was precipitated by centrifugation at 20,300 *g* for 30 min at 4 °C. The total RNA pellet was successively washed with 70% ethanol and 100% ethanol followed by centrifugation at 21,200 *g* for 5 min at 4 °C. The total RNA pellet was air-dried for 5 min at room temperature and then dissolved in 50 µl of DEPC-treated water. The concentration of total RNA was determined using the NanoDrop. Five µg of total RNA was checked for quality by 1% agarose gel electrophoresis. The total RNA was stored at -80 °C.

2.3.1.2. Removal of genomic DNA from total RNA

The reaction mixture for purifying total RNA was 30-50 µg of total RNA, 10 µl of 10x reaction buffer with $MgCl_2$ (Thermo Scientific), 5 µl of DNase I (1 U/µl) (Thermo Scientific) and up to 50 µl of DEPC-treated water. The mixture was incubated at 37 °C for 1 h, followed by purification using 100 µl of DEPC-treated water and an equal volume of phenol/chloroform (1:1). Subsequently, the mixture was vortexed and then centrifuged at 16,700 *g* at 4 °C for 5 min. The purification was repeated twice. The supernatant was transferred into a new Eppendorf tube, and then added with 1/10 volume of 3 M sodium acetate (pH 5.2) and 2.5 volumes of ethanol. The mixture was stored at -20 °C overnight. After ethanol precipitation, the mixture was centrifuged at 20,300 *g* for 20 min at 4 °C. The pellet was washed with 70% ethanol and 100% ethanol and then centrifuged at 20,300 *g* for 5 min at 4 °C. The RNA pellet was air-dried for 5 min and re-suspended in 20 µl of DEPC-treated water. The concentration and quality of total RNA were determined using a NanoDrop.

2.3.1.3. cDNA synthesis

The first-strand cDNA was synthesized from 1 µg of DNase I-treated total RNA using the Moloney Murine Leukimia Virus Reverse Transcriptase (M-MLV RT) (Promega), as follows: 1 µg of total RNA, 1 µl of Random Hexamers (50 µM), 1 µl of dNTPs (10 mM) and up to 12 µl DEPC-treated water. Twelve microliter of the reaction mixture was incubated at 65 °C for 5 min and then cooled on ice for 2 min. Then, the following reagents were added 4 µl of M-MLV 5×reaction buffer (250 mM Tris-HCl (pH 8.3), 375 mM KCl, 15 mM $MgCl_2$, 50 mM DTT) (Promega), 2 µl 0.1 M DTT, 1 µl of recombinant RNasin® Ribonuclease Inhibitor (40 U/µl) (Promega). Nineteen microliter of the reaction mixture was incubated at 37 °C for 2 min. Afterward, 1 µl of M-MLV RT (200 U/µl) was added into the mixture and incubated in three stages: 25 °C for 10 min, 50 °C for 60 min, and 70 °C for 15 min. Finally, the first-strand cDNA was stored in -20 °C or used directly as a template for PCR reaction or a quantitative real-time PCR analysis.

2.3.1.4. Polymerase Chain Reaction (PCR)

The reaction mixture for PCR consisted of 1 µl of template DNA or cDNA, 1 µl of forward primer (10 µM), 1 µl of reverse primer (10 µM), 1 µl of dNTPs (2.5 µM), 0.5 µl of Phusion® DNA polymerase (2 U/µl) (Thermo Scientific), and 6 µl of 5x Phusion® GC buffer (New England Biolabs) with the total volume of 30 µl. PCR was performed with the following program in 35 cycles (Table 13).

Table 13. PCR program

Step		Temperature (°C)	Time
Initial denaturation		95	5 min
Denaturation	35x	95	45 sec
Annealing		55	30 sec
Elongation		72	1 min
Termination		72	10 min

2.3.1.5. Real Time Polymerase Chain Reaction (RT-PCR)

A SYBR Green qPCR kit with ROX dye passive reference was used in RT-PCR to monitor dscDNA synthesis. RT-PCR was performed in a StepOnePlus™ real-time PCR system (Applied Biosystems). RT-PCR data for FvXTHs were normalize against the expression levels of an interspacer 26S-18S RNA housekeeping gene. Gene specific primers and interspacer (IS) primers were used to amplify the target gene and the IS gene, respectively. RT-PCR mixture was 10 µl of 2x Power SYBR Green Mix, 0.8 µl of forward primer (10 µM), 0.8 µl of reverse primer (10 µM), 2 µl of cDNA, and 6.8 µl of ultrapure H_2O. The dilution of cDNA for target gene and IS gene were 20x and 8000x, respectively. Three technical and 2-3 biological replicates of each sample were performed under the following standard thermal conditions (Table 14).

Table 14. RT-PCR program

Step		Temperature (°C)	Time
Holding stage		95	10 min
Cycling stage		95	15 sec
	40x	60	15 sec
		72	15 sec
Melt curve stage		95	15 sec
		60	1 min
		95	15 sec

The threshold cycle (C_T) values (the number of cycles required to reach a defined fluorescence intensity threshold) of target gene and IS genes were calculated using StepOne™ Software V.2.1. For data analysis of all samples, relative gene expression was quantified using the $2^{-\Delta\Delta CT}$ method (Livak and Schmittgen, 2001) to indicate fold changes of each sample related to the selected reference sample. In addition, the IS gene was used as an internal control for normalized expression values. The following formulas were used for calculating the $2^{-\Delta\Delta CT}$.

$\Delta C_T = C_T$ (target gene) – C_T (internal spacer gene) (1)

$\Delta\Delta C_T = \Delta C_T$ (target) – ΔC_T (reference) (2)

Relative gene expression = $2^{-\Delta\Delta CT}$ (3)

The numerical values obtained from $2^{-\Delta\Delta CT}$ were transformed into graphics by using either the R software or SigmaPlot software.

2.3.1.6. Colony PCR

Colony PCR was performed to proof the successful recombinant plasmid transformation in bacteria or yeast cells by amplification of the target gene. Reaction mixture for colony PCR was 1 µl of template DNA or cDNA, 1 µl of forward primer (10 µM), 1 µl of reverse primer (10 µM), 1 µl of dNTPs (2.5 µM) (Thermo scientific), 0.5 µl of *Taq* DNA polymerase (5 U/µl) (New England Biolabs), 3 µl of 10x ThermoPol reaction buffer (New England Biolabs) in a total of 30 µl reaction. Colony PCR was performed with the following program in 35 cycles (Table 15).

Table 15. Colony PCR program

Step		Temperature (°C)	Time
Initial denaturation		95	5 min
Denaturation	35x	95	45 sec
Annealing		55	30 sec
Elongation		72	1 min
Termination		72	10 min

2.3.1.7. Agarose gel electrophoresis

For nucleotide separation, agarose 1% w/v and 1×TAE buffer (40 mM Tris (pH 7.6), 20 mM acetic acid, 1 mM EDTA) were dissolved using microwave. Eighty milliliter of liquid agarose was added 4 µl of Roti®-Load DNA stain (10 mg/ml) (Carl Roth) and poured into an electrophoresis chamber with comb. After the gel was dry, 20 µl of the sample or 6 µl of the DNA marker was mixed with 2 µl of 10× DNA loading dye and loaded into each well. The electrophoresis was run in 1× TAE buffer for 20 min, 125 Volt. The DNA or RNA fragments were visualized using a UV box (Bioimaging system G:Box).

2.3.1.8. PCR clean up and gel extraction

PCR clean up and gel extraction was performed using NucleoSpin® Gel and PCR Clean-up kit from Macherey-Nagel according to the manufacturer's protocol.

2.3.1.9. Plasmid isolation

Plasmid isolation from *E. coli* cell was done using Wizard® Plus SV Minipreps DNA Purification System from Promega according to the manufacturer's method.

2.3.1.10. Restriction endonuclease reaction

One microgram of PCR product or plasmid DNA was added to 5-10 units of restriction enzyme for digestion. Twenty µl reaction volume contained 1-5 µg of DNA fragment, 2 µl of 10x reaction buffer, and 1 µl of restriction enzyme (20 U/µl)

and was incubated at 37 °C overnight. Agarose gel electrophoresis was performed to confirm digestion.

2.3.1.11. Ligation reaction

Six microliter DNA fragments (50 ng/µl) and 2 µl vector DNA (20 ng/µl) which was cut using the same restriction enzymes were mixed with 1 µl of T4 DNA ligase (3 Weiss units/µl) (Promega) and 1 µl of 10x ligation buffer (Promega) in a total volume of 10 µl. The ligation reaction was incubated at 4 °C for overnight.

For pGEM-T Easy vector (Promega) cloning, PCR products were added with A-tailing at the 5'-ends by treatment with *Taq* DNA polymerase and dATP (Thermo scientific). Afterwards, 3 µl of PCR fragments with A-tailing (50 ng/µl) and 1 µl of linear pGEM-T Easy vector containing 3´-terminal deoxythymidine (50 ng/µl) were mixed with 1 µl of T4 DNA ligase (3 Weiss units/µl) (Promega) and 5 µl of 2x Rapid Ligation Buffer (Promega) in a total volume of 10 µl. The ligation reaction was incubated at 4 °C, overnight.

2.3.1.12. DNA sequencing

Plasmid DNA sample containing target gene was sequenced by Eurofins MWG Operon, Ebersberg, Germany. Plasmid DNA sample for sequencing was 15 µl of 50-100 ng/µl purified DNA. Universal primer for sequencing was provided by the manufacturer. Premix sample was 15 µl of purified DNA (50-100 ng/µl) and 2 µl of specific primer (10 µM).

2.3.2. Biochemical method

2.3.2.1. Protein production from *S. cerevisiae*

Fresh or frozen cell pellets were re-suspended in 500 µl of breaking buffer (50 mM sodium phosphate (pH 7.4), 1 mM EDTA, 5% glycerol, 1 mM PMSF) and then centrifuged at 1,500 *g* for 5 min at 4 °C to pellet cells. The cells were re-suspended in a volume of breaking buffer to obtain an OD_{600} of 50–100. An equal volume of acid-washed glass beads was added and then vortexed for 30 sec followed by 30 sec on ice. The procedure was repeated ten times. The mixture

was centrifuged for 10 min at maximum speed. The supernatant was collected in a microcentrifuge tube.

2.3.2.2. Protein concentration

Protein concentration was measured using the Bradford (1976) method. Five microliter of protein solution was added to 95 µl of H_2O (1:20 dilution) and 1 ml of Bradford reagent (8.5% (v/v) phosphoric acid, 5% (v/v) ethanol and 0.01% (w/) Coomassie). The absorbance was measured at 595 nm. Serum albumin (0.2 µg, 0.4 µg, 0.8 µg, 10 µg, 15 µg and 20 µg) was used as standard.

2.3.2.3. Sodium Dodecyl Sulphate Polyacrylamide Gel Electrophoresis (SDS-PAGE)

The 12% Tris-glycine SDS-PAGE gel was set in a gel tank and 1x TAE running buffer was added. A mixture of 10 µg protein sample with 8 µl of 4x protein loading dye (Carl Roth) in a total volume of 32 µl was heated at 95 °C for 5 min and then cooled in ice for 2 min. The protein mixture or a protein marker (PageRuler Plus Prestained Protein Ladder, Thermo Scientific) was loaded carefully into each well and then electrophoresis was performed at 160 Volt for 1.5 h. The proteins were stained with Commasie Blue staining solution (0.33 g Coomassie Brilliant Blue G250, 120 ml methanol, 24 ml acetic acid, and 120 ml H_2O) with shaking at 20 rpm overnight at room temperature. The staining solution was discarded, and the gel was de-stained twice with a de-staining solution (20% ethanol, 10% acetic acid) at room temperature with shaking at 20 rpm for 3 h.

2.3.2.4. Western Blot

SDS gel and filter papers was incubated in semidry blotting buffer (25 mM TRIS base, 200 mM glycin, 20% (v/v) methanol) for 5-10 min. The PVDF membrane (Roth) was activated in methanol for 1 min and then equilibrated in semidry blotting buffer for 5 min. From the bottom part (anode) of semidry blotter was placed in order: 4x filter papers, membrane, polyacrylamide gel, and then 4x filter papers. A current of 10 Volt (0.8 mA/cm^2 gel) was applied for 60 min. The membrane was removed from the blotter and incubated in blocking buffer (5% BSA or milk powder in washing buffer) on a shaker for 60 min at room

temperature. The membrane was washed three times for 5 min in washing buffer (20 mM TRIS base, 140 mM NaCl, 0.1% (v/v) Tween 20). The membrane was incubated in a 50 ml falcon tube with 3 ml blocking buffer and 1 µl of Anti-His-AP (Abcam) monoclonal antibody with rotation for overnight at 4 °C. The membrane was washed three times for 10 min in washing buffer and then two times for 5 min in detection buffer (100 mM Tris (pH 9.5), 100 mM NaCl, 5 mM $MgCl_2$). The membrane was incubated in 20 ml of detection buffer containing 50 µl NBT substrate (5 mg NBT in 100 µl 70% DMF) and 25 µl BCIP (5 mg BCIP Na-salt in 100 µl H_2O) for 15 min to 3 h in the dark with shaking until bands appear. Finally, the membrane was washed with water.

2.3.2.5. Affinity chromatography

The purification of His tag recombinant protein was done using HisTrap FF column 5 ml (GE Healthcare) in a FPLC system (ÄKTA FPLC, GE Healthcare). HisTrap FF column was equilibrated in 1x His wash/bind buffer (50 mM NaPi (pH 7.4), 300 mM NaCl, 30 mM imidazol). Sample was equilibrated using 1x His wash/bind buffer at 0.5 ml/min for 30 min. Elution of target protein was done using step gradient elution of 1x His elution buffer (50 mM NaPi (pH 7.4), 300 mM NaCl, 250 mM imidazol) for 20 min and then continued with 1x His elution buffer containing 500 mM imidazole for 20 min. Two milliliter fractions were collected for enzyme assay.

2.3.2.6. Protein purification from *F.* × *ananassa* fruits

Fruit of *F.* × *ananassa* (50 g) were frozen in liquid N_2 and ground in a precooled rotor-stator homogenizer. The frozen powder was mixed with 10 g prewashed PVP and stirred for 30 min with a mixture of 100 ml of Tris HCl buffer (0.05 M, pH 8.5). The homogenate was squeezed through four layers of muslin, followed by centrifugation of the filtrate (20,000 *g*, 20 min). Two percent of protamine sulphate was added dropwise under stirring to the filtrate until a final concentration of 2 mg protamine sulphate per 100 mg protein was reached. After stirring for 15 min, the solution was centrifuged. The supernatant was fractionated with solid ammonium sulphate ($(NH_4)_2SO_4$) at concentration of 0-40% and then 40-60%. Pellet was dissolved in a minimal volume (5 ml) of Tris HCl buffer (0.05

M, pH 7.5), clarified by centrifugation (20,000 g, 10 min) and desalted by dialysis (Tris HCl buffer (0.05 M, pH 7.5))

2.3.3. Cultivation Method

2.3.3.1. *E. coli* strain NEβ 10

2.3.3.1.1. Competence cell preparation

A single colony of *E. coli* strain was inoculated in 10 ml of LB (Luria-Bertani) medium (10 g tryptone, 10 g NaCl, 5 g yeast extract, pH 7.0 ad 1L H_2O) containing appropriate antibiotics at 37°C, with shaking at 150 rpm overnight. Two ml of overnight culture was diluted in 200 ml LB medium containing 20 mM $MgSO_4$, and incubated additionally at 37 °C, with shaking at 150 rpm for 2-3 h until the OD_{600} reached 0.4 - 0.6. Afterward, the bacterial culture was submerged in an ice-water bath for 30 min. Cells were harvested by centrifugation at 4,500 *g* for 5 min at 4 °C. The cell pellet was re-suspended in 0.4 volume of ice-cold trituration buffer TFB1 (30 mM potassium acetate, 10 mM $CaCl_2$, 50 mM $MnCl_2$, 100 mM RbCl, 15% glycerol, pH 5.8) and incubated on ice for 5 min. Following centrifugation at 4,500 *g* for 5 min at 4 °C, the pellet was re-suspended in 0.04 ml of ice-cold trituration buffer TFB2 (10 mM MOPS or PIPES, 75 mM $CaCl_2$, 10 mM RbCl, 15% glycerol, pH 6.5). Finally, 200 µl aliquots of competent cells were frozen in liquid nitrogen and stored at -80 °C or used directly for transformation.

2.3.3.1.2. Transformation

One tube of 50 µl of competent cells was thawed at room temperature, 5 µl was added to 1 µg vector DNA and mixed by flicking the tube. The transformation reaction was incubated for 30 min on ice. Heat shock was performed by incubating the tube for 45 sec to 1 min in a 42°C water bath and put immediately on ice for 2 minutes. Nine hundred fifty microliter of SOC medium (2% trypton, 0.5% yeast extract, 10 mM NaCl, 2.5 mM KCl, 10 mM $MgCl_2$, 10 mM $MgSO_4$, 20 mM $_D$-glucose) was added and then incubated at 37 °C in a shaking incubator (150 rpm) for 1 hour. One hundred microliter of the transformation reaction was plated on appropriate selection plates using a sterile spreader and then incubated for 15 to 18 h at 37 °C.

2.3.3.1.3. Culture for plasmid isolation and colony PCR

One colony of *E. coli* from LB plate (LB medium containing 1.5% agar) with appropriate antibiotic (100 µg/ml) was inoculated in 5 ml LB medium with similar antibiotic and then incubated at 37 °C and 150 rpm overnight until OD_{600} reached 1.5 to 2.0. For stock culture, 700 µl of this culture was added to the same volume of sterile glycerol for cryo stock (65% (v/v) glycerin, 1.2% (w/v) $MgSO_4$, 0.3% (w/v) Tris-HCl pH 8) and then stored at -80 °C.

2.3.3.2. *Saccharomyces cerevisiae* strain INVSc1

2.3.3.2.1. Competence cell preparation

The competent cell for yeast was prepared using S. c. EasyComp Transformation Kit (Invitrogen). A single colony of *S. cerevisiae* strain INVSc1 was inoculated in 10 ml of YPD (Yeast Extract Peptone Dextrose) medium (1% yeast extract, 2% peptone, 2% D-glucose) at 28 – 30 °C in a shaking incubator (150 rpm) overnight. The OD_{600} of the overnight culture was determined and then diluted to an OD_{600} of 0.2 to 0.4 in a total volume of 10 ml of YPD. Then, the cells were grown at 28 – 30 °C in a shaking incubator for approximately 3 to 6 h until the OD_{600} reached 0.6 to 1.0. The cells were pelleted by centrifugation at 500 *g* for 5 min at room temperature. The cell pellet was re-suspended in 10 ml of Solution I (wash solution) and then centrifuged at 500 *g* for 5 min at room temperature. The cell pellet was re-suspended in 1 ml of Solution II (lithium cation solution). Cells were competent and could be used immediately for transformation or stored in -80 °C for future use.

2.3.3.2.2. Transformation

One tube of 50 µl of competent cells was thawed at room temperature. One micro gram of vector DNA (recombinant plasmid PYES2) in 5 µl volume was added to the competent cells. Then, 500 µl of Solution III (Transformation solution) of S. c. EasyComp Transformation Kit, Invitrogen was added to the DNA/cell mixture and mixed by vortexing vigorously. The transformation reaction was incubated for 1 h in a 30°C water bath and mixed every 15 min by vortexing vigorously. One

hundred microliter of the transformation reaction was plated on appropriate selection plates and then incubated for 2 to 4 days at 30°C.

2.3.3.2.3. Expression of PYES2 recombinant plasmid in *Saccharomyces cerevisiae* strain INVSc1

In *S. cerevisiae* strains INVSc1, transcription from the GAL1 promoter is repressed in the presence of D-glucose (West *et al.,* 1984). Transcription induced by removing D-glucose and adding galactose as a carbon source (Giniger *et al.,* 1985). A single colony of INVSc1 containing PYES2 construct was inoculated into 15 ml of SC-U medium (0.67% yeast nitrogen base (without amino acids), 2% carbon source (D-glucose, 0.01% (adenine, arginine, cysteine, leucine, lysine, threonine, tryptophan, uracil), 0.005% (aspartic acid, histidine, isoleucine, methionine, phenylalanine, proline, serine, tyrosine, valine)) and incubated overnight at 30 °C at 150 rpm. Next day, the OD_{600} of the overnight culture was determined and diluted to obtain an OD_{600} of 0.4 in 50 ml of induction medium. The cells were pelleted by centrifugation at 1,500 *g* for 5 min at 4 °C and then inoculated into 50 ml of induction medium (SC-U medium containing 2% galactose). The cells were grown at 30 °C, 150 rpm. An aliquot of cells was harvested at 0, 2, 4, 6, 8, and 10 h after addition of cells to the induction medium. For each time point, 5 ml of culture from the flask was removed and the OD_{600} determined of each sample. The cells were pelleted by centrifugation at 1,500 *g* for 5 min at 4 °C and then re-suspended in 500 µl of sterile water. The cells were transferred into a sterile microcentrifuge tube and then centrifuged for 30 sec at top speed. The cell pellet was stored at –80 °C until ready to use.

Small-scale preparation of cell lysates was performed using acid-washed glass beads. Fresh or frozen cell pellets were re-suspended in 500 µl of breaking buffer and then centrifuged at 1,500 *g* for 5 min at 4 °C. The cell pellet was re-suspended in a volume of breaking buffer to obtain an OD_{600} of 50 - 100. An equal volume of acid-washed glass beads was added and then vortexed for 30 sec, followed by 30 sec on ice. This step was repeated ten times for a total of ten min to lyse the cells. The cells debris was pelleted by centrifugation for 10 min at

maximum speed. Supernatant was transferred to a new microcentrifuge tube. The lysate was the crude protein extract.

2.3.3.3. Agrobacterium tumefaciens GV3101

2.3.3.3.1. Competent cell preparation

A single colony of *A. tumefaciens GV3101* (Van Larebeke *et al.,* 1974) was inoculated in LB medium and incubated at 28 °C and 150 rpm overnight. The overnight culture was inoculated into 200 mL LB medium to an OD_{600} of 0.2 and incubated at 28 °C and 150 rpm to an OD_{600} of 0.8. The culture was cooled on ice for 10 min. Cells were pelleted by centrifugation at 1,860 *g*, 4 °C for 10 min and then re-suspended in 20 ml of ice-cold 10% glycerol. The step was repeated four times. Finally, the cells were re-suspended in 2 ml of ice-cold 10% glycerol, aliquoted (200 µl of cells suspension) into microfuge tubes and then stored at -80°C.

2.3.3.3.2. Transformation

The competent cells were transformed using electroporation method. Forty-five microliter of electrocompetent cells was mixed with 1 µl plasmid DNA in a cold 2 mm electroporation cuvette. An electric pulse of 1.8 kV was applied for transformation. Afterward, the cuvette was transferred on ice and 1 ml of LB medium was added. The liquid was transferred to a sterile microfuge tube and incubated at 28 °C for at least 1 h. The cells were plated on LB agar containing appropriate antibiotic and incubated for 2 to 4 days at 28 °C.

2.3.3.3.3. Expression of recombinant pGWR8–YFP plasmid in *A. tumefaciens* GV3101

A single colony of *A. tumefaciens GV3101* was inoculated in 5 ml of LB medium with kanamycine (25 µg/ml) and incubated at 28 °C, 150 rpm overnight. One hundred microliter of the overnight culture was transferred into 20 ml of AB Medium (1 g/l NH_4Cl, 0.3 g/l $MgSO_4$ x $7H_2O$, 0.15 g/l KCl, 0.01 g/l $CaCl_2$ x $2H_2O$, 0.0025 g/l $FeSO_4$ x $7H_2O$, 0.27 g/l KH_2PO_4, 10 g/l D-glucose, 3.90 g/l MES, 100 µM acetosyringone, pH 5.6) and incubated at 28 °C and 150 rpm overnight. OD_{600} of the cell culture was measured before pelleting the cell by centrifugation for 10

min at 1,860 *g*. The cell pellet was re-suspended in infiltration buffer (10 mM $MgSO_4$, 10 mM MES, 100 µM acetosyringone, pH 5.5) to an OD_{600} of 0.8±0.1. The suspension was used for infiltration the bottom side of tobacco leaves using a blunt ended 1 ml syringe.

2.3.3.4. Agrobacterium tumefaciens AGL0

2.3.3.4.1. Competent cell preparation

A single colony of agrobacterium cells was grown in 10 ml LB medium with appropriate antibiotic (Rifampicin, 25 µg/ml) at 28 °C, 150 rpm for overnight. Four milliliter of overnight culture was added in 100 ml LB medium and incubated at 28 °C with shaking until the OD_{600} of the culture reaches 0.5–1.0. Afterward, the culture was incubated on ice for 30 min and then centrifuged for 20 min at 4 °C, 5,000 *g*. Cell pellet was re-suspended in 2 ml ice cold 20 mM $CaCl_2$ and then aliquoted (100 µl) in Eppendorf tubes. The competent cells were frozen in liquid nitrogen and stored at -80 °C or used directly for transformation.

2.3.3.4.2. Transformation

One µg of plasmid DNA was added into 50 µl of competence cells and then incubated for 5 min on ice. Afterward, the tube was frozen in liquid nitrogen for 5 min. Heat shock was performed at 37 °C for 5 min without shaking. Nine hundred fifty microliter of LB medium was added and then incubated for 2 – 4 h at 28 °C and 150 rpm. Finally, the cells were plated in LB agar with appropriate antibiotics and incubated at 28 °C for 2 days.

2.3.3.4.3. Expression of recombinant pBI121 plasmid in *A. tumefaciens* AGL0

The *A. tumefaciens* strain AGL0 (Lazo *et al.*, 1991) containing the recombinant pBI121, was grown at 28 °C in LB medium with appropriate antibiotics. When the culture reached an OD_{600} of about 0.8, *Agrobacterium* cells were harvested and washed twice with 30 ml modified MacConkey agar (MMA) medium (Murashige and Skoog salts, 10 mM MES (morpholine ethane sulphonic acid pH = 5.6), 20 g/l sucrose, according to Spolaore *et al.*, 2001). Finally, the cell pellet was re-suspended in 10 ml of MMA medium for infiltration into the strawberry fruit.

2.3.4. *In vitro* assay

2.3.4.1. XET assay

Endotransglucosylase assays were based on the method of Fry *et al.* (1992). In brief, radioactive XET activity assays were performed in a reaction volume of 64 µl that contained sodium succinate buffer pH 5.5 at a final concentration of 300 mM, 0.5% (w/v) tamarind xyloglucan, 1 kBq [^{3}H]XXXGol and 4 µl of FvXTH enzyme extract. After incubation for various time periods at 25°C the reaction was stopped by the addition of 20 µl 90% (v/v) formic acid. However, when water-soluble cellulose acetate (WSCA) was the donor-substrate, 20 µl of 35% NH_3 was used so that the WSCA was converted to cellulose. The reaction mixtures were then spotted on a 4 cm x 4 cm square Whatman 3MM filter paper, air dried, washed under running tap water overnight to remove unreacted radioactive oligosaccharide and dried again in an oven at 60°C. For ^{3}H scintillation counting, the dry paper was rolled into a cylinder with the loaded side facing outwards and placed into a 22 ml scintillation vial, which was subsequently wetted with approximately 2 ml of scintillation cocktail (0.5 % 2,5-diphenyloxazole/0.05 % 1,4-bis(5-phenyloxazol-2-yl) benzene in toluene; Wallac OptiPhase (Perkin Elmer, Waltham, MA, USA)). Radioactivity on dry paper was assayed by scintillation counting in WallacOptiScint (Perkin Elmer, Waltham, MA, USA). The measurements of blanks occurred in an identical way.

Cellohexaitol or MLG-derived heptasaccharides were assayed using a different method because these polysaccharides are difficult to elute from paper. Ethanol precipitation was performed as follow: ethanol was added to a final concentration of 75% (v/v), and the precipitated polysaccharides were then washed by re-suspension and pelleting in 75% ethanol. This step was repeated several times until the supernatants were non-radioactive. Finally, the pellet was re-dissolved in water and assayed for ^{3}H.

Various acceptor substrates including [^{3}H]XXXGol, [^{3}H]XXLGol, [^{3}H]XLLGol, [^{3}H]XXFGol, [^{3}H]XXGol, [^{3}H]XGol (each at 1 kBq per assay) and also various donor substrates such as tamarind xyloglucan, barley β-glucan, hydroxyethylcellulose, water-soluble cellulose acetate (WSCA) and cellulose

(each at a final concentration of 0.5% (w/v) in the assay) were used to determine the substrate specificity of enzyme. Various pH and temperature values were performed using 1kBq [^{3}H]XXXGol as acceptor substrate and 0.5% (w/v) of tamarind xyloglucan as donor substrate. Different buffers were used as follows: 300 mM acetate buffer (pH 3.6, pH 4.0, pH 4.6 and pH 5.2), 300 mM sodium succinate buffer (pH 5.0, pH 5.5, pH 6.0 and pH 6.5) and 300 mM sodium phosphate buffer (pH 6.2, pH 7.0, pH 7.4, and pH 8.0).

2.3.4.2. Xyloglucan hydrolysis by the XEH activity of FvXTH9 and FvXTH6

The reaction mixture (640 µl) contained 0.25% (w/v) of tamarind xyloglucan in 300 mM succinate buffer pH 5.5 with 0.5% (v/v) chlorobutanol and 40 µl of enzyme extract. The reaction was incubated 30°C, 68 hours. The solution was mixed with 200 µl formic acid to stop the reaction. The solution was size-profiled by gel-permeation chromatography (GPC) on Sepharose CL-6B (bed vol. 160 cm^3) in acetate buffer 0.05 M, pH 4.8, flow rate 1 ml/min together with internal markers of sucrose (2.5 mg) 15 kDa-25 kDa dextran (2.5 mg), 100 kDa dextran (2.5 mg), 670 kDa dextran (2.5 mg), 2000 kDa blue dextran (2.5 mg) and 2.5 ml fractions were collected and assayed for carbohydrate content by the anthrone method.

2.3.4.3. Kinetic assay of FvXTH9 and FvXTH6

XET kinetic parameters of the purified recombinant FvXTH9 and FvXTH6 were determined using radioactive assay according to Fry *et al.* (1992). K_m and V_{max} for XXXGol was determined using 1% (w/v) tamarind xyloglucan as donor substrate. This assay is for testing XET activities with trace of high-specific activity [^{3}H]XXXGol diluted with various amounts (0 – 357 µM) of unlabelled XXXGol. The K_m and V_{max} for xyloglucan was determined using [^{3}H]XXXGol at a concentration of 43 µM for FvXTH9 and 89 µM for FvXTH6 with various concentrations (0-4.55 mg/ml) of the polysaccharide.

2.3.4.4. Esterase assay

Esterase assay was performed using α-napthyl acetate, p-nitrophenyl acetate, benzyl acetate and phenyl acetate as substrates. Recombinant protein (10 µl) was mixed with 5 µl substrate 20 mM in 85 µl KPi buffer 0.1 M pH 6.0. The mixture was incubated at 30°C, 24h, 300 rpm and added 50 µl methanol to stop the reaction then centrifuged for 10 min, 4°C at 20,000 *g*. The supernatant (50 µl) was analyzed by LC-MS.

Esterase assay for various pH was performed using α-napthylacetat as substrate. Twenty-five microliter of recombinant protein was mixed with 25 µl of 0.016 M α-napthylacetat in 200 µl of 0.1 M KPi buffer pH 5.8, 6.0 and 7.0. The mixture was incubated at 30°C, 30 min, 300 rpm and then centrifuged for 10 min, 4°C at 20,000 *g*. Fifty microliter of the supernatant was analyzed by LC-MS.

2.3.5. *In vivo* assay

2.3.5.1. Transient expression in *Nicotiana tabacum* leaves

To study the subcellular localization of FvXTH9 and FvXTH6 in *N. tabacum* leaves, full-length gene of *FvXTH6* and *FvXTH9* were cloned into pGWR8 (Rozhon *et al.,* 2010) plasmid and then fused with the YFP gene. Primers of FP_FvXTH9_pGWR8 and RP_FvXTH9_pGWR8 were used to amplify *FvXTH9*, whereas FP_FvXTH6_pGWR8 and RP_FvXTH6_pGWR8 were used to amplify *FvXTH6*. The constructs were transformed into *Agrobacterium tumefaciens* GV3101/pSoup cells. Expression of recombinant protein was performed in leaves of *N. tabacum* for protein localization. The leaves were observed for the expression of recombinant protein after two days of infiltration. The infiltration area was investigated using an Olympus FV1000/IX81 laser scanning confocal microscope with a UPlanSApo ×60/1.20 objective (Olympus) and laser wavelength of 515 nm. Images were obtained and processed using FluoView software.

2.3.5.2. Transient expression in *F.* × *ananassa* fruit

Full-length ORF *FvXTH9* and *FvXTH6* genes were cloned into pBI121 vector. PCR fragments cut by BamHI and SacI were cloned into the binary vector pBI121 digested with the same enzymes. This placed the inserts under control of the CaMV35S promoter. Specific primers were used as follow: FP_FvXTH9_pBI121 and RP_FvXTH9_pBI121 for *FvXTH9* amplification, whereas FP_FvXTH6_pBI121 and RP_FvXTH6_pBI121 for *FvXTH6* amplification. The constructs were transformed into *E. coli* NEβ10 cell and absence of errors confirmed by sequencing. Correct clones were transformed into *A. tumefaciens* AGL0. Overexpression of recombinant protein was performed in fruit of *F.* × *ananassa.* The agrobacterium suspension was evenly injected into entire white fruits (14 days after pollination) that were still attached to the plant by using sterile 1 ml hypodermic syringes. Infiltrated fruits were harvested on 8, 10, 12 and 14 days post infiltration.

2.3.5.3. Fruit firmness analysis

The firmness was measured using a Texture Analyzer (TA.XT2i, Stable Micro Systems Texture Technologies, Scarsdale, NY) fitted with a 5 mm flat probe. Each fruit was penetrated 5 mm at a speed rate of 0.5 mm s^{-1} and the maximum force developed during the test was recorded in Newtons (N). Each fruit was measured twice in opposite sides of its equatorial zone.

2.3.5.4. Hemicellulose analysis

2.3.5.4.1. Fruit preparation

Fruit for hemicellulose content analysis was prepared as described by Renard *et.al.,* (1995). Four gram of lyophilized strawberry fruit powder was suspended in 200 ml of 6 M NaOH under magnetic stirring for 18 h at room temperature. The solution was then centrifuged (15,000 *g*, 15 min) and the supernatant was neutralized with acetic acid until pH neutral (pH 7). The extract was dialyzed against distilled water overnight. Water was removed by freeze-drying to obtain a powder of hemicellulose.

2.3.5.4.2. Xyloglucan fractionation

Xyloglucan fractionation was performed using Sepharose CL-6B column (Bed volume 160 cm^3). Gel medium was equilibrated in 0.05 M sodium acetate buffer pH 4.8 with a flow rate 1 ml/min. Sample was dissolved in 1 ml of 0.05 M acetate buffer pH 4.8 and eluted from the column using 0.05 M acetate buffer pH 4.8 at 1 ml/min. For size calibration a mixture of sucrose (2.5 mg), 15 kDa-25 kDa dextran (2.5 mg), 100 kDa dextran (2.5 mg), 670 kDa dextran (2.5 mg) and 2000 kDa blue dextran (2.5 mg) was loaded and eluted using 0.05 M acetate buffer pH 4.8 at 1 ml/min. Fractions (2.5 ml) were collected and assayed for carbohydrate content by the anthrone method.

2.3.5.4.3. Anthrone method for hemicellulose detection

To 100 µl of the test samples in a 96 well plate, 200 µl of 0.2% solution of anthrone in 95% sulphuric acid was added. Absorbance at 630 nm was measured using a plate reader. The blank was 0.05 M acetate buffer pH 4.8.

3. RESULT

3.1. Putative XTHs from *F. vesca*

3.1.1. The identification of putative XTH genes

Putative *XTH* genes were searched in the *F. vesca* ssp. vesca accession Hawaii 4 genome sequence to functionally characterize strawberry xyloglucan modifying enzymes in *Fragaria*. Mining of the publicly available *F. vesca* genome sequence yielded 28 apparently distinct putative XTH (Shulaev *et al.,* 2011). A phylogenetic analysis was performed to show the relationship of different XTH in diploid *F. vesca* (Figure 7).

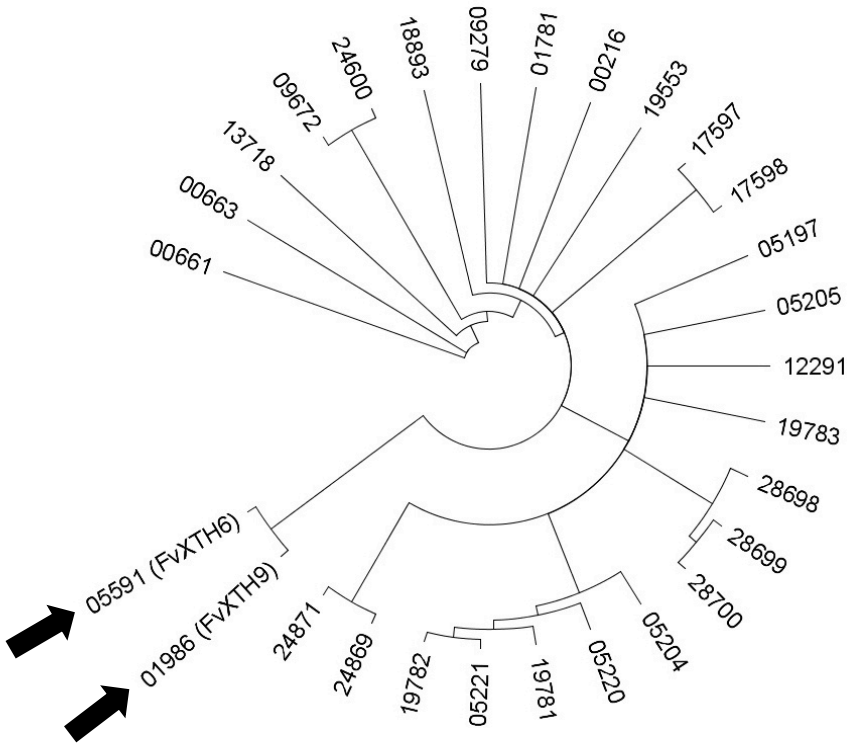

Figure 7. Phylogenetic tree of XTHs candidates from *F. vesca*.

The tree was constructed using Genious v5.6 software with the Neighbor-Joining method with 5000 bootstrap replications. Amino acid sequences were retrieved from the *F. vesca* Genome Browser database and their accession numbers as follows: gene00216, gene00661, gene00663, gene01781, gene01986, gene05197, gene05204, gene05205, gene05220, gene05221, gene05591, gene09279, gene09672, gene12291, gene13718, gene17597, gene17598, gene18893, gene19553, gene19781, gene19782, gene19783, gene24600, gene24869, gene24871, gene28698, gene28699, gene28700 (Shulaev *et al.,* 2011). FvXTH9 (gene01986) and FvXTH6 (gene05591) are indicated by arrows.

3.1.2. Selection of candidate genes

To functionally characterize fruit ripening-related strawberry XTHs, transcript levels of the putative XTHs were analyzed in a transcriptomic data set, obtained from fruit at different developmental stages (green, white and ripe) of three *F. vesca* varieties (Reine de Vallées, Hawaii 4 and Yellow Wonder; Härtl *et al.,* 2017). Gene 01986, namely *FvXTH9* (according to the *F. vesca* Annotation release 101) showed the highest expression level in green receptacle of all three genotypes. The *FvXTH9* transcript level in receptacle decreased with progressing ripening and was low in achenes throughout strawberry fruit development (Figures 8 and 9). The other genes were barely expressed in the receptacle (Figure 8). Genes 19783, 13718, 24871 and 05591 were predominantely expressed in the achenes (Figure 9).

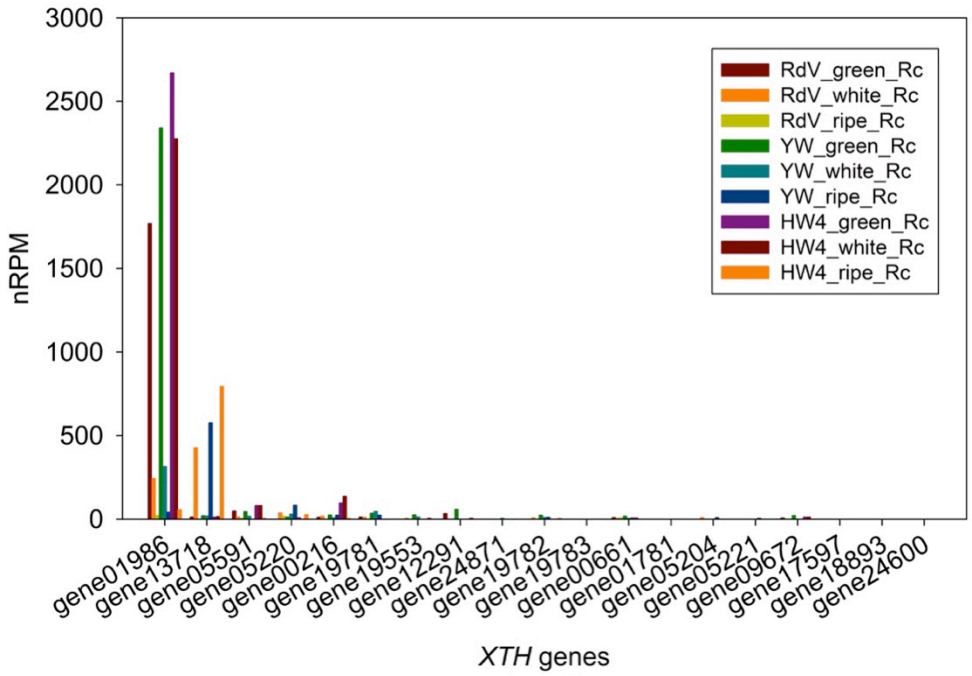

Figure 8. Next generation sequencing data of *XTH* gene candidates in receptacle.

Transcript levels of putative *XTH* genes from *F. vesca* varieties Hawaii 4 (HW4), Reine des Vallées (RdV) and Yellow Wonder (YW) in the receptacle (Rc), displayed as nRPM (normalized read per million).

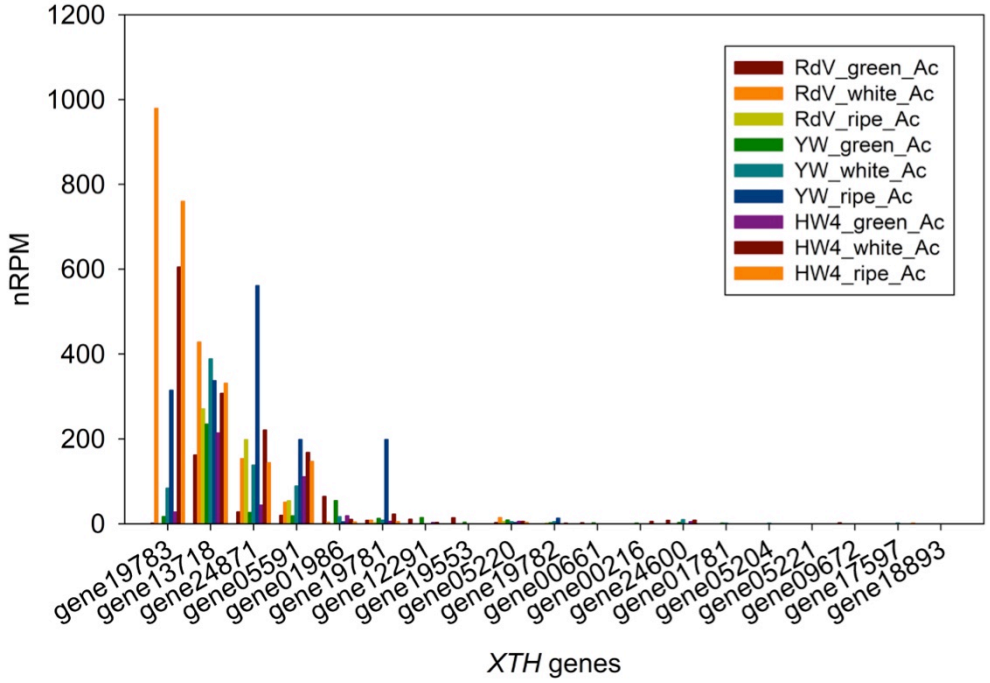

Figure 9. Next generation sequencing data of *XTH* gene candidates in achenes.

Transcript levels of putative *XTH* genes from *F. vesca* varieties Hawaii 4 (HW4), Reine des Vallées (RdV) and Yellow Wonder (YW) in the achenes (Ac), displayed as nRPM (normalized read per million).

A sequence analysis of different putative *F. vesca XTH* genes revealed that *FvXTH9* was closely related to gene05591 (*FvXTH6*) (48.5% identity of amino acid sequence homology) (Figure 7). Because *FvXTH9* might be involved in strawberry fruit ripening and and *FvXTH6* showed high sequence similarity they were selected for further investigation.

3.1.3. Phylogenetic analysis of XTH proteins from various plants species

In order to classify the different groups of XTHs (group I/II, IIIA and IIIB), a phylogenetic tree was generated using the deduced amino acid sequences of FvXTH9 and FvXTH6 and biochemically characterized XTHs from various plants species, including Arabidopsis, tomato, apple and others (Figure 10). FvXTH9 and FvXTH6 are classified in group I/II, with the well-characterized PttXET16A, a strict XET enzyme (Johansson *et al.,* 2004). Additionally, FvXTH9 and FvXTH6

are closely related to At-XTH9 and At-XTH6, respectively. Thus, proteins encoded by genes 01986 and 05591 were named FvXTH9 and FvXTH6 (Figure 10).

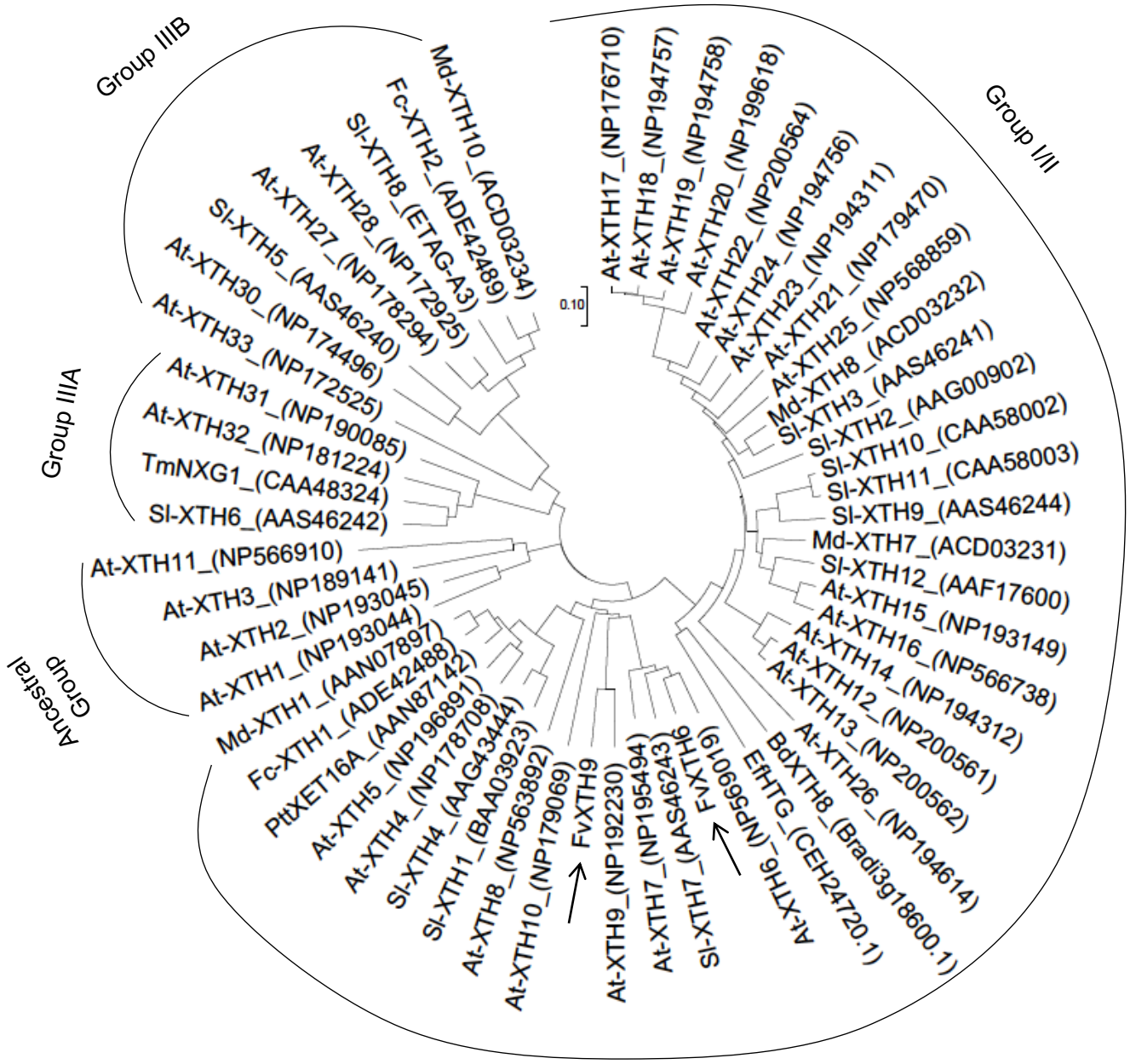

Figure 10. Phylogenetic tree of XTHs from different species.

*F. vesca (*Fv*)*, *A. thaliana (*At*), S. lycopersicum* (Sl*), M. x domestica (*Md*), F. chiloensis (*Fc*), Populus tremula x Populus tremuloides* (Ptt) and *Tropaeolum majus (*Tm*)*. FvXTH6 and FvXTH9 protein sequences (indicated by arrows) were aligned with other XTH sequences. The phylogenetic tree was constructed by the Neighbour-Joining method with 5000 bootstrap replications using MEGA 7 software. The GenBank accession numbers are indicated in the figure.

3.1.4. Amino acid sequence alignment of group I/II XTHs proteins from selected plants.

A multiple alignment was generated to access relationship among group I/II of XTHs (Figure 11). FvXTH9 consisted of 294 amino acid residues with a theoretical molecular mass and pI value of 33.15 kDa and 5.46, respectively (Appendix 1). FvXTH6 consisted of 293 amino acid residues with a theoretical molecular mass of 33.34 kDa and a pI value of 6.44, respectively. FvXTH9 and FvXTH6 contain the conserved motif of glycosyl hydrolase family 16 ((D/N)E(I/L/F)DFEFLGN), which is likely to be the active site (Campbell and Braam, 1998) and also a potential N-linked glycosylation (N-X-S/T) site, indicating that these proteins possess the common structural features of XTHs (Figure 11). FvXTH9 contains the NEFDFEFLG sequence at position 97-105, while FvXTH6 has the DELDFEFLG sequence at position 107-115. FvXTH9 and FvXTH6 have N-T-T and N-R-T as putative N-glycosylation domain directly after the catalytic domain, respectively. These findings identify FvXTH9 and FvXTH6 as typical class I/II XTHs.

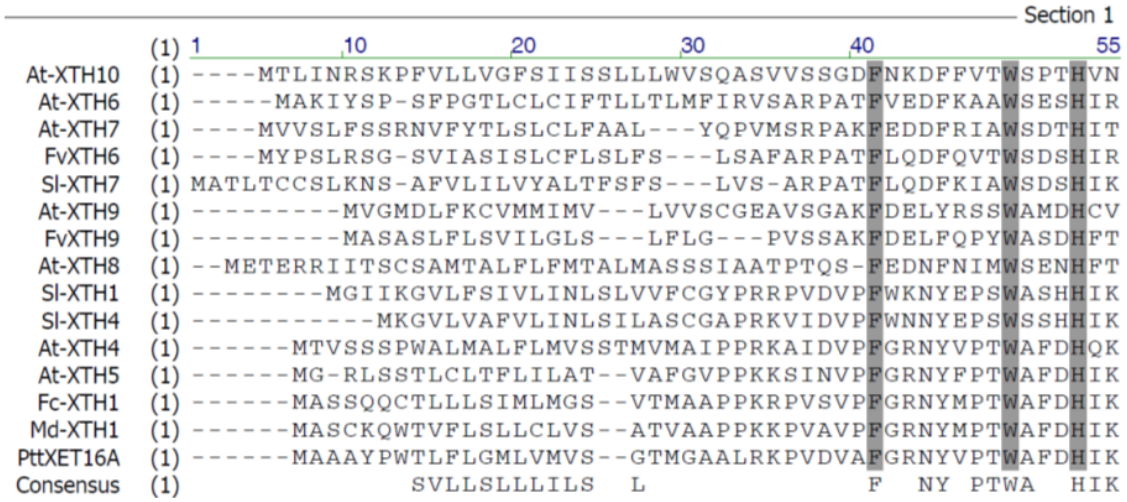

to be continued

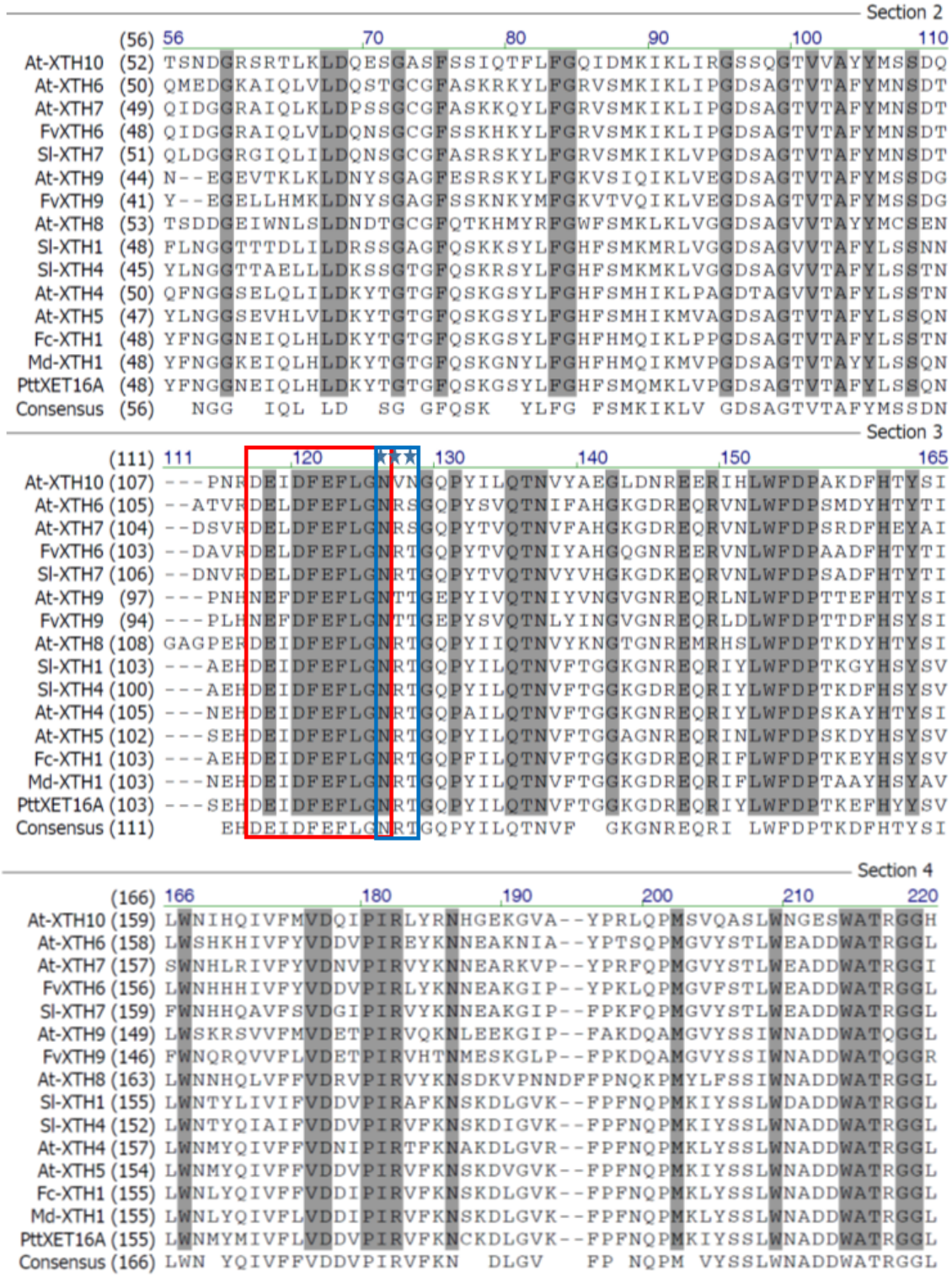

to be continued

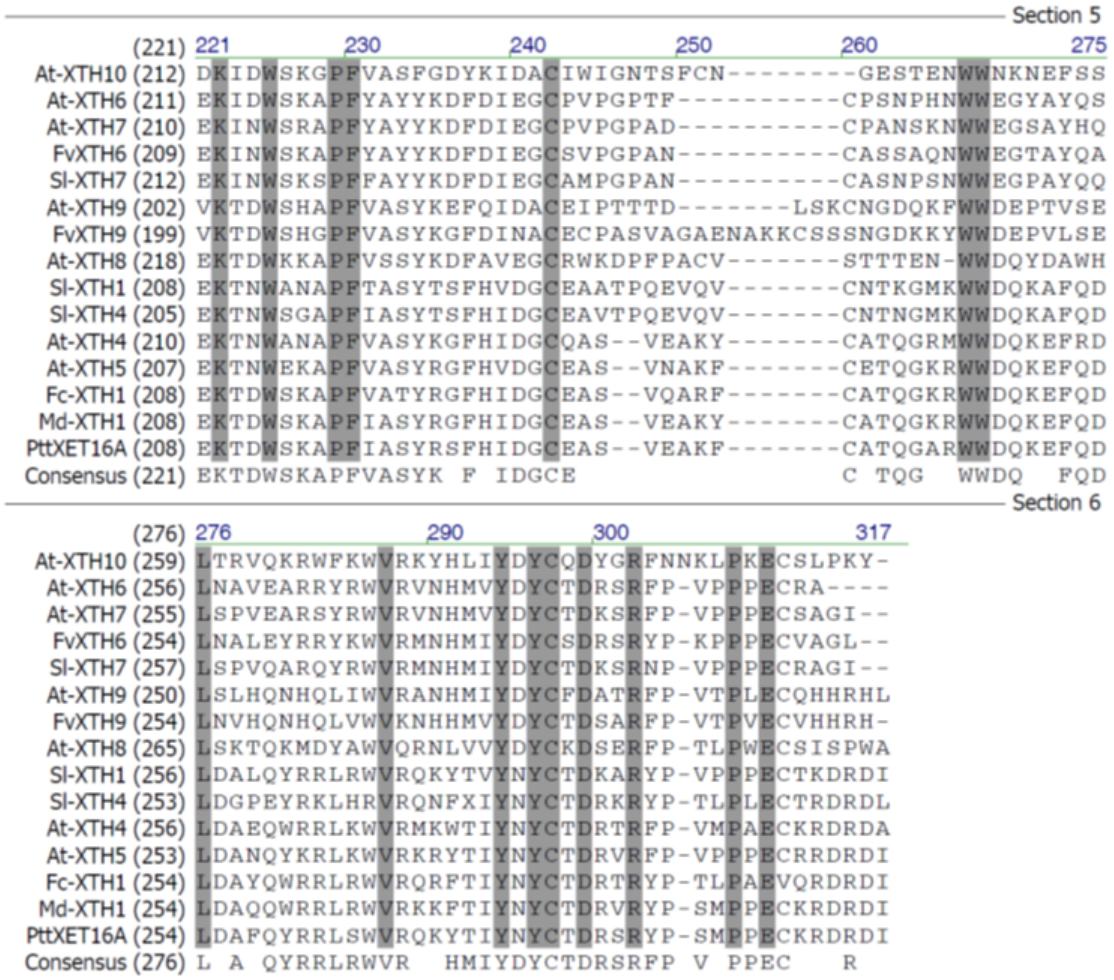

Figure 11. Amino acid sequence alignment of group I/II XTHs.

Sequences correspond to the following GenBank accession numbers: *A. thaliana* (At-XTH4 (NP 178708), At-XTH5 (NP 196891), At-XTH6 (NP 569019), At-XTH7 (NP 195494), At-XTH8 (NP 563892), At-XTH9 (NP 192230), At-XTH10 (NP 179069)), *S. lycopersicum* (Sl-XTH1 (BAA03923), Sl-XTH4 (AAG43444), Sl-XTH7 (AAS46243)), *M. x. domestica* (Md-XTH1 (AAN07897)), *F. chiloensis* (Fc-XTH1 (ADE42488)) and *Populus tremula x Populus tremuloides* (PttXET16A (AAN87142)). Identical amino acids in the sequences are shaded in black. Box indicates the conserved motif and stars (***) mark N-liked glycosylation site. AlignX Vector NTI Advance V.11.5 software was used.

3.1.5. Expression profiles of *FvXTH9* and *FvXTH6* in fruit, leaves and flowers of *F. vesca*

The expression levels of *FvXTH9* and *FvXTH6* were also examined by quantitative real-time PCR in fruit at different ripening stages, as well as in leaf and flower

tissue of *F. vesca* (Figure 12). Both genes displayed similar expression profiles during fruit development but had different transcript abundances. The expression level of *FvXTH9* from the small green fruit to the large green fruit showed a high increase, followed by a rapid decrease in the white fruit and the ripe fruit. *FvXTH6* slightly increased from the small green fruit to the large green fruit and then rapidly dropped in the white and the ripe fruit. Other tissue samples were probed to verify the tissue specific expression of *XTHs*. Both *FvXTH9* and *FvXTH6* are highly expressed in flower (Figure 12). Besides, *FvXTH6* is expressed at a high level in young leaf but a low level in old leaf, whereas *FvXTH9* is transcribed at a very low level in both young and old leaves.

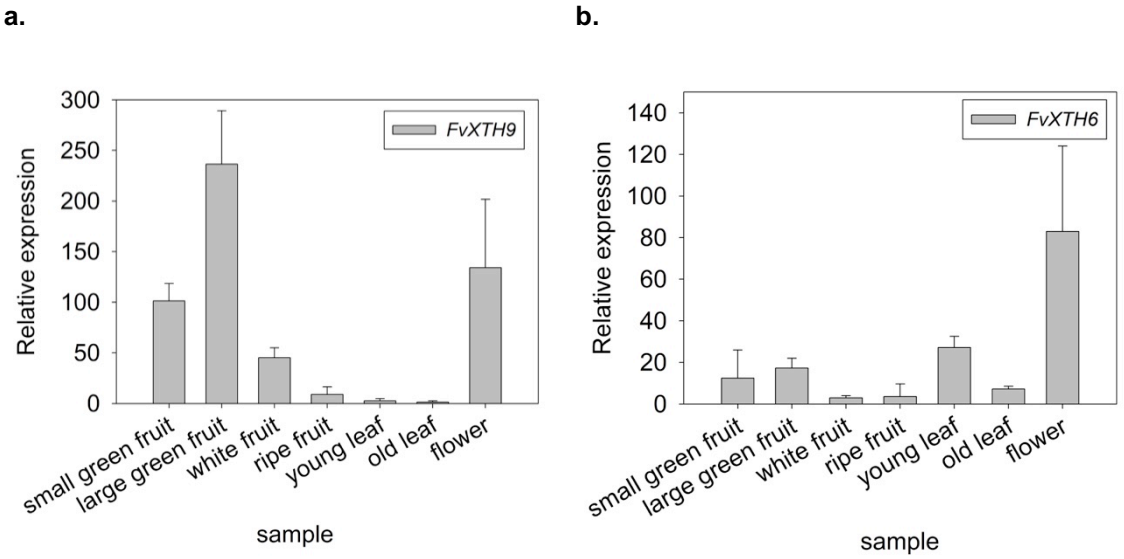

Figure 12. Quantitative PCR analysis of *FvXTH9* (a) and *FvXTH6* (b)

Analyses were performed in *F. vesca.* Hawaii 4 fruit tissue at different developmental stages (small green, large green, white and ripe fruit) and vegetative tissues (young leaf, old leaf and flower).

3.2. Cloning and characterization of *XTH* genes from *F. vesca*

The mRNA isolation was performed for both *F. vesca* Hawaii 4 and *F.* × *ananassa* fruit (Appendix 4). In *F. vesca,* only large green fruit was used for mRNA isolation based on the qPCR analysis. However, for *F.* × *ananassa* fruit in different

developmental stages such as small green, large green, white, tuning and red fruit were used for mRNA isolation.

FvXTH6 which consisted of 880 bp was amplified using forward primer (FP_FvXTH6) and reverse primer (RP_FvXTH6) from the cDNA of *F. vesca* large green fruit. Non-specific bands were found after amplification using cDNA from *F.* × *ananassa* fruit. Furthermore, these bands did not show the correct size of the target gene (Appendix 5). The sequence of the putative *FvXTH6* from *F. vesca* was cloned in PSK+ cloning vector with restriction of the Sma I enzyme and was then transformed in *E. coli* NEβ 10 cell.

Specific primers of FP_FvXTH9 and RP_FvXTH9 amplified target *FvXTH9*, which consisted of 882 bp from *F. vesca* cDNA (Appendix 7). The expected PCR band that corresponded to *FvXTH9* was cloned in pGEM-T cloning vector and then transformed in *E. coli* NEβ 10 cell. The identity of the recombinant plasmid was verified by restriction enzyme digestion.

3.3. Heterologous expression and protein characterization of XTHs

3.3.1. Cloning and expression of *FvXTH6* using pGEX-4T-2 vector in *E. coli* BL21 (DE3) cell.

The pGEX-4T-2 plasmid was used as expression vector for production of the FvXTH6-glutathione-S-transferase (GST) fusion protein. The plasmid and target gene were cut using BamHI and SmaI restriction enzymes. Target gene was purified and ligated into pGEX-4T-2 plasmid. *FvXTH6* was successfully cloned into pGEX-4T-2 plasmid (Appendix 6). *E. coli* BL21 (DE3) was used as host organism for protein expression. Induction was performed by 0.5 mM isopropyl β-D-1-thiogalactopyranoside (IPTG). Fusion protein FvXTH6-GST was purified using GST resin. Translation analysis of FvXTH6 using Compute pI/Mw tool (www.expaxy.org) resulted in a 33 kDa protein and 59 kDa for the GST fusion protein. Western blot analysis showed that FvXTH6-GST was succesfully expressed as 59 kDa protein in addition to GST (Figure 13). Preliminary assays

of the elution fraction (EL2) of FvXTH6-GST resulted no XET activity. Therefore, another expression vector and host cell were used to produce FvXTH6.

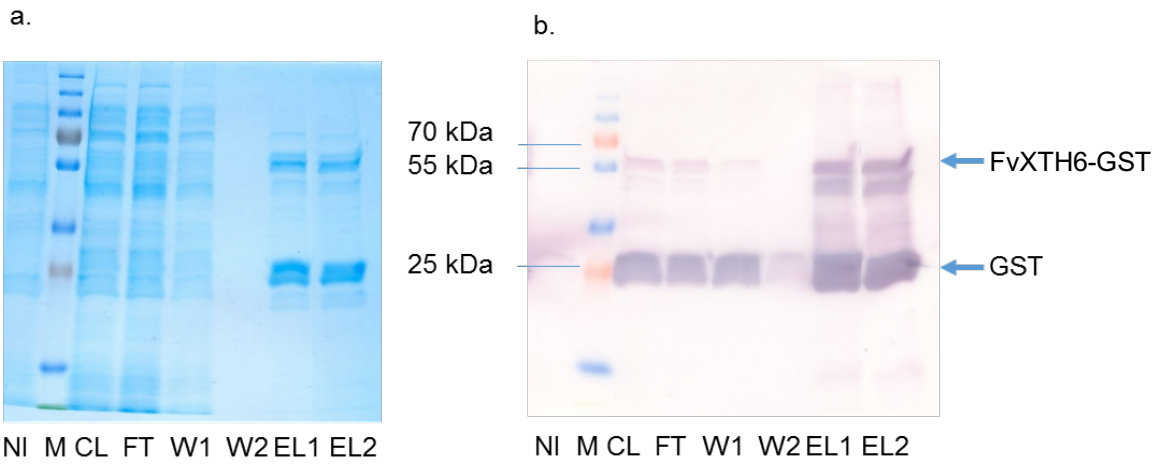

Figure 13. Purification of FvXTH6-GST using GST resin.

a, Commasie staining; b, Western blot. Purification steps: NI, non-induction; M, protein marker; CL, cell lysate; FT, flow-through; W1 and W2, wash; EL1, EL2, EL3, elution. Target protein and GST (59 kDa) are shown by arrows.

3.3.2. Cloning and expression of *FvXTH6* using PYES2 vector in *S. cerevisiae* yeast cell.

FvXTH6 was also produced in yeast cells. Thus, template DNA was amplified using a specific primer containing a yeast consensus sequence for PYES2, *FvXTH6* and an additional 6xHis sequence. Forward primer FP_FvXTH6_PYES2 and reverse primer RP_FvXTH6HIS_PYES2 amplified *FvXTH6* (880 bp) from *F. vesca* cDNA which was then ligated into PYES2 vector. Transformation was done in two steps, first using *E. coli* NEβ 10 for maintaining recombinant plasmid and then *S. cerevisiae* INVSc1 for protein expression. D-galactose was used to induce expression of the protein of interest from the GAL1 promoter in PYES2 vector. Purification was done using HisTag affinity chromatography. SDS-PAGE and western blot analysis of these fractions A4, A5 and A6 showed that FvXTH6-His was successfully expressed as 33 kDa protein (Figure 14a).

3.3.3. Cloning and expression of *FvXTH9* using PYES2 vector in *S. cerevisiae* yeast cell

A specific primer containing a yeast consensus sequence for PYES2 and an additional 6x His sequence successfully amplified *FvXTH9*, which consisted of 882 bp from *F. vesca* cDNA. Forward primer (FP_FvXTH9_PYES2) and reverse primer (RP_FvXTH9HIS_PYES2) were used for *FvXTH9* amplification. Cloning was conducted using the PYES2 vector. Similar to the cloning and expression of *FvXTH6*, transformation was also done in two steps. Purification was also performed by affinity chromatography. FvXTH9HIS was successfully expressed as 33 kDa protein as shown by SDS PAGE analysis (Figure 14b).

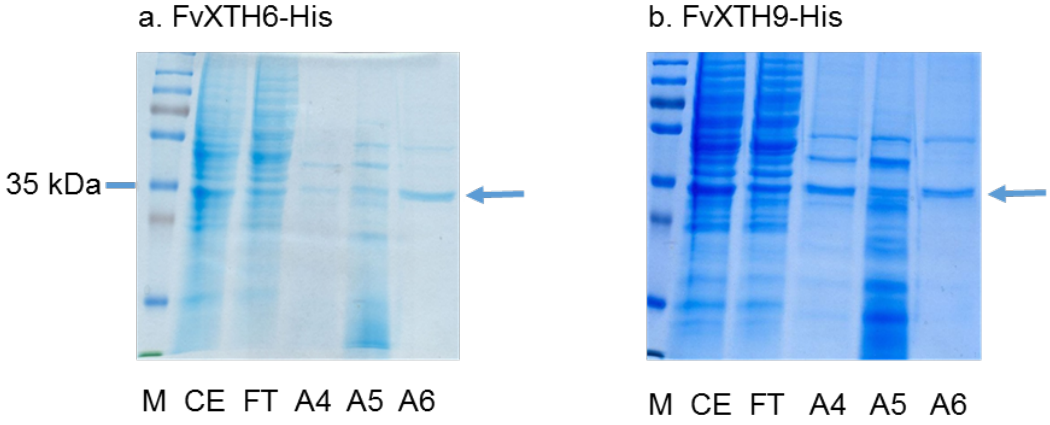

Figure 14. Purification of FvXTH6-His and FvXTH9-His using HisTrap FF column.

Coomassie staining; M, protein marker; CE, crude extract; FT, flow through; A4-, A5-, A6-, GPC fractions. Target proteins (33 kDa) are shown by arrows.

3.4. *In vitro* assay of FvXTH9 and FvXTH6

3.4.1. Determination of optimal pH and temperature for XET activity

Various pH and temperature values were tested using radiolabeled XXXGol as acceptor substrate, tamarind xyloglucan as donor substrate and crude extract of FvXTH9 or FvXTH6 expressed in yeast. The pH optimum of the XET activity of

FvXTH9 and FvXTH6 were 6.5 in 300 mM sodium succinate buffer (Figure 15a and 15b). FvXTH9 and FvXTH6 were inactive in XET assays at a pH of 4.0 and below. While FvXTH6 exhibited only 25% activity at pH 4.8, FvXTH9 still showed approximately 70% of its maximal activity at that pH, indicating a higher acid tolerance. Both enzymes displayed 50% of their maximal activities at pH 7.0, which dropped below 30% at pH 8.0. Their activities in sodium phosphate buffer were lower than in sodium succinate buffer at the same pH. The temperature optimum of FvXTH6 were 30 °C (Figure 14c). No XET activity was detected in crude extract of empty vector-transformed Saccharomyces cultures (control PYES2).

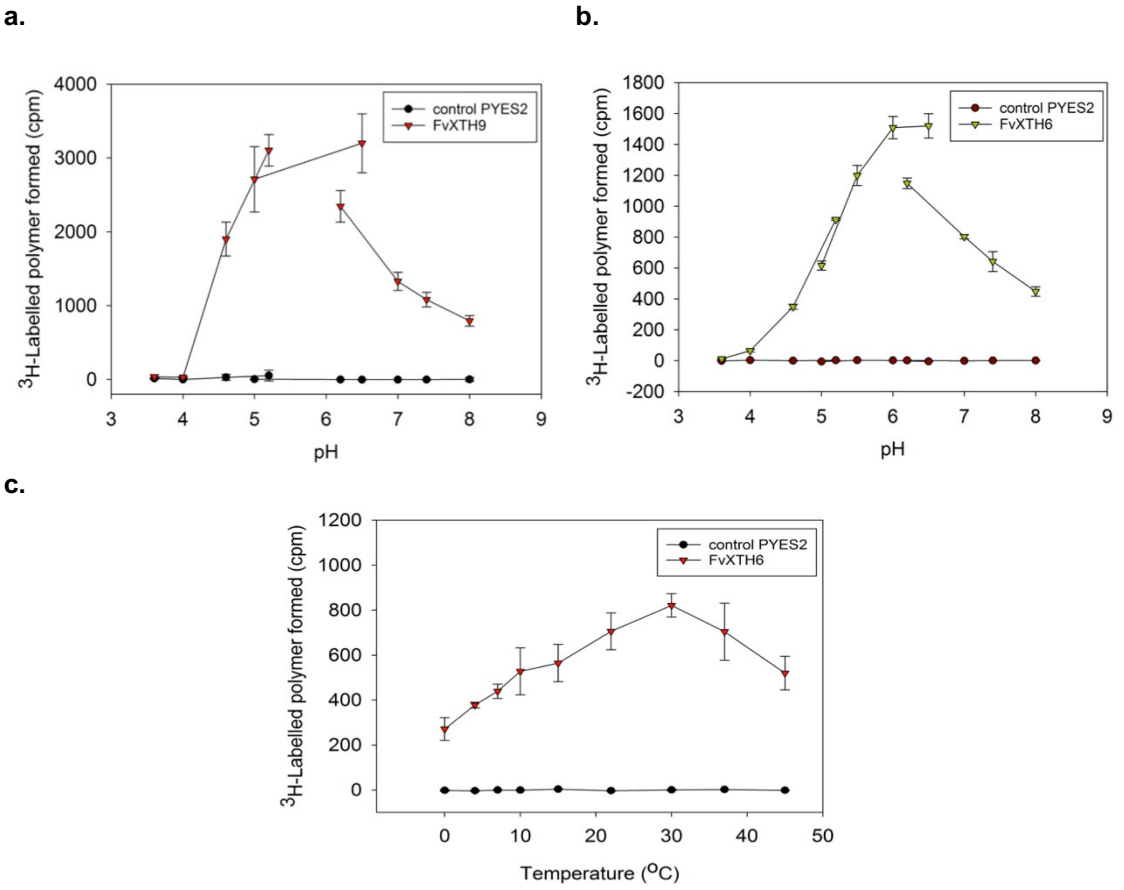

Figure 15. The pH and temperature optimum of FvXTH9 and FvXTH6.

The pH optimum of FvXTH9 (a) and FvXTH6 (b). Temperature optimum of FvXTH6 (c). No XET activity was detected for control PYES2. Different buffers were used as follows: acetate buffer (pH 3.6, pH 4.0, pH 4.6 and pH 5.2), sodium succinate buffer (pH 5.0, pH 5.5, pH 6.0 and pH 6.5) and sodium phosphate buffer (pH 6.2, pH 7.0, pH 7.4, pH 8.0). Each assay was performed in 4 replicates.

3.4.2. Substrate specificity (donor and acceptor substrate)

3.4.2.1. Substrate specificity of FvXTH9

To determine the substrate specificity of the FvXTH9 enzyme, various donor substrates such as tamarind xyloglucan, barley β-glucan, and HEC were used in assays whereas [^{3}H]XXXGol served as acceptor substrate (Figure 16a).

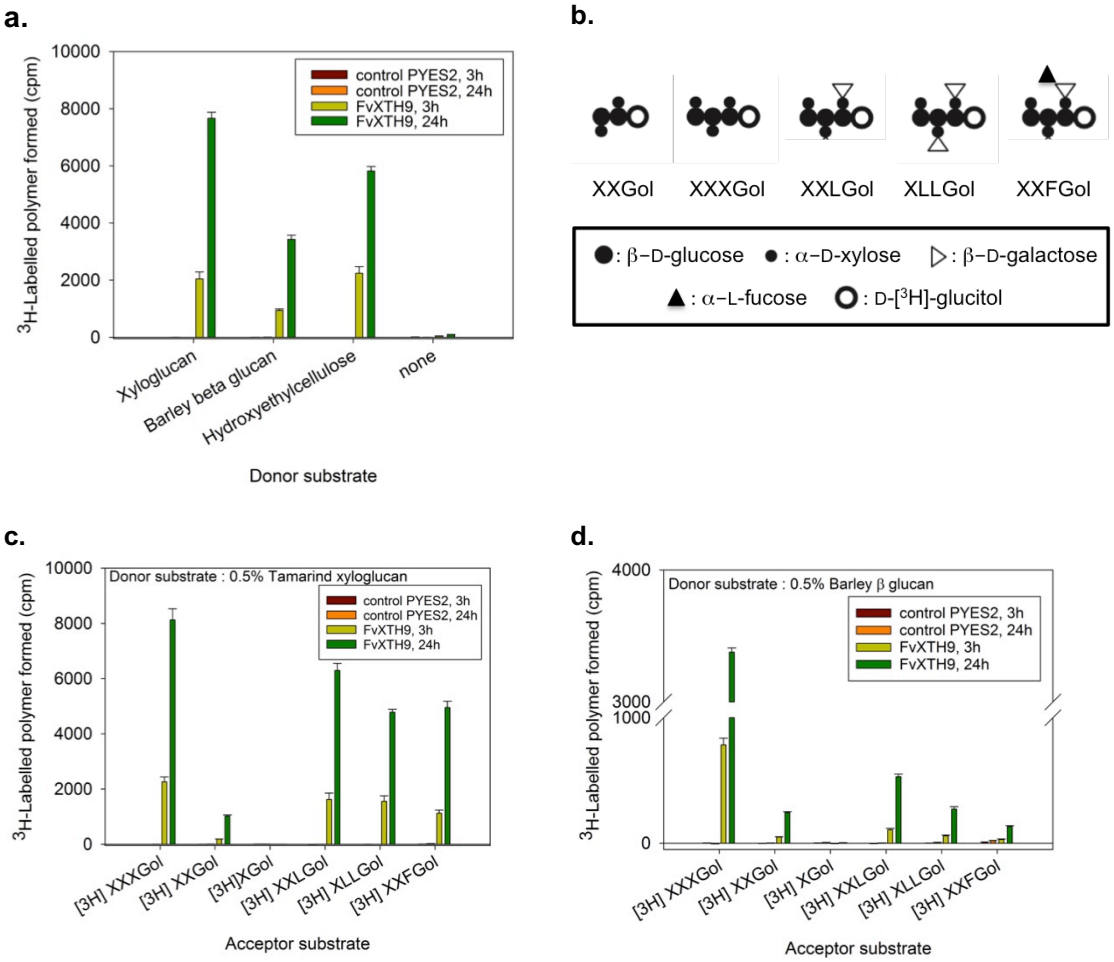

Figure 16. XET and MXE assays of FvXTH9.

a. Donor substrate preference (Xyloglucan, Barley β glucan, HEC), b. Structures of acceptor substrates, c. Acceptor substrate preference for XET assay (XXXGol, XXGol, XGol, XXLGol, XLLGol, XXFGol), d. Acceptor substrate preference for MEX assay (XXXGol, XXGol, XGol, XXLGol, XLLGol, XXFGol). No XET activity was found in crude extract of empty vector-transformed Saccharomyces cultures (control PYES2). Each assay was performed in 4 replicates. Unsubstituted glucose (Glc) residues are abbreviated as G, whereas X, L and F indicate Glc residues that are 6-O-substituted with α-D-Xylp, β-D-Galp-(1-2)-α-D-Xylp and α-L-Fucp-(1-2)-β-D-Galp-(1-2)-α-D-Xylp side chains, respectively (Fry *et al.,* 1992).

A crude extract of FvXTH9 accepted all three donor substrates tested efficiently with tamarind xyloglucan being the preferred one followed by HEC and barley β-glucan (Figure 16a). XET and MXE activity assay was performed using tamarind xyloglucan and barley β-glucan as a donor substrate, respectively. Both assays were performed using various acceptor substrates (Figure 16b). The result showed that FvXTH9 has XET and MXE activity. The acceptor substrate preference for XET was in the following order: XXXGol > XXLGol > XLLGol ≈ XXFGol > XXGol (Figure 16c). For the MXE activity assay, it was in the following order: XXXGol > XXLGol > XLLGol > XXGol > XXFGol (Figure 16d). No activity was found for XGol in both assays.

3.4.2.2. Substrate specificity of FvXTH6

Various acceptor substrates including radiolabeled XXXGol, XXLGol, XLLGol, XXFGol, XXGol, and cellohexaitol and various donor substrates such as tamarind xyloglucan, barley β-glucan, HEC, WSCA and cellulose were used to determine the substrate specificity of the FvXTH6 produced in yeast (Figure 17).

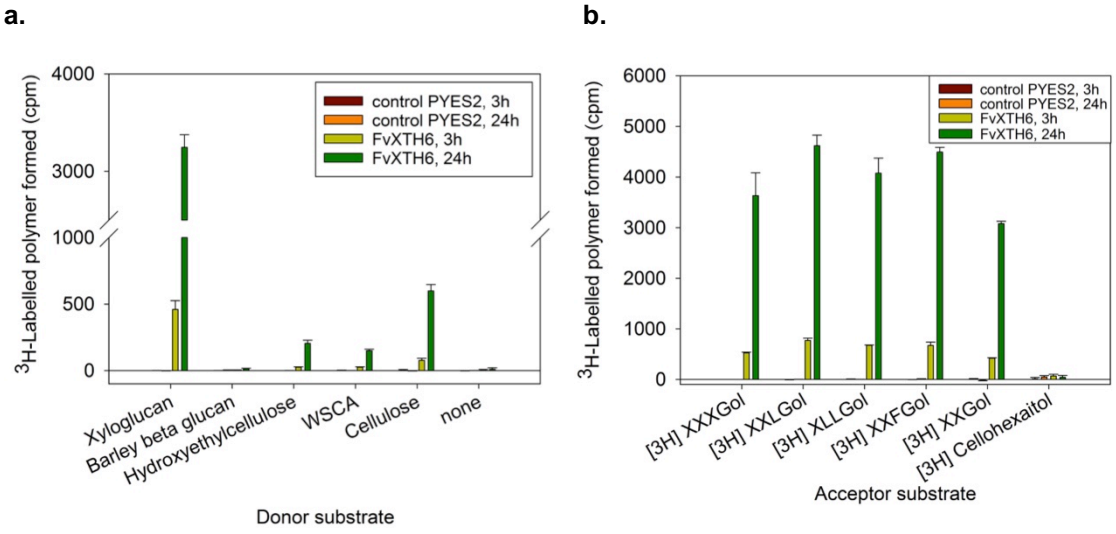

Figure 17. XET assay of FvXTH6.

a. Donor substrate preference (xyloglucan, barley β glucan, HEC, WSCA, cellulose), b. Acceptor substrate preference (XXXGol, XXLGol, XLLGol, XXFGol, XXGol, cellohexaitol). No XET activity was detected in a crude extract of empty vector-transformed Saccharomyces cultures (control PYES2). Each assay was performed in 4 replicates.

FvXTH6 used tamarind xyloglucan efficiently as a donor substrate, while low activity was observed for cellulose, HEC and WSCA. No enzyme activity was found using barley β-glucan. (Figure 17a). Acceptor substrates preference for FvXTH6 was XXLGol ≈ XXFGol > XLLGol > XXXGol > XXGol, although they showed only little differences in activity (Figure 17b).

3.4.3. Kinetic properties of FvXTH9 and FvXTH6

To investigate the kinetic parameters of FvXTH9 and FvXTH6 in more detail, both enzymes were expressed in yeast and purified as His_6 tag protein. XET activity was determined using a radioactive assay according to Fry *et al.* (1992).

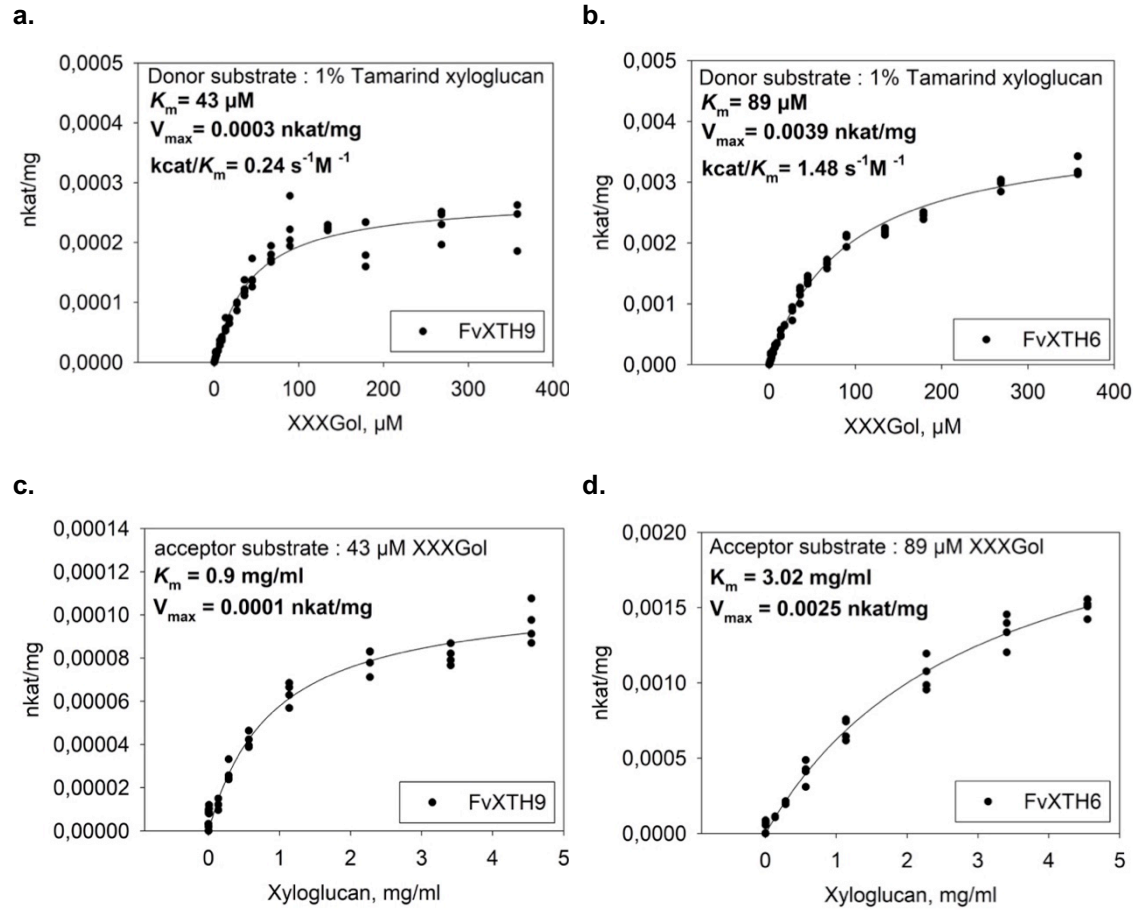

Figure 18. Kinetic properties.

Effect of acceptor-substrate concentration and donor-substrate concentration on transglucosylation rate catalysed by 1.01 mg/ml protein of FvXTH9 (a,c) and 0.86 mg/ml protein of FvXTH6 (b,d). K_m and V_{max} for XXXGol were determined using 1% (w/v) tamarind xyloglucan as donor substrate. K_m and V_{max} for xyloglucan were determined using [^{3}H]XXXGol at a concentration of approx. one time of the K_m for XXXGol, with various concentrations of the polysaccharide. Each assay was performed in 4 replicates.

For XXXGol, FvXTH9 displayed a K_m of 43 µM and a V_{max} of 0.003 nkat/mg. Recombinant FvXTH6 showed a K_m of 89 µM and a V_{max} of 0.039 nkat/mg for XXXGol. For xyloglucan, FvXTH9 showed K_m of 0.9 mg/ml and V_{max} of 0.0001 nkat/mg. The K_m and V_{max} of FvXTH6 for xyloglucan were 3 mg/ml and 0.0025 nkat/mg, respectively (Figure 18). K_m values for the donor substrate are quoted in mg/ml, not µM, because XTHs are able to utilize any segment of the polysaccharide chain equally, not only one site per molecule as with the acceptor substrate (Rose *et al.,* 2002).

3.4.4. XEH (xyloglucan endohydrolase) activity

To differentiate between XET and XEH activities, we used xyloglucan as a substrate and determined the molecular weight before and after the treatment with the putative XTH enzymes (Figure 19).

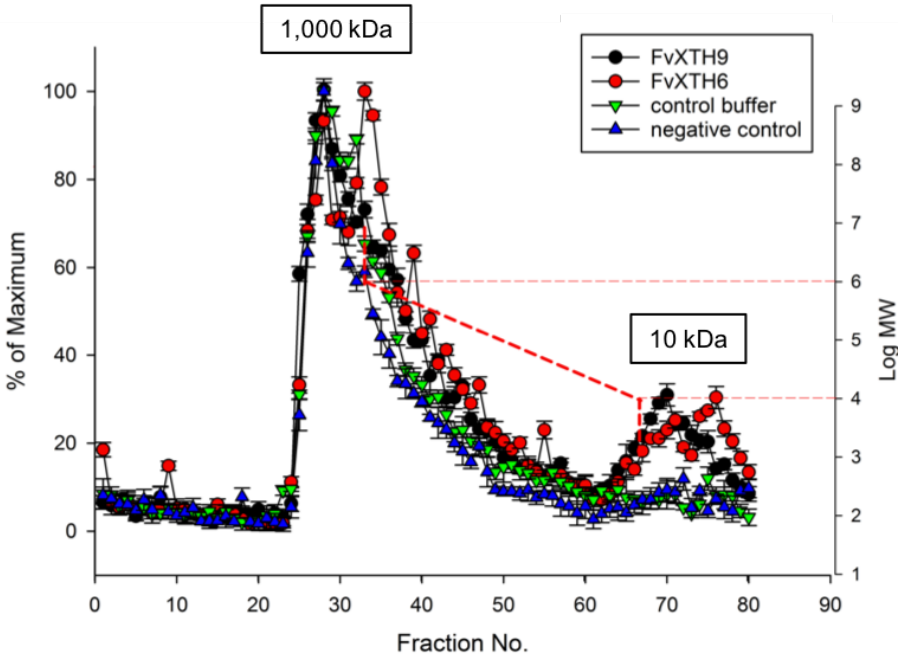

Figure 19. XEH activity of FvXTH6 and FvXTH9. The substrate was xyloglucan of median Mr 1,000 kDa. At intervals during xyloglucan hydrolysis, the median Mr was size-profiled by gel-permeation chromatography on Sepharose CL-6B. The red dashed line and right-hand y-axis indicate the scale used for approximating the Mr of the xyloglucan in each fraction. Dextrans (15 kDa - 25 kDa, 100 kDa, 670 kDa and 2000 kDa) and sucrose (342 Da) were used as markers. Buffer (control buffer) and crude extract of untransformed Saccharomyces culture (negative control) were used as control. XEH assay for each sample was performed in 3 replicates.

Analysis by gel permeation chromatography showed that the tamarind xyloglucan had a median molecular weight of approximaletly 1,000 kDa and no peaks were visible in the low molecular range (Figure 19). Also tamarind xyloglucan treated with a protein extract isolated from untransformed yeast showed a similar high molecular size distribution. In contrast, tamarind xyloglucan treated with FvXTH9 and FvXTH6 showed a significant peak in the low molecular range with median molecular weight of 10 kDa (Figure19), indicating that the used substrate was partially hydrolyzed by the expressed XTHs.

3.5. *In vivo* assay of FvXTH9 and FvXTH6

3.5.1. Direct localization of FvXTH9 and FvXTH6 in *Nicotiana tabacum* leaves.

3.5.1.1. Cloning of *FvXTH9* and *FvXTH6* using pGWR8 vector into *Agrobacterium tumefaciens* GV3101 cells.

To study the subcellular localization of FvXTH9 and FvXTH6 in plant cells, the full-length gene of *FvXTH9* and *FvXTH6* was fused with the *YFP* gene in the C-terminal position using the 35s CaMV promotor (Figure 20). The construct was transformed into *A. tumefaciens* GV3101 cells and agro-infiltrated via a syringe into *N. tabacum* leaves.

3.5.1.2. Fluorescent confocal microscopy analysis of FvXTH9-YFP and FvXTH6-YFP proteins.

Bioinformatic prediction of the sub-cellular localization for both FvXTH9 and FvXTH6 pointed to the endoplasmic reticulum using Predotar 1.04, the secretory pathway using TargetP 1.1 and MultiLoc2 and the cell wall using Plant-mPLoc online tools (Table 16). These predictions suggest that FvXTH9 and FvXTH6 travel from the ER via vesicles to the Golgi apparatus and finally to the cell membrane to be released into the extracellular environment.

Table 16. Prediction of the sub-cellular localization of FvXTH9 and FvXTH6.

Prediction tool	Reference	Results for FvXTH6	Results for FvXTH9
Predotar 1.04	(Small *et al.,* 2004)	ER (probability: 0.89)	ER (probability: 0.99)
TargetP 1.1	(Emanuelsson *et al.,* 2000)	Secretory pathway (probability: 0.958)	Secretory pathway (probability: 0.974)
Plant-mPLoc	(Chou and Shen, 2007, 2008, 2010)	Cell wall	Cell wall
MultiLoc2	(Blum *et al.,* 2009)	Secretory pathway (probability: 1.0)	Secretory pathway (probability: 0.99)

In order to provide experimental evidence for the subcellular localization of FvXTH9 and FvXTH6 in plant cells, the full-length coding sequence of *FvXTH9* or *FvXTH6* was fused C-terminal with the *YFP* gene and placed under control of the 35S CaMV promoter (Figure 20). The constructs were transformed into *A. tumefaciens* GV3101/pSoup cells and infiltrated into *Nicotiana tabacum* leaves. As a control, a construct expressing free YFP was infiltrated in the same way.

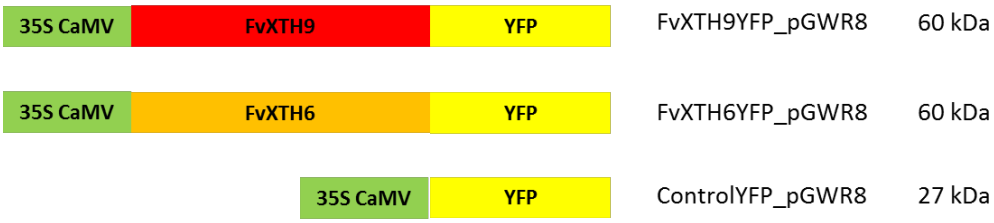

Figure 20. Schematic representation of recombinant pGWR8 constructs fused to YFP.

Confocal microscopy showed clear signals at the cell membrane and/or cell wall for both FvXTH9-YFP (Figure 21a) and FvXTH6-YFP (Figure 21b). For FvXTH6-YFP also clear signals could be observed in the cytoplasm. Interestingly, the signals of both proteins appeared mainly in spots of high intensity, indicating localization to sub-cellular structures like vesicles, the ER or specific regions of the cell membrane.

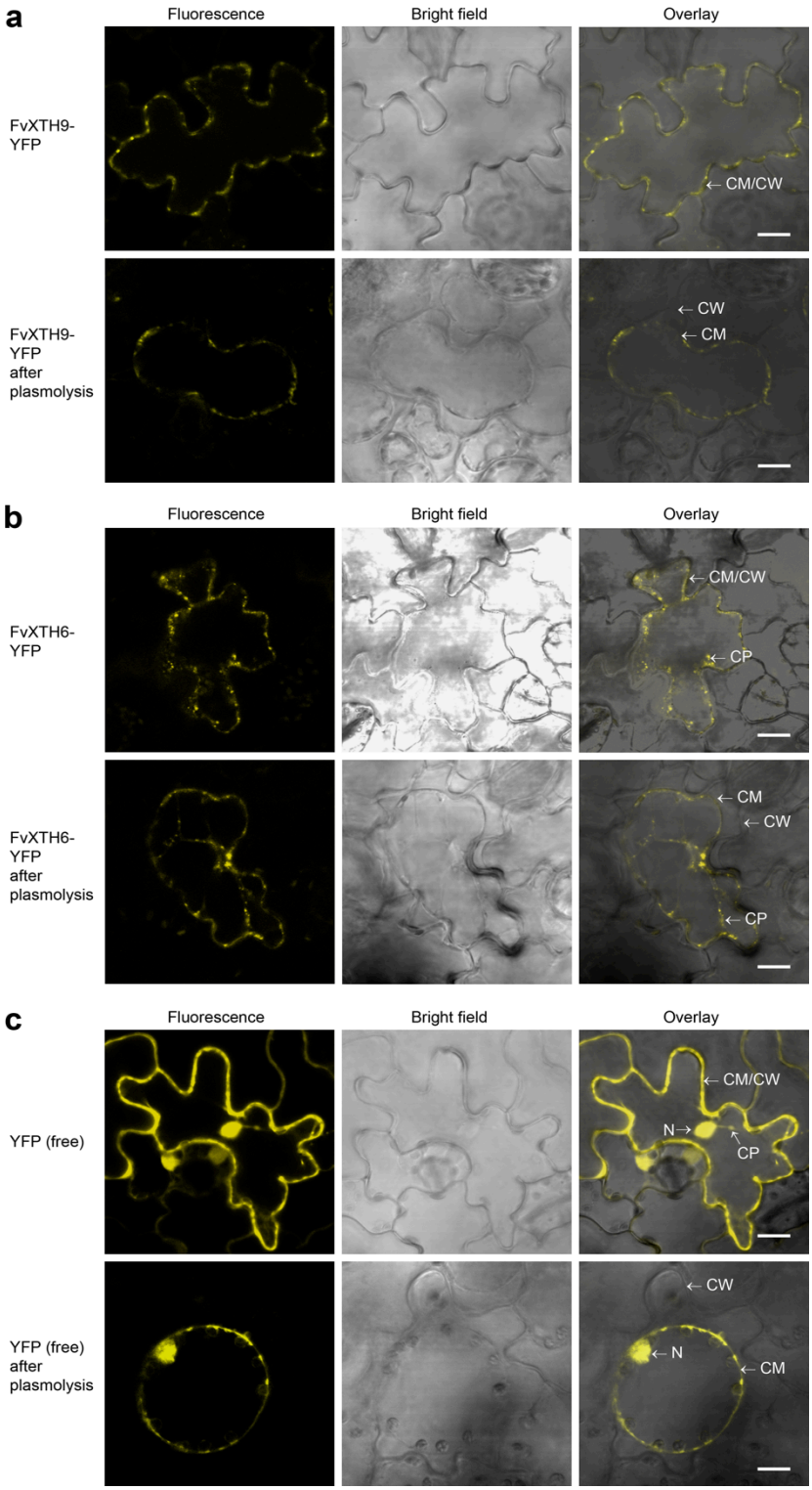

Figure 21. Localization of FvXTH9-YFP (a), FvXTH6-YFP (b), and control-YFP (c) in *N. tabacum* leaves.

Bright spots show high concentrations of XTH proteins fused to YFP in regions where the proposed substrate is localized. CW, cell wall; CM, cell membrane; CP, cytoplasm; N, nucleus.

In contrast, the signal for free YFP were more evenly distributed, as it is expected for a cytoplasmic protein (Figure 21c). To investigate a potential localization to the cell wall infiltrated plant cells were treated with 0.5% (w/v) NaCl for 30 min to induce plasmolysis. Under that condition no signals were visible in the cell wall while the spots in the cell were clearly visible, indicating that the proteins, if released from the cell, are not tightly associated with the cell wall. These results show that both, FvXTH9 and FvXTH6, are localized to the cell membrane. FvXTH6 appears also in spots in the cytoplasm, which represent likely vesicles of the secretory pathway.

3.5.2. Transient expression of FvXTH9 and FvXTH6 in *F. × ananassa* fruit

3.5.2.1. Cloning of *FvXTH9* and *FvXTH6* using pBI121 vector into *A. tumefaciens* AGL0 cells.

According to the RT-PCR data, large green fruit showed the highest expression level of the XTH genes, whereas red fruit have relatively low transcript levels (Figure 12). Therefore, overexpression of the target genes was performed to investigate the functional role of XTH genes in strawberry fruit. Full-length *FvXTH9* and *FvXTH6* genes were successfully cloned into pBI121 vector using 2x CAMV 35S promotor and transformed into *A. tumefaciens* AGL0 strain.

3.5.2.2. *F. × ananassa* fruit phenotypes after transient expression of *XTH* genes.

A. tumefaciens strain AGL0 transformed with pBI121 harboring the full-length *FvXTH9* and *FvXTH6* genes were evenly injected into completely white immature *F. × ananassa* fruits while they were still attached to the plant about 14 days after pollination. Infiltrated fruits were harvested 8, 10, 12 and 14 days post-infiltration (DPI). *F. × ananassa* fruit phenotypes showed that fruits infiltrated with *FvXTH9* and *FvXTH6* ripened faster compared to the control fruits at 8, 10 and 12 DPI (Figure 22).

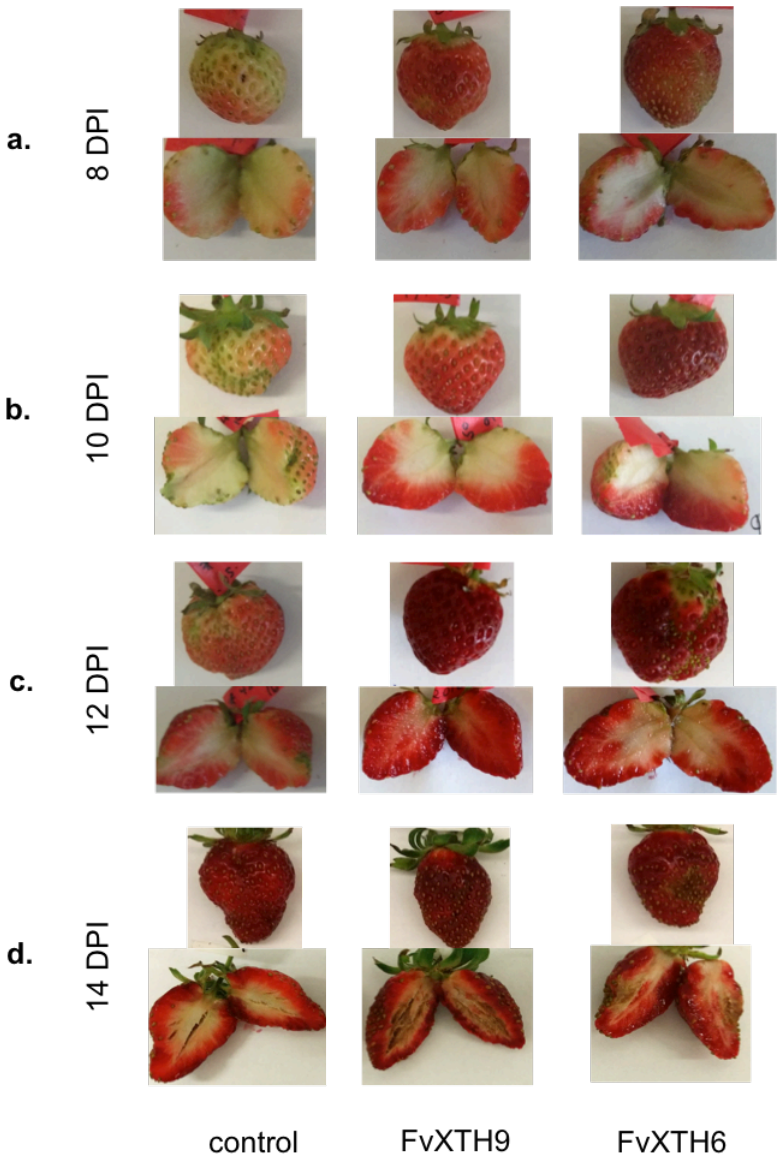

Figure 22. *F.* × *ananassa* fruit phenotypes after agro-infiltration of *FvXTH9* and *FvXTH6*

Fruit phenotypes at 8 DPI (a), 10 DPI (b), 12 DPI (c) and 14 DPI (d). Control pBI121 represented the empty vector-transformed Agrobacterium cultures. DPI, days post infiltration.

3.5.2.3. qPCR analysis after transient expression of *XTH* genes.

Quantitative PCR (qPCR) was performed to determine *XTH* transcript abundances in strawberry fruit after transient expression of *XTH* genes. *XTH* genes were highly expressed in both *FvXTH6* and *FvXTH9* infiltrated fruits

compared to control pBI121 fruits (Figure 23). Furthermore, expression level of *FvXTH9* and *FvXTH6* were increased from 8 to 12 DPI and dropped in 14 DPI. These data confirmed that *FvXTH9* and *FvXTH6* were successfully overexpressed in strawberry fruit.

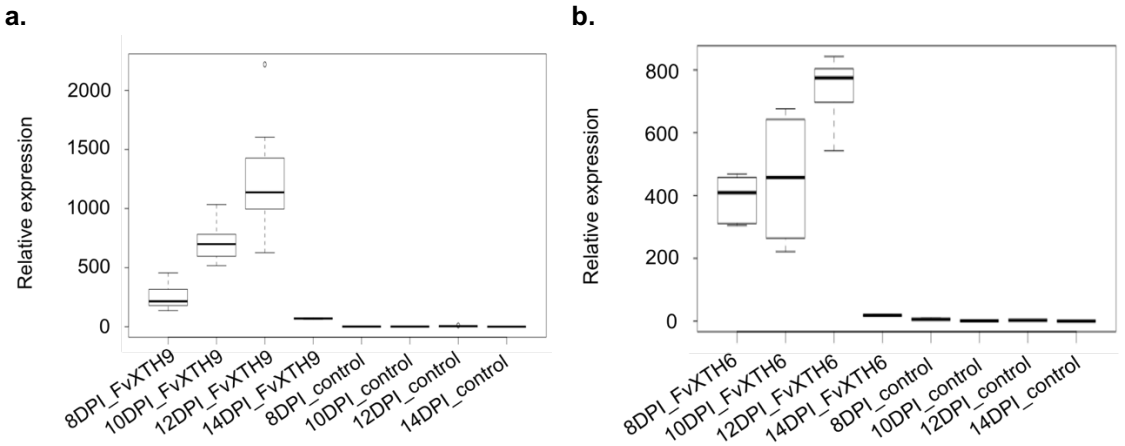

Figure 23. Quantitative PCR analysis of *FvXTH9* (a) and *FvXTH6* (b).

Analyses were performed with *F.* × *ananassa* fruit after agro-infiltration of *FvXTH9* and *FvXTH6* at 8 DPI, 10 DPI and 12 DPI. Control, control pBI121. Data was obtained by analyzing 2-3 biological replicates and 3 technical replicates.

3.5.2.4. Fruit firmness analysis

To evaluate the effect of *FvXTH6* and *FvXTH9* up-regulation on the rigidity of the strawberry fruit, the firmness of the fruit was measured using a texture analyzer (Figure 24). The result showed that a lower force was required to penetrate *FvXTH6* and *FvXTH9* agro-infiltrated fruits in comparison with control pBI121. This means that the fruit infiltrated with *FvXTH6* or *FvXTH9* were softer than control pBI121 fruit. The texture analysis data support the observation that both transgenic fruits ripened faster than the control pBI121 fruit.

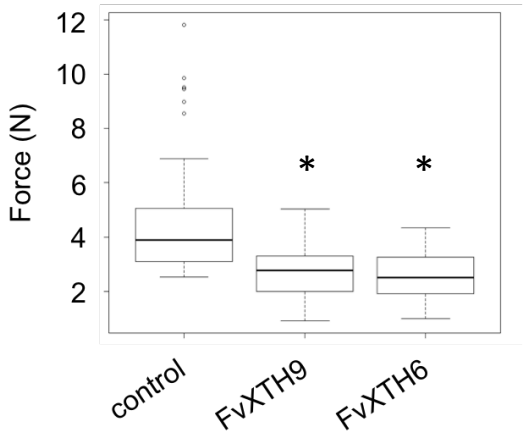

Figure 24. Texture analysis of *control pBI121*, *FvXTH9,* and *FvXTH6* agro-infiltrated fruits 12 DPI.

Texture analyzer was fitted with a 5 mm flat probe. Each fruit was penetrated 5 mm at a speed rate of 0.5 mm s^{-1} and the maximum force developed during the test was recorded in Newtons (N). The data was obtained by analyzing 60 fruits of each agro-infiltration experiment. The asterisks indicate statistically significant differences ($p < 0.05$) between fruits agroinfiltration with *XTHs* and the empty plasmid. Control fruit was infiltrated with *A. tumefaciens* AgL0 contained pBI121 empty plasmid.

3.5.2.5. Hemicellulose analysis

Hemicellulose analysis of *FvXTH9*, *FvXTH6,* and *control pBI121* agro-infiltrated fruits 12 DPI detected low molecular weight polymers of about 10 kDa in hemicellulose fractions in both infiltrated fruits and in negative control fruit in red fruit 12 DPI. (Figure 25). Unfortunately, hemicellulose distribution in unripe fruit was not investigated. It seems that overexpression of *FvXTH9* and *FvVTH6* did not further change the size distribution of 10 kDa hemicellulose oligomers.

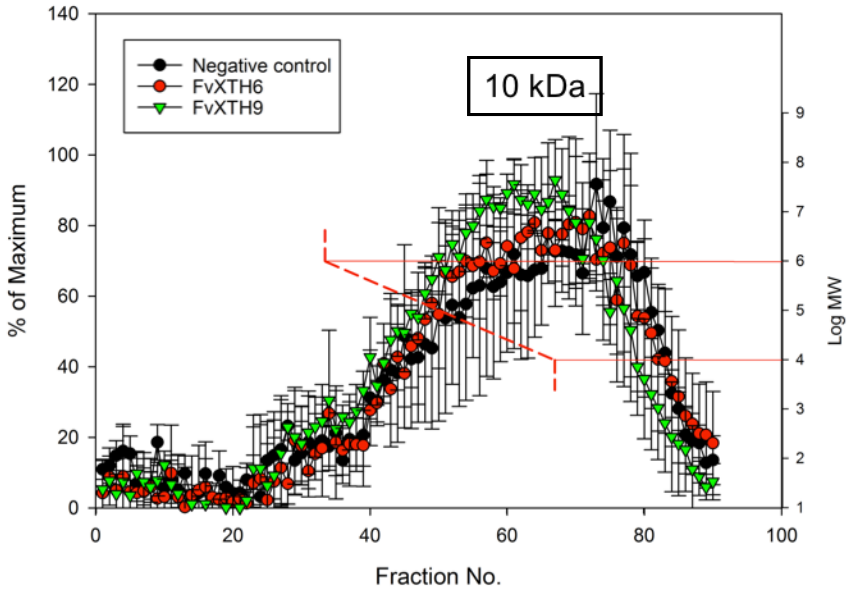

Figure 25. Hemicellulose analysis of *FvXTH9*, *FvXTH6,* and *control pBI121* agro-infiltrated fruits 12 DPI.

The median Mr was size-profiled by gel-permeation chromatography on Sepharose CL-6B. The red dashed line and right-hand y-axis indicate the scale used for approximating the Mr of the xyloglucan in each fraction. Dextrans (15 kDa - 25 kDa, 100 kDa, 670 kDa and 2000kDa) and sucrose (342 Da) were used as markers. The data was obtained by analyzing 3 replicates for each experimental set-up. Control fruit was infiltrated with *A. tumefaciens* AgL0 contained pBI121 empty plasmid.

3.6. Investigation of enzyme candidates related to the strawberry fruit ripening

3.6.1. Native PAGE purification from the ammonium sulphate 40-60% *F.* × *ananassa* fruit extract and detection of esterase activity in the gel

To investigate enzymes related to the strawberry fruit ripening, native proteins from a *F.* × *ananassa* fruit extract were isolated and purified. Esterases are good candidates because of their putative role in the degradation of cell wall components. Therefore, a *F.* × *ananassa* fruit protein extract was isolated using the ammonium sulphate precipitation. The ammonium sulphate 40-60% protein extract of *F.* × *ananassa* was then separated using native PAGE. Esterase activity was detected in the gel by application of α-naphthyl acetate as a substrate (Gabriel, 1971). Coupling of the released α-naphtol with a diazonium salt formed an insoluble yellow to red colour product (Figure 26B).

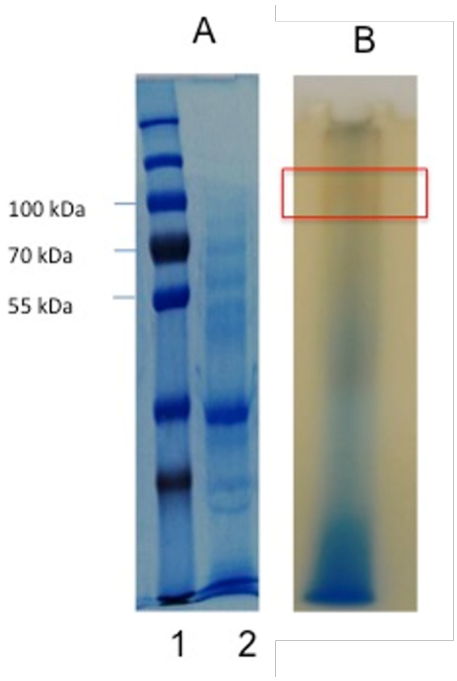

C

Protein	Gene	MW (kDa)
Pectinesterase 3 (PE3), Precursor (putative)	gene05463	65
Pectinesterase 1 (PE1), Precursor (putative)	gene05465	58
GDSL esterase/lipase At5g14450, Precursor (putative)	gene27964	43
Pectinesterase 34 (PE34) (similar to)	gene12871	72

Figure 26. SDS PAGE (A), native PAGE (B) analysis of an *F.* × *ananassa* fruit extract and results of the protein sequence analysis (C).

A yellow colour (in box) showed positive band of esterase assay in native PAGE.

3.6.2. Protein sequence analysis of the positive band

The protein band showing putative esterase activity in native PAGE was cut from the gel and sent for protein sequence analysis. The result showed several esterases as possible candidates (Figure 26C). Among these enzymes, GDSL esterase/lipase (gene27964) was chosen as a candidate for further analysis and cloning purpose. Four pectinesterase (PE) genes from strawberry, FaPE1, FaPE2, FaPE3, and FaPE4 have already been cloned (Castillejo *et al.,* 2004).

3.7. Putative GDSL esterase/lipase from *F. vesca*

3.7.1. NGS data of gene27964 (GDSL esterase/lipase At5g14450, Precursor (putative))

Transcriptomic data set of gene27964, namely *FvGDSL esterase/lipase* showed high expression level in green fruit of both receptacle and achenes from three *F. vesca* varieties: Reine de Vallées, Hawaii 4 and Yellow Wonder (Härtl *et al.,* 2017). Decreasing expression level was displayed during fruit ripening except in receptacle of Yellow Wonder variety. Expression level in receptacle is higher than in achene (Figure 27).

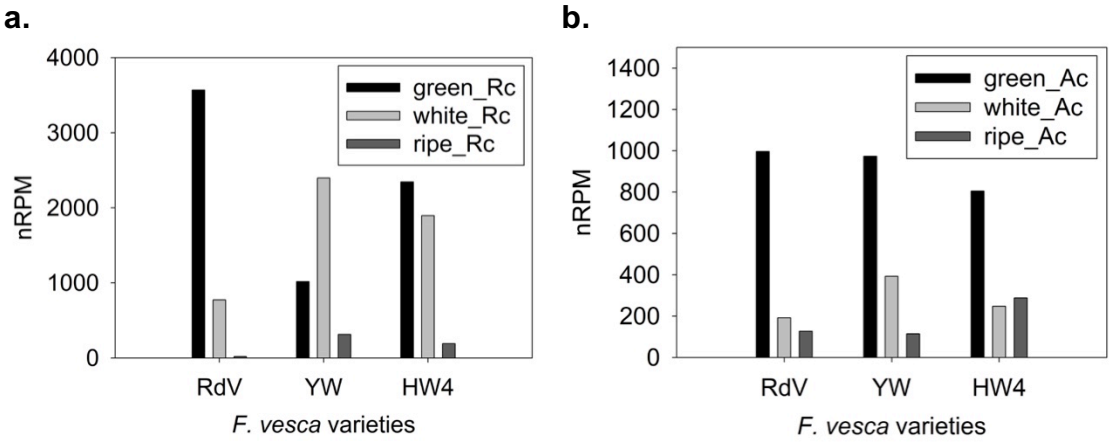

Figure 27. NGS data of gene27964 from three *F. vesca* varieties: Hawaii 4 (HW4), Reine des Vallées (RdV) and Yellow Wonder (YW).

Putative XTH genes were sorted in decreasing order of their expression levels in the receptacle (Rc) and achenes (Ac), displayed as nRPM (normalized read per million).

3.7.2. Quantitative PCR of gene27964 in *F. vesca* Hawaii 4 fruit and vegetative tissues

Quantitative real-time PCR was performed to investigate the expression levels of *FvGDSL esterase/lipase* in fruit, leaf and flower tissue of *F. vesca* (Figure 28). The result indicated a down up down expression pattern in fruit at different maturation stages. The expression level increased from small green to large green fruit and then decreased during fruit ripening. In vegetative tissue, the expression level in flower is higher than in both young and old leaves.

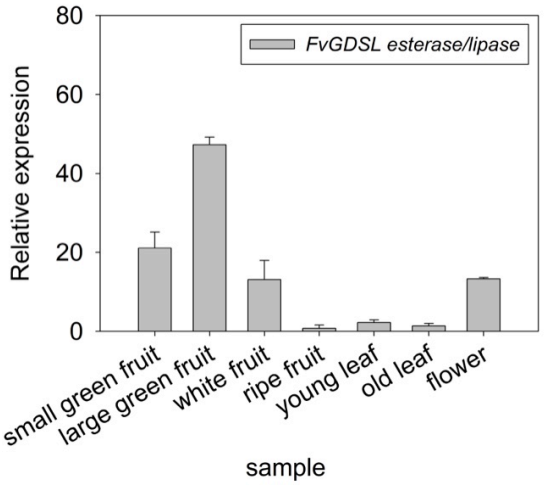

Figure 28. qPCR analysis of gene27964 in *F. vesca.* Hawaii 4

Analyses were performed in fruit tissues at different developmental stages (small green, large green, white and ripe fruit) and vegetative tissues (young leaf, old leaf and flower).

3.7.3. Multiple alignment sequence of FvGDSL esterase/lipase with others GDSL esterase/lipase enzyme

The primary sequence of FvGDSL esterase/lipase contained several conserved amino acid residues typical of the GDSL family. These include Gly-Asp-Ser-Asn (substitute Asn for Leu in FvGDSL) in the N-terminal region (Figure 29). Like other GDSL-motif proteins, FvGDSL contains the catalytic triad of residues Ser45, Asp364, and His367 (Upton and Buckley, 1995). Recently, the SGNH hydrolases were defined as a subgroup of the GDSL family based on the presence of four residues Ser (block I), Gly (block II), Asn (block III), and His (block V) (Molgaard

et al., 2000). Analysis of the FvGDSL primary sequence revealed the presence of four conserved peptides at Ser45, Gly84, Asn91, and His367 (Figure 29).

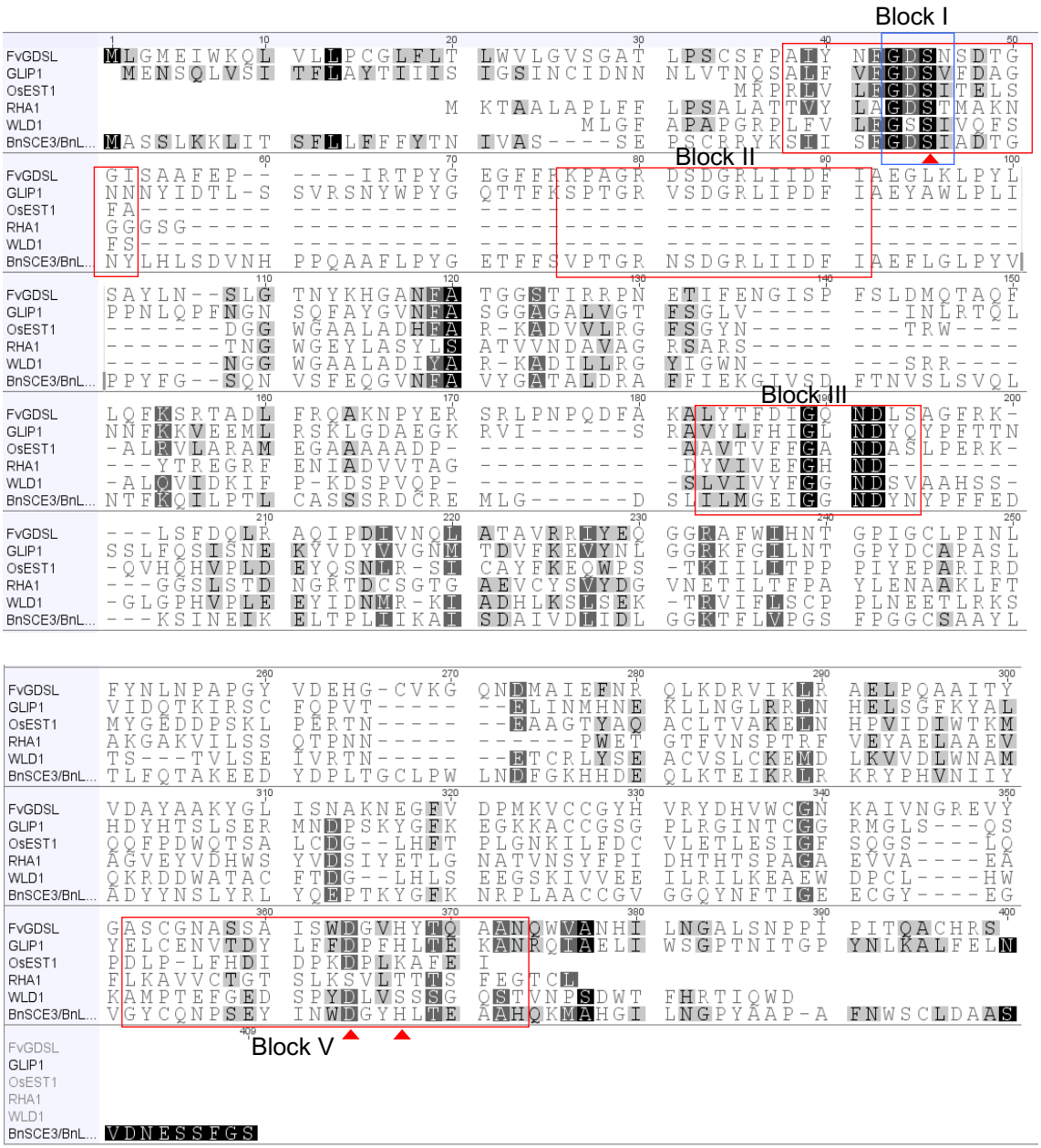

Figure 29. Amino acid sequence alignment of GDSL esterase/lipase enzymes using Clustal W software.

Sequences correspond to the following accession numbers: *A. thaliana* (GLIP1 (NP_198915.1), *Oryza sativa* (OsEST1 (AK061229.1), WLD1 (AK067429)), *Aspergillus aculeatus* (RHA 1 (UniProtKB-Q00017), *Brassica napus* (BnSCE3 (AAX62802.1)). Fully conserved residues are in blue frame box. Four conserved blocks in the SGNH-hydrolases family are in red lines box (I, II, III, V; Akoh *et al.,* 2004; Ling *et al.,* 2006). Amino acid residues forming the catalytic triad (Ser, Asp, His) in the consensus sequences of blocks I and V are marked by red triangles. One of the Gly residues in block II and Asn in block III potentially may also act as catalytic residues.

3.8. Cloning and heterologous expression of gene27964 (putative GDSL esterase/lipase At5g14450)

The gene27964 consists of 1.161 bp according to the *F. vesca* genome database (Shulaev *et al.,* 2011). Forward primer FP_GDSL 27964 and reverse primer RP_GDSL 27964 were used for target gene amplification from cDNA of *F.× ananassa* and *F. vesca* fruits. Bands of the correct size (1.2 kb) could be amplified from cDNA of *F.* × *ananassa* and *F. vesca* fruits except from small green fruit of *F.* × *ananassa* cDNA (Appendix 8).

The putative GDSL esterase gene from *F. vesca* and *F.* × *ananassa* was successfully cloned into PSK+ cloning vector in *E. coli* NEβ10 cell (Appendix 8). However, the sequence analysis of the isolated genes from *F. vesca* and *F.* × *ananassa* fruit cDNA showed 100% and 51% identity with gene27964 (putative GDSL esterase/lipase) of the *F. vesca* genome database, respectively. Furthermore, translation of the nucleotide sequence isolated from *F.* × *ananassa* fruit cDNA resulted many stop codons inside the sequence.

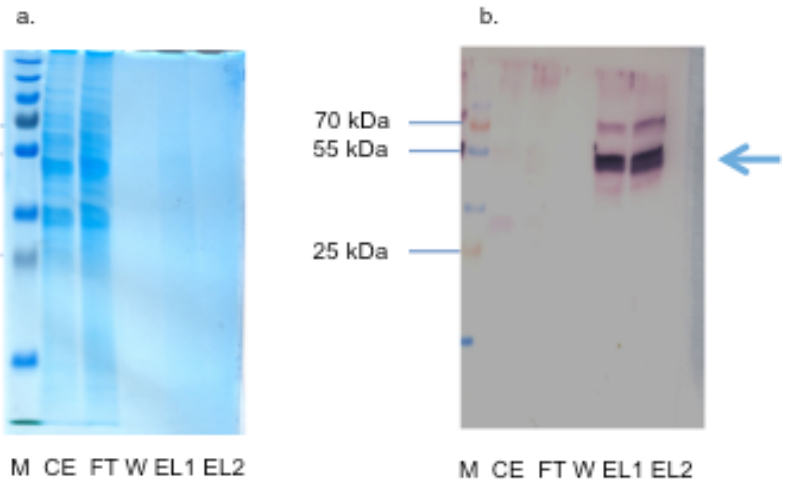

Figure 30. SDS PAGE (a) and western blot analysis (b) of recombinant FvGDSL esterase/lipase produced in *S. cerevisiae.*

M, protein marker; CE, crude extract; FT, flow through; W, wash; EL1, EL2, elution .

Therefore, only the target gene amplified from *F. vesca* fruit cDNA namely *FvGDSL esterase/lipase* was used for further cloning using the PYES2 expression vector. SDS-PAGE and Western blot analysis of the crude extract of the recombinant protein produced in yeast showed that FvGDSL esterase/lipase was successfully expressed as 43 kDa HisTag fusion protein (Figure 30).

3.9. Esterase assay of FvGDSL esterase/lipase

To investigate the enzymatic activity of FvGDSL esterase/lipase, preliminary esterase assays were performed using α-napthyl acetate, p-nitrophenyl acetate (p-NA), benzyl acetate and phenyl acetate as substrates. The result showed that crude extract of FvGDSL esterase/lipase produced high levels of the aromatic alcohol products (Figure 31). Although control PYES2 also hydrolyzed p-nitrophenyl acetate and benzy acetate to a certain extent, extracts containing FvGDSL esterase/lipase released higher amounts of the alcohols than crude extracts of control PYES2 (Figure 31).

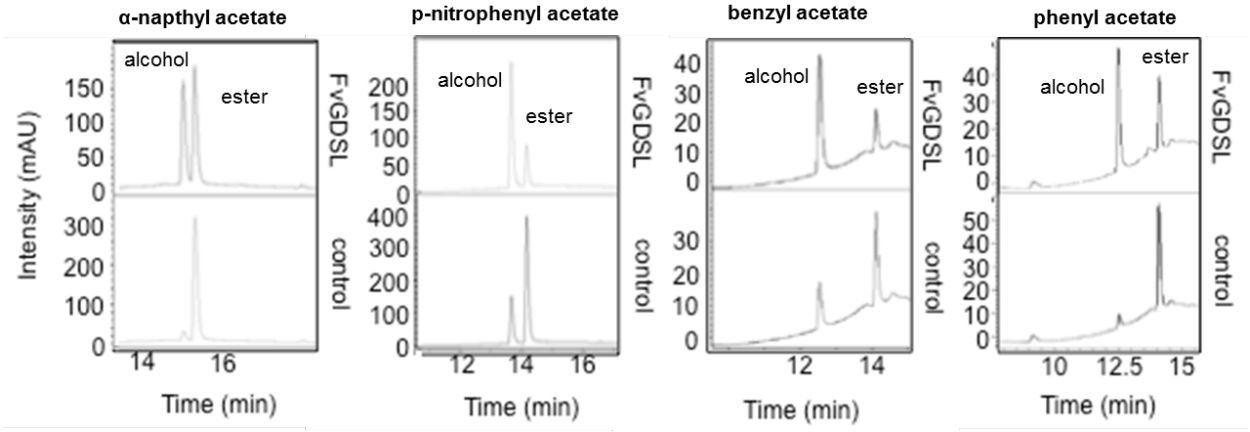

Figure 31. HPLC-UV esterase assay of FvGDL esterase/lipase.

Ester such as α-napthyl acetate (a), p-nitrophenyl acetate (b), benzyl acetate (c) and phenyl acetate (d) were used as substrate and incubated with crude extract of FvGDSL esterase/lipase. Crude extract of *S. cerevisiae* transformed with empty PYES2 vector (control PYES2) was used as negative control.

Finally, various pH values were tested using α-napthyl acetate as substrate, and crude extract of FvGDSL esterase/lipase expressed in yeast. The optimum pH for the esterase activity of FvGDSL esterase/lipase was pH 6.0 in potassium phospate buffer (Figure 32).

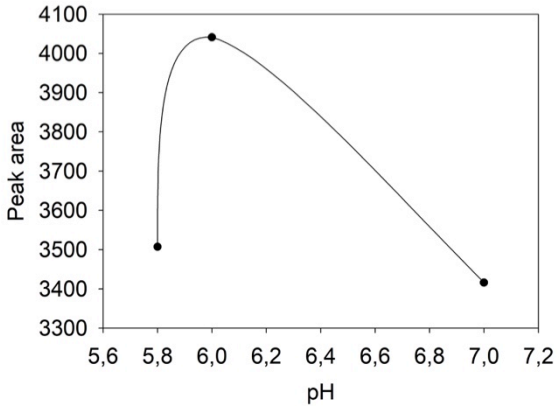

Figure 32. The pH optimum of FvGDSL esterase/lipase.

The ester α-napthyl acetate was used as substrate and incubated with crude extract of FvGDSL esterase/lipase. The product α-napthol was detected using LC-MS analysis. Assay was perform at 30ºC in potassium phosphate buffer at pH 5.8, pH 6.0, and pH 7.0.

The results showed that FvGDSL esterase/lipase is a promiscuous hydrolase accepting a range of small molecule esters as substrate.

4. DISCUSSION

4.1. Putative XTH family from *F. vesca*

Xyloglucan endotransglucosylase/hydrolases (XTHs) are cell wall-modifying enzymes and have been implicated in fruit softening during ripening. Here, we functionally characterized two phylogenetically related XTHs from *F. vesca,* which are differently transcribed during fruit development. There are 28 XTHs candidates in the *F. vesca* genome database (Shulaev *et al.,* 2011). The expression pattern of putative XTHs during strawberry fruit development displayed the highest expression level for *FvXTH9* (gene 01986) (Härtl *et al.,* 2017) (Figure 8). Since a phylogenetic analysis of different XTHs in diploid *F. vesca* showed that FvXTH9 was closely related to FvXTH6 (gene 05591) (Figure 7) we therefore selected *FvXTH9* and *FvXTH6* for biochemical and *in vivo* analysis.

The NGS data of *FvXTH9* and *FvXTH6* in fruit at different ripening stages of *F. vesca* was supported by qPCR data (Figure 12). The expression pattern of *FvXTH9* showed a low transcript abundance at the small green stage, the highest level at the large green stage and then a decrease by the end of ripening (ripe stage). *FvXTH6* displayed a similar pattern during ripening but at considerably lower absolute transcript levels. This gene expression pattern could be related to fruit growth in *F. vesca* (Perkins-Veazie, 1995). The higher expression of endogenous *FvXTH9* and *FvXTH6* genes during fruit growth than during ripening indicated that the primary role of these genes during fruit development maybe in cell expansion in the growing fruit. In addition, both *FvXTH9* and *FvXTH6* are highly expressed in flower. Furthermore, their expression in young leaves are higher than in old leaves suggesting that these genes could be related to cell wall modifications in vegetative tissues during growth.

The expression profile of *FvXTH9* and *FvXTH6* is comparable with *Fc-XTH1* (*F. chiloensis*), with high level in lower green (LG) and tuning (T) stages (Opazo *et al.,* 2010). In tomato fruit, SlXTH1 and SlXTH4 have a high expression level at the tomato immature green stage and the tomato mature green stage,

respectively (Miedes *et al.,* 2009). In kiwifruit, genes Ad-XTH1 and Ad-XTH4 have a “down-up-down” expression profile during softening (Atkinson *et al.,* 2009). In persimmon fruit, the expression of DkXTH1, DkXTH4, and DkXTH5 was very high in immature growing fruit and peaked before the mature stage (Yan *et al.,* 2015).

XTHs are grouped, according to phylogenetic analysis and biochemical data into class I/II, IIIA and IIIB (Baumann *et al.,* 2007). FvXTH9 and FvXTH6 are members of group I/II, together with PttXET16A (known as PttXET16-34; Johansson *et al.,* 2004). The classification of XTHs reflects the different biochemical mechanisms of enzyme action (Rose *et al.,* 2002). Members of groups I/II predominantly exhibit only XET activity (Maris *et al.,* 2011; Nishitani and Tominaga, 1992; Rose *et al.,* 2002), whereas members of group III have shown both XEH and XET activity (De Silva *et al.,* 1993; Fanutti *et al.,* 1993; Zhu *et al.,* 2012; Baumann *et al.,* 2007).

The common structural feature of XTH enzymes is the (D/N)E(I/L/F)DFEFLGN motif, which includes the catalytic active-site residues ExDxE (Campbell and Braam, 1999; Johansson *et al.,* 2004; Rose *et al.,* 2002). The amino acid sequences of FvXTH6 and FvXTH9 (Figure 11) also contain the conserved motif of XTH enzymes, suggesting that they have XET/XEH activities (Campbell and Braam, 1998). The first E (Glutamate) of the conserved sequence is proposed to be a crucial amino acid for the cleavage of (1-4)-β-glucosyl linkages (de Silva *et al.,* 1993; Okazawa *et al.,* 1993; Xu *et al.,* 1995). The substitution of the first E with Q (Glutamine) in At-XTH22, converting DEIDFEFL to DQIDFEFL, abolished XET activity (Campbell and Braam 1998). Although I (Isoleucine) is replaced by by F (Phenylalanine) at position 99 in FvXTH9 and L (Leucine) at position 109 in FvXTH6, the changes conserve the non-polar and uncharged nature of the residue and would not change the protein’s structure and property. The alteration of the first I to V (Valine) in XTH31 (*A. thaliana*) (Zhu *et al.,* 2012) and also to F (Phenylalanine) in a nasturtium seed XTH (de Silva *et al.,* 1993) caused no change in XET activity.

Beside this conserved motif, a potential N-linked glycosylation (N-X-S/T) site was present and cysteine residues were found in the carboxyl-terminal region indicating a potential anchor for the attachment of fatty acids. FvXTH9 and FvXTH6 have the putative N-glycosylation domain directly after the catalytic domain. Most of the XTH proteins have the N-glycosylation domain immediately or spaced by 5 to 15 amino acids from the catalytic domain, indicating that glycosylation modulates the enzyme function (Kallas *et al.,* 2005). The removal of this N-glycosylation site by site directed mutagenesis promotes a partial or total loss of XTH activity in *A. thaliana* (Champbell and Braam, 1998). The importance of the N-glycosylation domain could explain why the expression of FvXTH6 and FvXTH9 in *E. coli* yielded non-functional proteins.

4.2. Cloning of XTH genes from *F. vesca* and characterization of the recombinant proteins

Two full-length ORF sequences named *FvXTH6* and *FvXTH9* were successfully amplified from *F. vesca* Hawaii 4. The *FvXTH6* and *FvXTH9* cDNA were 880 and 882 bp long, respectively. *FvXTH6* was successfully cloned into pGEX-4T-2 plasmid in *E. coli* BL21 (DE3) cells and expressed as 59 kDa protein. Unfortunately, this recombinant protein FvXTH6 did not show any enzymatic activity using the XET assay. Therefore, *FvXTH6* was ligated into PYES2 and *S. cerevisiae* was chosen for expression the recombinant protein. Besides, FvXTH9 was similarly produced in *S. cerevisiae*.

The molecular weight (33 kDa) of FvXTH9 and FvXTH6 are comparable to other XTHs. In kiwifruit, Ad-XTH13 and Ad-XTH14 have 35.5 kDa and 36.7 kDa, respectively. Md-XTH10 in apple has 36 kDa (Atkinson *et al.,* 2009). Molecular weight of XTHs in barley, cauliflower and poplar were 33 kDa (Hrmova *et al.,* 2009), 32 kDa (Steele and Fry, 1999) and 30 kDa (Bourquin *et al.,* 2002), respectively.

4.3. *In vitro* assay of FvXTH9 and FvXTH6

4.3.1. Determination of optimal pH and temperature for XET activity

The XET activities of FvXTH9 and FvXTH6 showed optima at pH 6.5. The fact that both enzymes have very similar pH–activity profiles is not surprising as they are phylogenetically very closely related (Yokoyama and Nishitani, 2001; Baumann *et al.,* 2007). These acidic pH optima are typical of XTHs (Purugganan *et al.,* 1997; Campbell and Braam, 1999; Steele and Fry, 2000; Maris *et al.,* 2011). The pH optima of the recombinant PttXET16-34 is between 5 and 5.7 (Kallas *et al.,* 2005). AtXTH12 and the highly-sequence similar AtXTH13 show optima at pH 5.0 and 6.0, respectively (Maris *et al.,* 2011). The activity of hydrolases secreted into the cell wall is influenced by the wall environment, especially the pH value (Hoson, 1993; Hoson, 1998). The molecular mass of xyloglucans in azuki bean epicotyls has been shown to be decreased in acidic conditions (Nishitani and Masuda 1982). Since FvXTH9 and also FvXTH6 showed high activity in acidic conditions, it may also be involved in acid-induced cell wall expansion.

FvXTH6 showed the highest activity at 30 °C and has a very broad temperature range for activity, maintaining about 50% of their maximal activity between 4 °C and 45 °C. FvXTH6 still retained 60% of its maximal activity at 45 °C but at 0 °C its activity dropped to 30% of its maximum activity. Most XTH enzymes show broad temperature–activity profiles. The optimum temperatures of XTHs typically range from 18 °C to 37 °C. Extremes have been reported for heat-tolerant (55 °C) as well as cold-tolerant (–5 °C) enzymes (Purugganan *et al.,* 1997; Campbell and Braam, 1999; Steele and Fry, 2000; Kallas *et al.,* 2005; Van Sandt *et al.,* 2006).

4.3.2. Substrate specificity of FvXTH9 and FvXTH6

4.3.2.1. Donor substrate preference

Xyloglucan is the preferred donor substrate for both FvXTH9 and FvXTH6. Crude extract of FvXTH9 showed enzyme activity using barley β-glucan as well as HEC

as donor substrate (Figure 16). In contrast to FvXTH9, FvXTH6 did not accept barley β-glucan as donor substrate, indicating that it has no MXE activity. FvXTH6 could utilize also artificial substrates in the following order: cellulose > HEC > WSCA (Figure 17).

XTHs attack not only xyloglucan polymer but also some soluble artificial substrates. A pure XTH isoenzyme from barley could utilize xyloglucan (100% rate), HEC (44% rate), WSCA (5% rate), and CMC (0.4%) as donor-substrates (Hrmova´ *et al.,* 2007). For AtXTH12, AtXTH13, AtXTH17, AtXTH18, and AtXTH19 enzymes the non-xyloglucan polymers were preferred in the order: WSCA > HEC > MLG > CMC, but with very low activity rates for MLG and CMC (Maris *et al.,* 2010). Enzyme extracts from young shoots of *Equisetum* and the grass *H. lanatus* share similar donor-substrate profiles on artificial soluble β-glucans, with relative activities on xyloglucan:WSCA:HEC:CMC being 100:(20–24):(11–17):(0.4–1.5), suggesting that these four (1→4)-β-D-glucans are attacked by common XTHs (Fry *et al.,* 2008).

WSCA resembles the natural grass xyloglucans (Poaceae), which carrying an O-acetyl group on carbon 6 of the (1→4)-β-D-glucan backbone (Gibeaut *et al.,* 2005). Cellulose acetate with approximately 0.5–1.0 acetyl groups per Glc residue is water-soluble (Gomez-Bujedo *et al.,* 2004). Similar to the xylose residues of xyloglucan, most of the –CO-CH_3 groups in WSCA would be attached to position 6 of the Glc residues. Therefore, WSCA mimics xyloglucan sufficiently well to act as a donor-substrate for XTHs. HEC also resembles xyloglucan, but with –CH_2-CH_2OH groups in place of the xylose residues, and acts as an XTH donor-substrate (Mohand and Farkas, 2006; Hrmova *et al.,* 2007). Whereas, CMC has –CH_2-COO^- groups in place of xylose side chains.

4.3.2.2. Acceptor substrate preference

The acceptor substrate preference was studied on a selection of oligosaccharidyl-[^{3}H]alditols with various side-chains and backbones differing in the number of glucose units. XET activity for FvXTH9 and FvXTH6 differ in their oligosaccharide acceptor-substrate preference. The best acceptor substrate for

FvXTH9 is XXXGol followed by XXLGol and then XXFGol (Figure 16), whereas, both XXLGol and XXFGol are strongly preferred acceptor substrates for FvXTH6 followed by XLLGol. (Figure 17). The activity with the pentasaccharide XXGol compound is relatively low for both enzymes. FvXTH9 and FvXTH6 had lower activity with the doubly galactosylated acceptor substrate (XLLGol) and FvXTH9 also with the fucosylated substrate (XXFGol). The fucosyl residues are predicted to alter the conformation of the xyloglucan polymer (Levy *et al.,* 1997). This altered conformation may reduce XTHs binding.

XTHs are capable of attaching xyloglucan to xyloglucan-derived oligosaccharides with various side chains, but they show clear differences in their preferred side-chain substitutions. The composition of the xyloglucan side-chains substitutions on the glucan backbone, leading to different donor and acceptor substrates, was found to affect XET action differentially among XTHs isoforms (Purugganan *et al.,* 1997; Campbell and Braam, 1999; Steele and Fry, 2000).

These results may be compared with those published for other XTH isoenzymes. In pea seedling extracts, the preference for non-reduced acceptor-substrates was in the order XLLG > XXXG > XXFG > XXG; pea XET activity cannot act on GXG, XGG, XG, XGol or cello-oligosaccharides (Fry *et al.,* 1992; Lorences and Fry, 1993). Eight native XTH isoenzymes from Vigna and Brassica have the consistent order of acceptor substrate preference: XLLGol > XXLGol > XXXGol > XXGol (XGol was ineffective) (Steele and Fry, 2000). Seven Arabidopsis group-I/II XTHs (XTH12, XTH13, XTH14, XTH17, XTH18, XTH19, XTH26) operated satisfactorily on XXXGol, XXLGol, XLLGol and XXFGol (Maris *et al.,* 2009, 2011). Of these four acceptor substrates, the mono-galactosylated octasaccharide XXLGol gave the highest (or joint-highest) rate with XTHs 13, 14, 17, 18, 19 and 26. Only XTH12 showed a noticeably higher rate with XXFGol. Acceptor preferences were XXXGol > XXFGol > XXLGol > XLLGol > XLFGol for Arabibdosis XTH31 and XXXGol > XLLGol > XLFGol > XXLGol > XXFGol for Arabibdosis XTH15 (Shi *et al.,* 2015).

Our result also showed that FvXTH9 has not only XET but also MXE activity because barley β-glucan functioned as donor-substrate. The acceptor substrate

preference for MXE was XXXGol > XXLGol > XLLGol > XXGol > XXFGol > XGol (Figure 16). The order of the acceptor preference of MXE activity is slightly different from that of XET but the relative activities of the less preferred substrates are considerably lower. For XET activity, heptasaccharide XXXGol which lacks Gal and Fuc is the best acceptor-substrate tested, followed by XXLGol, XXFGol and then by XLLGol. The pentasaccharide XXGol is a poor acceptor substrate. However, for MXE activity, although the first three preferred substrates are identical to XET (XXXGol, XXLGol and XLLGol), the following substrate is different: XXGol. Here, the fucosylated form XXFGol is ineffective. Both have no activity for XGol. Furthermore, MXE activity is lower than XET for FvXTH9.

In case of MXE activity of Equisetum (Fry *et al.,* 2008), the acceptor-substrate profile was distinctly different from that of XET. The best acceptor-substrate tested was XXXGol (both XLLGol and XXGol being much less effective) whereas, XLLGol was the best acceptor-substrate for XET, followed by XXXGol and then XXGol. The finding that MXE activity can exceed XET activity indicates that Equisetum possesses enzymes in which the favoured donor-substrate was MLG. These data emphasize enzymological differences between the proteins catalyzing MXE and XET activities.

4.3.3. Kinetic properties of the recombinant XTH

XET catalytic properties of the purified recombinant FvXTH9 and FvXTH6 towards tamarind xyloglucan and XXXGol were determined. Various amount of the XXXGol concentration (at a constant 1% (w/v) tamarind xyloglucan) produced classical hyperbolic Michaelis-Menten curves. FvXTH9 showed a higher affinity for XXXGol (K_m = 43.22 µM) than FvXTH6 (K_m = 89.45 µM) probably because XXXGol is the preferred acceptor substrate for FvXTH9. K_m values for XXXGol of both enzymes are within the range of others XTHs. For example, Arabidopsis XTH15 and XTH31 had K_m values of 31 µM and 86 µM, respectively (Shi *et al.,* 2015) whereas, XET activity from Equisetum and barley showed K_m value of 80 µM (Fry *et al.,* 2008) and 40 µM (Hrmova *et al.,* 2009), respectively. Higher K_m values were found in cultured poplar cells and ripening kiwifruit with the values of 320 µM and 100 µM, respectively (Schröder *et al.,* 1998; Takeda *et al.,* 1996).

Calculation of the catalytic properties of FvXTH6 towards xyloglucan revealed a K_m of 3.02 mg/ml indicating a lower affinity than FvXTH9 (K_m = 0.9 mg/ml). These results were comparable to others XETs. XET activity for xyloglucan was reported in Equisetum (K_m = 0.35 mg/ml; Fry *et al.,* 2008), in kiwifruit (K_m = 0.6 mg/ml; Schröder *et al.,* 1998), in Arabidopsis (XTH22; K_m = 1.8 and 0.6 mg/ml for fucosylated and non-fucosylated xyloglucans respectively; Purugganan *et al.,* 1997 and XTH15, K_m = 2.87 mg/ml; Shi *et al.,* 2015). There was no decrease in the rate of ^{3}H incorporation at the highest concentrations of non-radioactive xyloglucan, indicating that 4.5 mg/ml polysaccharide (20 µM) did not appreciably compete with [^{3}H]XXXGol (43.22 µM for FvXTH9 and 89.45 µM for FvXTH6) as acceptor substrate.

4.3.4. XEH activity

FvXTH9 and FvXTH6 showed XEH activity. XEH activity was measured using tamarind xyloglucan as sole substrate. In the absence of acceptor substrate, XET activity will be a rare occurrence since the only available acceptor substrates for a transglycosylation reaction are other xyloglucan molecules. FvXTH9 and FvXTH6 hydrolyzed 1,000 kDa tamarind xyloglucan, which resulted in 10 kDa oligosaccharides (Figure 19). Interestingly, although FvXTH9 and FvXTH6 belong to the group I/II of XTHs they also exhibit XEH activity. This activity finding is different from the member of groups I XTHs that exhibit only XET activity (Maris *et al.,* 2011; Nishitani and Tominaga, 1992; Rose *et al.,* 2002). Wildtype enzymes of PttXET16-34, as well as its respective glycosylation mutants were considered as transglycosylases, since no hydrolytic activity could be measured with the bicinchoninic acid (BCA) assay (Kallas *et al.,* 2005).

Proteins with XEH activity can reduce the molecular weight of xyloglucan, for example during fruit ripening (Rose and Bennett 1999). One XTH gene product from azuki bean (*Vigna angularis* Ohwi et Ohashi cv. Takara) epicotyls has been reported to be purely hydrolytic (Tabuchi *et al.,* 2001). An increase in reducing power in xyloglucan solution was clearly detected after treatment with the purified enzyme. Xyloglucans with molecular masses of 500 and 25 kDa were gradually hydrolyzed to 5 kDa for 96 h without production of any oligo- or monosaccharide

with the purified enzyme. The purified enzyme did not show an endo-type transglycosylation reaction, even in the presence of xyloglucan oligosaccharides. Another enzyme has been purified from kiwifruit cell wall (Schröder *et al.,* 1998). Kiwifruit core XET was capable of depolymerising xyloglucan in the absence of [^{3}H]XXXGol by hydrolysis, and in the presence of [^{3}H]XXXGol by hydrolysis and endotransglycosylation.

4.4. *In vivo* assay of recombinant FvXTH9 and FvXTH6

4.4.1. Direct localization of FvXTH9 and FvXTH6 in *N. tabacum* leaves.

Prediction of the sub-cellular localization revealed for both FvXTH9 and FvXTH6 localization to the secretory pathway or to organelles associated with the secretory pathway. This could be confirmed by confocal microscopy of tobacco leaves agroinfiltrated with YFP-tagged versions of FvXTH9 and FvXTH6, which localize to the cell membrane and the vesicle of the secretory pathway (Figure 21a and 21b). In contrast, cell transformed with YFP alone (control YFP) showed uniform YFP fluorescence throughout the cell wall, cell membrane, cytoplasm and nucleus (Figure 21c). Non-plasmolyzed cell showed that FvXTH9-YFP fusion protein was obviously found in the cell wall and/or in the cell membrane. After plasmolysis, FvXTH9-YFP was specifically localized in the cell membrane (Figure 21a). FvXTH6-YFP fusion protein was found not only in the cell wall and/or cell membrane but also in the cytoplasm before plasmolysis. Plasmolyzed cell showed that localization of FvXTH6-YFP was clearly in plasma membrane and also in the cytoplasm, which indicated likely vesicles of the secretory pathway (Figure 21b).

This finding suggests that FvXTH9 and FvXTH6 could be anchored to the cell membrane as they contain predicted N-terminal signal peptides targeting the proteins. Further research need to verify the presumed signal peptides (N-terminal amino acids) of FvXTH6 and FvXTH9. Since xyloglucan is synthesized in the Golgi and transported via exocytosis to undergo transglycosylation immediately upon release into the wall (Thompson and Fry, 2001), the

membrane-localized FvXTH9 and FvXTH6 may be well positioned for catalyzing either this process or the partial hydrolysis of newly secreted xyloglucans.

Other XTHs have also been reported to be plasma membrane localized. The full-length Arabidopsis XTH31-GFP fusion protein was targeted to the plasma membrane by an N-terminal signal peptide (Zhu *et al.,* 2012). Arabidopsis XTH33 was also plasma membrane localized (Ndamukong *et al.,* 2009). In contrast, the *PeXTH* gene from *Populus euphratica* localized exclusively to the endoplasmic reticulum and cell wall in transgenic tobacco (Han *et al.,* 2013). DkXTH8 protein was directly localized to the cell wall via its signal peptide in onion epidermal cells (Han *et al.,* 2016).

4.4.2. Transient expression in *F. × ananassa* fruit

To confirm whether FvXTH9 and FvXTH6 are involved in fruit ripening and softening, overexpression of the target genes in strawberry fruit was performed. Quantitative PCR analyses confirmed that *XTX* genes were successfully overexpressed in both *FvXTH9*- and *FvXTH6*-agroinfiltrated fruits. The expression patterns of both genes increased from 8 to 12 DPI and then decreased significantly in 14 DPI (Figure 23). In contrast, low transcript levels of *FvXTH9* and *FvXTH6* were detected in control pBI121 fruits.

Overexpression of gene products in plants may change the phenotypes. The results showed that fruits infiltrated with *FvXTH9* and *FvXTH6* exhibited accelerated color change and ripened faster compared to the control pBI121 (Figure 22). To support this finding, the differences in fruit firmness at 12 DPI were recorded. Compared to control pBI121 fruit, the *FvXTH9* and *FvXTH6* infiltrated fruits showed decreased firmness (Figure 24). The texture analysis supported the observation that fruits of both transgenics ripened faster than the control fruit. Opazo *et al.,* 2010 reported the changes in fruit firmness during development and ripening in *F. chiloensis.* The finding showed that the main reduction in firmness occurs between large green (LG) and turning (T) stages. Because the expression profile for *Fc-XTH1* transcripts showed a high level at LG and T stages, it was suggested that Fc-XTH1 might be involved in *F.*

chiloensis softening. Similarly, overexpression of *DkXTH8* in tomato fruit led to accelerated color change and decreased firmness compared to wild type fruit (Han *et al.,* 2016) whereas UV-C irradiation of tomato fruit reduced the activity of cell wall-degrading enzymes and delayed the ripening of tomato fruit. Irradiated fruit were firmer than control (Barka *et al.,* 2000).

We also investigated the modification of hemicelluloses to elucidate the role of these polymers in fruit softening. The average molecular weight of hemicellulose in red, ripe strawberry fruit (12 DPI) was 10 kDa not only of the *FvXTH9* and *FvXTH6* infiltrated fruits but also in the negative control fruit (Figure 25). Unfortunately, we did not investigate the molecular weight of hemicellulose in unripe strawberry fruit. However, this finding implies that in the ripe fruits hemicellulose is already completely hydrolysed to 10 kDa breakdown products that cannot be further degraded by FvXTH6 and FvXTH9. We hypothesize that these degradation products are no longer substrates of XTHs.

During fruit ripening, hydrolytic enzymes are produced to achieve efficient cell wall degradation (Johansson *et al.,* 2004). A significant reduction of hemicelluloses was detected in the high-molecular-weight region *(*Mr > 170 kDa) of green strawberry fruit (Nogata *et al.,* 1996). Huber, 1984 also reported depolymerization of hemicellulosic polymers during ripening in strawberry. Hemicelluloses from small green and large green strawberry fruit show a consistent predominance of high-molecular weight polymers. Changes were first evident in fruit at the onset of ripening (white fruit) and more alteration was apparent as ripening proceeded. Similarly, the maintenance of fruit firmness was associated with the increased molecular mass of xyloglucan in tomato fruit, and the depolymerization of xyloglucan molecules resulted in tomato fruit ripening (Miedes *et al.,* 2009).

The qPCR analysis of different maturation stages of *F. vesca* Hawaii 4 fruit (Figure 11) revealed that expression of endogenous FvXTHs decreased significantly at fruit ripening. Therefore, the degradation of xyloglucan in ripe fruit might be also induced by another factor such as auxin. Auxin induced degradation (Labavitch and Ray 1978), solubilization (Terry *et al.,* 1981),

decrease in molecular mass (Nishitani and Masuda 1981, Nishitani and Masuda 1983), and stimulation of autolysis (Hoson 1990) of xyloglucans, when it stimulates elongation of stem segments in dicotyledons.

Overexpresion of FvXTH9 and FvXTH6 in strawberry fruit accelerated color change and decreased firmness compared to wild type fruit. These results suggested that the genes *FvXTH9* and *FvXTH6* might be involved in the texture changes associated with ripening of strawberry fruit through involvement in cell wall restructuring such as hemicellulose metabolism. Thus, genetic regulation of hemicellulose metabolism during fruit development and ripening appears to be particularly crucial.

4.5. GDSL esterase/lipase

Fruit softening is mainly the result of the action of hydrolytic enzymes such as hydrolases that modify the carbohydrate components of the cell wall. In association with xylanases, cellulases, and mannanases, acetylxylan esterase may participate in the degradation of plant cell walls. Three *Neocallimastix patriciarum* esterases involved in the degradation of complex polysaccharides were found to belong to the GDSL-family (Dalrymple *et al.,* 1997). They have acetylxylan esterase activity, able to remove O-acetyl groups from xylose residues in xylan and xylo-oligomers. *Aspergillus aculeatus* produces rhamnogalacturonan acetylesterase (RGAE), a member of the SGNH-family that is able to perform a synergistic degradation of rhamnogalacturonan (Molgaard *et al.,* 2000). GDSL1 can exhibit both hydrolase and transferase activities. Indeed, a plant GDSL-lipase involved in pyrethrins biosynthesis harbors transferase activity *in vivo* and esterase activity *in vitro* (Kikuta *et al.,* 2012). These dual activities are similar to XTH that display hydrolase and transferase activities (Rose *et al.,* 2002). Pectin esterase (PE) activity has also been reported in ripening strawberry fruits (Neal, 1965; Barnes and Patchett, 1976). Therefore, native protein from *F.* × *ananassa* fruit extract were isolated and purified to investigate a new esterase enzyme.

Ammonium sulphate precipitation was used to isolate target proteins from *F.* × *ananassa* fruit. Esterase activity assay in the native PAGE gel resulted a positive band of α-naphtol production. This band was sequenced and resulted several esterases candidates such as pectinesterase 3 (gene05463), pectinesterase 1 (gene05465), GDSL esterase/lipase (gene27964), pectinesterase 34 (gene12871) and other enzymes. Pectinesterase 1 (PE1) and pectinesterase 3 (PE3) have been characterized (Castillejo *et al.,* 2004). Therefore, FvGDSL esterase/lipase was chosen as a candidate.

GDSL esterases/lipases might play a role in the regulation of plant development and morphogenesis. Plant GDSL-lipases are generally depicted as acylhydrolases (Abdelkafi *et al.,* 2009; Updegraff *et al.,* 2009). Their hydrolytic activity has been widely associated with seed germination (Clauss *et al.,* 2008), pollen hydration (Updegraff *et al.,* 2009), pathogen defense (Oh *et al.*, 2005; Kwon *et al.,* 2009; Lee *et al.,* 2009), and the abiotic stress response (Hong *et al.,* 2008; Zhou *et al.,* 2009).

The NGS data of *FvGDSL esterase/lipase* in fruit at different ripening stages (Härtl *et al.,* 2017) of *F. vesca* Hawaii 4 variety was supported by qPCR data. The highest expression level was found in green fruit and then decreased during fruit ripening. The expression pattern of *FvGDSL* resembled those of *FvXTH6* and *FvXTH9*.

Multiple alignment sequence of FvGDSL esterase/lipase with others GDSL esterase/lipase enzyme revealed the conserved motif and catalytic triad of the FvGDSL esterase/lipase (Figure 29). GDSL lipases constitute a subclass of lipolytic enzymes characterized by a distinct GDSL sequence motif. These include Gly-Asp-Ser-(Leu) in the N-terminal region (Akoh *et al.,* 2004). Conserved residues in FvGDSL are Gly-Asp-Ser-Asn at position 43-46, whereas OsEst1 (*Oriza sativa*) and BnSCE3/ BnLIP2 (*Brassica napus*) have Ile for Leu substitution (Hamada *et al.,* 2012; Clauss *et al.,* 2008). The active centre of these enzymes is formed by a catalytic triad consisting of the seryl residue from the GDSL motif, which is part of the conserved peptide block I, and aspartyl and histidyl residues that are both located in the conserved peptide block V. This implies that, in

FvGDSL, the catalytic triad is most probably composed of Ser^{45}, Asp^{364}, and His^{367}. Within the GDSL subclass, FvGDSL belongs to the subgroup of SGNH hydrolases that are characterized by the presence of the four strictly conserved residues Ser, Gly, Asn and His in four conserved peptide blocks I, II, III, and V, respectively (Molgaard *et al.,* 2000; Ling *et al.,* 2006). Each of the four residues plays an important role in enzyme catalysis. The Ser residue in block I serve as the catalytic nucleophile and proton donor to the oxyanion hole. The Gly residue in block II and the Asn in block III serve as two proton donors to the oxyanion hole. The His residue in block V acts as a base to make the active site Ser more nucleophilic by deprotonating the hydroxyl group (Akoh *et al.,* 2004).

GDSL esterases/lipases are hydrolytic enzymes with multifunctional properties such as broad substrate specificity. Preliminary esterase assays showed positive results for all tested small molecule ester substrates. The result showed that FvGDSL esterase/lipase has carboxylesterases activity.

The p-nitrobenzyl esterase (PNB carboxy-esterase) catalyzed rapid ester hydrolysis for simple organic esters such as PNB-acetate, benzyl acetate and α-naphthyl acetate (Chen *et al.,* 1995). OsEST1 showed high activity using α-naphthyl acetate as a substrate with K_m and V_{max} values of 172 µM and 63.7 µmol/min/mg protein, respectively. The relative activity for 1-naphthyl butyrate was only 0.87% of the value for 1-naphthyl acetate. Furthermore, when triacylglycerols, such as trybutyrine and olive oil, were used as substrates, OsEST1 did not show any detectable activity. These data indicate that OsEST1 strictly recognizes small molecule esters and cannot be considered a lipase (Hamada *et al.,* 2012). Cbes-AcXE2 hydrolyzed p-nitrophenyl (pNP) acetate, pNP-butyrate, and phenyl acetate with approximately equal efficiency. The specific activity and K_M for the most preferred substrate, phenyl acetate, were 142 U/mg and 0.85 mM, respectively (Soni *et al.,* 2017). Enod8 is a Medicago nodule specific gene of the GDSL family of lipases and esterases found in *Medicago sativa* (alfalfa) and *M. truncatula* (model legume) as well as in bacteria. Purified Enod8 proteins were found to possess esterase activity on acetyl and butyryl esters but no longer chain aliphatic esters (Pringle *et al.,* 2004).

Recombinant *Arabidopsis* GDSL lipase 2 (GLIP2) protein possessed lipase activity. This enzyme hydrolyzed p-nitrophenyl acetate and p-nitrophenyl butyrate (Lee *et al.,* 2009).

Esterase assays showed that the crude extract of FvGDSL esterase exhibited highest enzymatic activity at pH 6.0 in phosphate buffer. OsEST1 was most active at pH around 8.0-8.5 (Hamada *et al.,* 2012) and a purified enzyme Cbes-AcXE2 showed an optimum pH of 7.5 (Soni *et al.,* 2017). It appears that GDSL hydrolases have quite different pH optima. Although first enzymatic activity of FvGDSL has been demonstrated further experiments are required to study the biological function of this enzyme during strawberry ripening.

5. CONCLUSION

Two functional xyloglucan endotransglucosylase/hydrolases, FvXTH9 and FvXTH6 were identified from *F. vesca. FvXTH9* is highly expressed in immature fruits and then the transcript levels decrease until full maturity. The recombinant FvXTH9 and FvXTH6 protein showed strict XET activity and XEH activity. In addition, FvXTH9 has also MXE activity. Overexpression of FvXTH9 and FvXTH6 resulted in accelerated fruit softening in strawberry fruit. Thus, FvXTH9 and probably also FvXTH6 are likely to be capable of modifying the structure of xyloglucan in the cell wall. Further research is needed to investigate the hemicellulose content in different fruit maturation stage to support the hypothesis that the depolymerization of xyloglucan molecules resulted in strawberry fruit ripening.

A novel enzyme FvGDSL esterase/lipase was cloned and expressed in yeast. Preliminary enzyme assays showed that this enzyme has hydrolase activity toward low molecular weight esters. Since *FvGDSL* is co-expressed with *FvXTH6* and *FvXTH9,* it can be suspected that FvGDSL has a function in fruit ripening and might also be involved in the degradation of hemicellulose, possibly by deacetylation of the polysaccharide.

References

Abdelkafi, S., Ogata, H., Barouh, N., Fouquet, B., Lebrun, R., Pina, M., Scheirlinckx, F., Villeneuve, P., Carrière, F. (2009) Identification and biochemical characterization of a GDSL-motif carboxylester hydrolase from *Carica papaya* latex. *Biochim. Biophys. Acta.* **1791**, 1048–1056.

Aharoni, **A.** (2002) Gene expression analysis of strawberry achene and receptacle maturation using DNA microarrays. *J Exp Bot.* **53** (377), 2073–2087.

Akoh, C.C., Lee, G.C., Liaw, Y.C., Huang, T.H., Shaw, J.F. (2004) GDSL family of serine esterases/lipases. *Prog Lipid Res.* **43**(6), 534-552.

Antosiewicz, D.M., Purugganan, M.M., Polisensky, D.H., Braam, J. (1997) Cellular localization of Arabidopsis xyloglucan endotransglycosylas-related proteins during development and after wind stimulation. *Plant Physiol.* **115**, 1319–1328.

Arrowsmith, D.A., de Silva, J. (1995) Characterization of two tomato fruit expressed cDNAs encoding xyloglucan endotransglucosylases. *Plant Mol Biol.* **28**, 391–403.

Atkinson, R.G., Johnston, S.L., Yauk, Y.K., Sharma, N.N., Schroder, R. (2009) Analysis of xyloglucan endotransglucosylase/hydrolase (XTH) gene families in kiwifruit and apple, *Postharvest Biol Tec.* **51**, 149-157.

Barka, A.E., Kalantari, S., Makhlouf, J., Arul, J. (2000) Impact of UV-C irradiation on the cell wall-degrading enzymes during ripening of tomato (*Lycopersicon esculentum* L.) Fruit. *J. Agric. Food Chem.* **48**, 667−671.

Barnes, M.F., Patchett BJ. (1976) Cell wall degrading enzymes and the softening of the strawberry fruit. *J. Food Sci*. **41**, 1392-1395.

Baumann, M.J., Eklöf, J.M., Michel, G., Kallas, Å.M., Teeri, T.T., Czjzek, M., Brumer, H. (2007) Structural evidence for the evolution of xyloglucanase activity from xyloglucan endo -transglycosylases: biological implications for cell wall metabolism. *Plant Cell.* **19**(6), 1947–1963.

Beisson, F., Li, Y., Bonaventure, G., Pollard, M., Ohlrogge, J.B. (2007) The acyltransferase GPAT5 is required for the synthesis of suberin in seed coat and root of Arabidopsis. *Plant Cell*. **19**, 351–368.

Bibikova, T.N., Jacob, T., Dahse, I., Gilroy, S. (1998) Localized changes in apoplastic and cytoplasmic pH are associated with root hair development in Arabidopsis thaliana. *Development.* **125**, 2925–2934.

Bourquin, V., Nishikubo, N., Abe, H., Denman, S., Eklund, M.,

Christiernin, M., Teeri, T.T., Sundberg, B., Mellerowicz, E.J. (2002) Xyloglucan endotransglycosylases have a function during the formation of secondary cell walls of vascular tissues. *Plant Cell.* **14**, 3073–3088.

Brick, D.J., Brumlik, M.J., Buckley, J.T., Cao, J-X., Davies, P.C., Misra, S., Tranbarger, T.J., Upton, C. (1995) A new family of lipolytic plant enzymes with members in rice, arabidopsis and maize. *FEBS Lett.* **377**(3), 475–480.

Brummell, D.A. (2006). Cell wall disassembly in ripening fruit. *Funct. Plant Biol.* **33**, 103–119.

Cabib, E., Farkas, V., Kosik, O., Blanco, N., Arroyo, J., McPhie, P. (2008) Assembly of the yeast cell wall Crh1p and Crh2p act as transglycosyl- ases in vivo and *in vitro*. *J Biol Chem.* **283**, 29859–29872

Campbell, P. and Braam, J. (1998) Co- and/or post-translational modifications are critical for TCH4 XET activity. *Plant J.* **15**, 553-561.

Campbell, P., Braam, J. (1999a) Xyloglucan endotransglycosylases: diversity of genes, enzymes and potential wall-modifying functions. *Trends Plant Sci.* **4**, 361–366

Campbell, P. and Braam, J. (1999b) *In vitro* activities of four xyloglucan endotransglycosylases from Arabidopsis. *Plant J.* **18**(4), 371-382.

Cantarel, B.L., Coutinho, P.M., Rancurel, C., Bernard, T., Lombard, V., Henrissat, B. (2009) The Carbohydrate-Active EnZymes database (CAZy): an expert resource for glycogenomics. *Nucleic Acids Res.* **37**, 233–238.

Carpita, N.C., Defernez, M., Findlay, K., Wells, B., Shoue, D.A., Catchpole, G., Wilson, R.H., McCann, M.C. (2001) Cell wall architecture of the elongating maize coleoptile. *Plant Physiol.* **127**, 551-565.

Castillejo, C., Fuente, J.I., Pietro Iannetta, P., Botella M. A., Valpuesta, V., (2004) Pectin esterase gene family in strawberry fruit: study of FaPE1, a ripening-specific isoform. *J Exp Bot*. **55** (398), 909-918.

Clauss, K., Baumert, A., Nimtz, M., Milkowski, C., Strack, D. (2008). Role of a GDSL lipase-like protein as sinapine esterase in Brassicaceae. *Plant J.* **53**, 802–813.

Cutillasiturralde, A., Zarra, I., Fry, S.C., Lorences, E.P. (1994) Implication of persimmon fruit hemicellulose metabolism in the softening process-importance of xyloglucan endotransglycosylase. *Physiol Plant.* **91**, 169-176.

Darrow, **G.M.** (1966) The strawberry. History, breeding and physiology. New York: Holt, Rinehart and Winston.

Dalrymple, B., Lowry, J. (1997) Three *Neocallimastix patriciarum* esterases associated with the degradation of complex polysaccharides are members of a new family of hydrolases. *Microbiology.* **143**, 2605-2614.

de Silva J, Jarman CD, Arrowsmith DA, Stronach MS, Chengappa S, Sidebottom C, Reid JS (1993) Molecular characterization of a xyloglucan-specific endo-(1→4)-β-d-glucanase (xyloglucan endotransglycosylase) from nasturtium seeds. *Plant J.* **3,** 701–711.

Edelman, H.G., Fry, S.C., (1992) Factors that affect the extraction of xyloglucan from the primary cell walls of suspension-cultured rose cells. *Carbohydr. Res*. **228**, 423-431.

Edwards, M., Dea, I.C.M., Bulpin, P.V., Reid, J.S.G. (1986) Purification and properties of a novel xyloglucan-specific endo-(1-4)-β-D-glucanase from germinated nasturtium seeds (*Tropaeolum majus* L). *J Biol Chem*. **261**, 9489–9494.

Fanutti, C., Gidley, M.J., Reid, J.S.G. (1993) Action of a pure xyloglucan endo- transglycosylase (formerly called xyloglucan-specific endo-(1-4)- β-D-glucanase) from the cotyledons of germinated nasturtium seeds. *Plant J.* **3**, 691-700

Fanutti, C., Gidley, M.J., Reid, J.S.G. (1996) Substrate subsite recognition of the xyloglucan endo-transglycosylase or xyloglucan-specific endo-(1-4)- β -D-glucanase from the cotyledons of germinated nasturtium (Tropaeolum majus) seeds. *Planta*. **200**, 221-228

Farkas, V., Sulova, Z., Stratilova, E., Hanna, R., Maclachlan, G. (1992) Cleavage of xyloglucan by nasturtium seed xyloglucanase and transglycosylation to xyloglucan subunit oligosaccharides. *Arch. Biochem. Biophys.* **298,** 365-370.

Fasano, J., Swanson, S., Blancaflor, E., Dowd, P., Kao, T., Gilroy, S. (2001) Changes in root cap pH are required for the gravity response of the Arabidopsis root. *Plant Cell.* **13**, 907–921.

Folta, K.M., Dhingra, A. (2007) Transformation of strawberry: the basis for translational genomics in Rosaceae. *In Vitro Cell Dev Biol Plant* **42**,482–490.

Franková, L., Fry, S.C. (2012) Trans-α-xylosidase, a widespread enzyme activity in plants, introduces (1→4)-α-D-xylobiose side-chains into xyloglucan structures. *Phytochemistry* **78**, 29–43.

Franková, L., Fry, S.C. (2013) Biochemistry and physiological roles of enzymes that ‘ cut and paste ’ plant cell-wall polysaccharides. *J Exp Bot.* **64**, 3519–3550.

Fry, S.C. (1989) Cellulases, hemicelluloses and auxin-stimulated growth: a possible relationship. *Physiol Plant.* **75**, 532-536.

Fry, S.C., Smith, R.C., Renwick, K.F., Martin, D.J., Hodge, S.K., Matthews, K.J. (1992) Xyloglucan endotransglycosylase, a new wall-loosening enzyme activity from plants. *Biochem. J.* **282**, 821–828.

Fry S.C., Aldington S., Hetherington P.R., Aitken J. (1993) Oligosaccharides as Signals and Substrates. *Plant Physiol.* **103**(1), 1-5.

Fry, S.C., Mohler, K.E., Nesselrode, B.H., Franková, L. (2008) Mixed-linkage β -glucan: xyloglucan endotransglucosylase, a novl wall-remodelling enzyme from Equisetum (horsetails) and charophytic algae. *Plant J.* **55**, 240–252.

Geisler-Lee, J., Geisler, M., Coutinho, P.M. (2006) Poplar carbohydrate-active enzymes. Gene identification and expression analyses. *Plant Physiol.* **140**, 946–962.

Gibeaut, D.M., Pauly, M., Bacic, A., Fincher, G.B. (2005) Changes in cell wall polysaccharides in developing barley (*Hordeum vulgare*) coleoptiles. *Planta.* **221**, 729–738.

Giovannoni, **J.J.** (2004) Genetic regulation of fruit development and ripening. *Plant Cell.* **16**, 170-180.

Gomez-Bujedo, S., Fleury, E., Vignon, M.R. (2004) Preparation of cellouronic acids and partially acetylated cellouronic acids by TEMPO–NaClO oxidation of water-soluble cellulose acetate. *Biomacromolecules.* **5**, 565–571.

Grishutin, S.G., Gusakov, A.V., Dzedzyulya, E.I., Sinitsyn, A.P. (2006) A lichenase-like family 12 endo-(l→4)-β-glucanase from *Aspergillus japonicus*: study of the substrate specificity and mode of action on β-glucans in comparison with other glycoside hydrolases. *Carbohydr. Res.* **341**, 218-229.

Härtl K., Denton A., Franz-Oberdorf K., Hoffmann T., Spornraft M., Usadel B., Schwab W. (2017) Early metabolic and transcriptional variations in fruit of natural white-fruited *Fragaria vesca* genotypes. *Sci. Rep.* **7**, 45113.

Hamada, S., Hasegawa, Y., Suzuki, Y. (2012) Identification of a GDSL-motif carboxylester hydrolase from rice bran (*Oryza sativa* L.). *J Cereal Sci*. **55**, 100-105.

Han, Y., Zhu, Q., Zhang, Z., Meng, K., Hou, Y., Ban, Q., Suo, J., Rao, J. (2015) Analysis of xyloglucan endotransglycosylase/hydrolase (XTH) genes and diverse roles of isoenzymes during persimmon fruit development and postharvest softening. *PLoS One.* **10**(4).

Han, Y., Wang, W., Sun, J., Ding, M., Zhao, R., Deng, S., Wang, F., Hu, Y., Wang, Y., Lu, Y., Du, L., Hu, Z., Diekmann, H., Shen, X., Polle, A., Chen S., (2013) *Populus euphratica* XTH overexpression enhances salinity tolerance by the development of leaf succulence in transgenic tobacco plants. *J Exp Bot.* **64**, 4225–4238.

Han, Y., Ban, Q., Li, H., Hou, Y., Jin, M., Han, S., Rao, J. (2016) DkXTH8, a novel xyloglucan endotransglucosylase/hydrolase in persimmon, alters cell wall structure and promotes leaf senescence and fruit postharvest softening. *Sci. Rep.* **6**, 39155.

Hancock, **J.F.** (1999) *Strawberries*. Crop production science in horticulture. Oxon *et al.,* CABI Pub.

Harada, T., Torii, Y., Morita, S., Onodera, R., Hara, Y., Yokoyama, R., Nishitani, K., Satoh, S. (2011) Cloning, characterization, and expression of xyloglucan endotransglucosylase/hydrolase and expansin genes associated with petal growth and development during carnation flower opening. *J Exp Bot.* **62,** 815–823.

Hayashi, T. (1989) Xyloglucans in the primary cell wall. *Annu Rev Plant Physiol Plant Mol Biol.* **40**, 139–168.

Hong, J.K., Choi, H.W., Hwang, I.S., Kim, D.S., Kim N.H., Choi, D.S., Kim, Y.J., Hwang, B.K. (2008) Function of a novel GDSL-type pepper lipase gene, CaGLIP1, in disease susceptibility and abiotic stress tolerance. *Planta.* **227**, 539-558.

Hoson, T. (1990) Effect of auxin on autolysis of cell walls in azuki bean epicotyls. *Plant Cell Physiol.* **31**, 281–287.

Hoson, T. (1993) Regulation of polysaccharides breakdown during auxin-induced cell wall loosening. *J. Plant Res.* **106**, 369–381.

Hoson, T. (1998) Apoplast as the site of response to environmental signals. *J. Plant Res.* **111**, 167–177.

Hrmova, M., Farkas, V., Lahnstein, J., Fincher, G.B. (2007) A barley xyloglucan xyloglucosyl transferase covalently links xyloglucan, cellulosic substrates and (1,3;1,4)-β-D-glucans. *J. Biol. Chem.* **282**, 12951–12962.

Hrmova, M., Farkaš, V., Harvey, A.J., Lahnstein, J., Wischmann, B., Kaewthai, N., Ezcurra, I., Teeri, T.T., Fincher, G.B. (2009) Substrate specificity and catalytic mechanism of a xyloglucan xyloglucosyl transferase HvXET6 from barley (*Hordeum vulgare* L.). *FEBS J.* **276**, 437–456.

Huber, D.J. (1984) Strawberry fruit softening: the potential roles of polyuronides and hemicelluloses. *J. Food Sci.* **49**, 1310–1315.

Jiménez-Bermúdez, S.,Redondo-Nevado, J., Muñoz-Blanco, J., Caballero, J.L., López-Aranda, J.M., Valpuesta, V., Pliego-Alfaro, F., Quesada, M.A., Mercado, J.A. (2002) Manipulation of strawberry fruit softening by antisense expression of a pectate lyase gene. *Plant Physiol.* **128**, 751–759.

Johansson, P., Brumer, H., Baumann, M.J., Kallas, A.M., Henriksson, H., Denman, S.E., Teeri, T.T., Jones, T.A. (2004) Crystal structures of a poplar xyloglucan endotransglycosylase reveal details of transglycosylation acceptor binding. *Plant Cell.* **16**, 874–886.

Kallas, A. M, Piens, K., Denman, S.E., Henriksson, H., Fäldt, J., Johansson, P., Brumer, H., Teeri, T.T. (2005) Enzymatic properties of native and deglycosylated hybrid aspen (*Populus tremula-tremuloides*) xyloglucan endotransglycosylase 16A expressed in *Pichia pastoris*. *Biochem. J.* **390**, 105–113.

Kaewthai, N., Harvey, A.J., Hrmova, M., Brumer, H., Ezcurra, I., Teeri, T.T., Fincher, G.B. (2010) Heterologous expression of diverse barley XTH genes in the yeast Pichia pastoris. *Plant Biotechnol*. **27**, 251–258.

Kikuta, Y., Ueda, H., Takahashi, M., Mitsumori, T., Yamada, G., Sakamori, K., Takeda, K., Furutani, S., Nakayama, K., Katsuda, Y., Hatanaka, A., and Matsuda, K. (2012). Identification and characterization of a GDSL lipase-like protein that catalyzes the ester-forming reaction for pyrethrin biosynthesis in Tanacetum cinerariifolium- A new target for plant protection. *Plant J.* **71**(2),183-93.

Kim, K.J., Lim, J.H., Kim, M.J., Kim, T., Chung, H.M., Paek, K.H. (2008) GDSL-lipase1 (CaGL1) contributes to wound stress resistance by modulation of CaPR-4 expression in hot pepper. *Biochem. Biophys. Res. Commun.* **374,** 693– 698.

Kannangara, R., Branigan, C., Liu, Y., Penfield, T., Rao, V., Mouille, G., Höfte, H., Pauly, M., Riechmann, J.L., Broun, P. (2007) The transcription factor WIN1/SHN1 regulates cutin biosynthesis in *Arabidopsis thaliana*. *Plant Cell.* **19**,1278–1294.

Knee, M., Sargent, J.A., Osborne, D.J. (1977) Cell wall metabolism in developing strawberry fruits. *J Exp Bot.* **28**, 377–396.

Kram, B.W., Bainbridge, E.A., Perera, M.A., Carter, C. (2008) Identification, cloning and characterization of a GDSL lipase secreted into the nectar of Jacaranda mimosifolia. *Plant Mol. Biol.* **68**, 173–183.

Kusumawati, L., Imin, N., and Djordjevic, M.A. (2008) Characterization of the secretome of suspension cultures of Medicago species reveals proteins important for defense and development. *J. Proteome Res.* **7**, 4508–4520.

Kwon, S.J., Jin, H.C., Lee, S., Nam, M.H., Chung, J.H., Kwon, S.I., Ryu, C.M., Park, O.K. (2009) GDSL lipase-like 1 regulates systemic resistance associated with ethylene signaling in Arabidopsis. *Plant J.* **58**, 235–245.

Labavitch, J.M., Ray, P.M. (1978) Structure of hemicellulosic polysaccharides of *Avena sativa* coleoptile cell walls. *Phytochemistry.* **17**, 933-937.

Lazo, G.R., Stein, P.A., Ludwig, R.A. (1991) A DNA transformation competent *Arabidopsis* genomic library in *Agrobacterium*. *Biotechnology.* **9**, 963–967.

Lee, Y-L., Chen, J.C., Shaw, J-F. (1997) The thioesterase I of *Escherichia coli* has arylesterase activity and shows stereospecificity for protease substrates. *Biochem Biophys Res Commun*. **231**(2), 452-456.

Lee, D.S., Kim, B.K., Kwon, S.J., Jin, H.C., Park, O.K. (2009) Arabidopsis GDSL lipase 2 plays a role in pathogen defense via negative regulation of auxin signaling. *Biochem. Biophys. Res. Commun.* **379**, 1038-1042.

Lefever, G., Vieuille, M., Delage, N., D´Harlingue, A., de Monteclerc, J., Bompeix, G. (2004) Characterization of cell wall enzyme activities, pectin composition, and technological criteria of strawberry cultivars (*Fragaria* × *ananassa* Duch). *J. Food Sci.* **69**, 221-226.

Lemaire-Chamley, M., Petit, J., Garcia, V., Just, D., Baldet, P., Germain, V., Fagard, M., Mouassite, M., Cheniclet, C., Rothan, C. (2005). Changes in transcriptional profiles are associ- ated with early fruit tissue specialization in tomato. *Plant Physiol.* **139**, 750–769.

Lerouxel, O., David, M., Cavalier, D.M., Liepman, A.H., Keegstra, K. (2006) Biosynthesis of plant cell wall polysaccharides-a complex process. *Curr Opin Plant Biol.* **9**, 621-630.

Levy, S. Maclachlan, G. and Staehelin, L.A. (1997) Xyloglucan sidechains modulate binding to cellulose during *in vitro* binding assays as predicted by

conformational dynamics simulation. *Plant J*. **11**, 373-386.

Li, W., Cui, S.W., Kakuda, Y. (2006) Extraction, fractionation, structural and physical characterization of wheat β-d-glucans. *Carbohydr Polym.* **63**, 408-416.

Liao, Z., Chen, M., Guo, L., Gong, Y., Tang, F., Sun, X., Tang, K. (2004) Rapid isolation of high-quality total RNA from Taxus and Ginkgo preparative. *Biochemistry & Biotechnology.* **34**(3), 209–214.

Ling, H., Zhao, J., Zuo, K., Qiu, C., Yao, H., Qin, J., Sun, X., Tang K. (2006) Isolation and expression analysis of a GDSL-like lipase gene from Brassica napus L. *J. Biochem. Mol. Biol.* **39**, 297-303.

Ling, H. (2008) Sequence analysis of GDSL lipase gene family in Arabidopsis thaliana. *Pak J Biol Sci.* **11**(5), 763-767.

Livak, K.J., Schmittgen, T.D. (2001) Analysis of relative gene expression data using real-time quantitative PCR and the 2-ΔΔCt method. *Methods.* **25**, 402–408.

Lo, Y.C., Lin, S.C., Shaw, J.F., Liaw, Y.C. (2003) Crystal structure of *Escherichia coli* thioesterase I/protease I/lysophospholipase L1: consensus sequence blocks constitute the catalytic center of SGNH-hydrolases through a conserved hydrogen bond network. *J Mol Biol.* **330**(3), 539-551.

Lorences, E.P. and Fry, S.C. (1993) Xyloglucan oligosaccharides, acting as acceptor substrates for xyloglucan endotransglycosylase, promote the depolymerization of xyloglucan. *Physiol Plant.* **88**,105-112.

Maclachlan, G., Brady, C. (1994) Endo-1, 4-b-glucanase, xyloglucanase and xyloglucan endotransglucosylase activities versus potential substrates in ripening tomatoes. *Plant Physiol*. **105**, 965–974.

Maris, A., Suslov, D., Fry, S.C., Verbelen, J.P., Vissenberg, K. (2009) Enzymic characterization of two recombinant xyloglucan endotransglucosylase/ hydrolase (XTH) proteins of Arabidopsis and their effect on root growth and cell wall extension. *J Exp Bot.* **60**, 3959–3972.

Maris, A., Kaewthai, N., Eklöf, J.M., Miller, J.G., Brumer, H., Fry, S.C., Verbelen, J.P., Vessenberg, K. (2011) Difference in enzymic properties of five recombinant xyloglucan endotransglucosylase/hydrolase (XTH) proteins of Arabidopsis. *J Exp Bot.* **62**, 261–271.

Matas, A.J., Agustí, J., Tadeo, F.R., Talón, M., Rose, J.K. (2010) Tissue specific transcriptome profiling of the citrus fruit epidermis and sub-epidermis using laser capture microdissection. *J Exp Bot.* **61**, 3321–3330.

Mathews, I., Soltis, M., Saldajeno, M., Ganshaw, G., Sala, R., Weyler, W., Cervin, M.A., Whited, G., Bott, R. (2007) Structure of a novel enzyme that catalyzes acyl transfer to alcohols in aqueous conditions. *Biochemistry*. **46** (31), 8969–8979.

Matsui, A., Yokoyama, R., Seki, M., Ito, T., Shinozaki, K., Takahashi, T., Komeda, Y., Nishitani, K. (2005) *AtXTH27* plays an essential role in cell wall modification during the development of tracheary elements. *Plant J.* **42**, 525-534.

Medford, J. I., Elmer, J. S. and Klee, H. J. (1991) Molecular cloning and characterisation of genes expressed in shoot apical meristems. *Plant Cell.* **3**, 359–370.

Meikle, P.J., Hoogenraad, N.J., Bonig, I., Clarke, A.E., Stone, B.A. (1994) A (1→3,1→4)-β-glucan-specific monoclonal antibody and its use in the quantification and immunocytochemical location of (1→3,1→4)-β-glucans. *Plant J.* **5**, 1-9.

Mellerowicz, E.J., Immerzeel, P., Hayashi, T. (2008) Xyloglucan: The molecular muscle of trees. *Ann Bot.* **102**(5), 659–665.

Mercado, J.A., Trainotti, L., Jiménez-Bermúdez, L., Santiago-Doménech, N., Posé, S., Donolli, R., Barceló, M., Casadoro, G., Pliego-Alfaro, F., Quesada, M.A. (2010) Evaluation of the role of the endo-β-(1,4)-glucanase gene FaEG3 in strawberry fruit softening. *Postharvest Biol Technol.* **55**, 8–14.

Miedes, E., Lorences, E.P. (2009) Xyloglucan endotransglucosylase/ hydrolases (XTHs) during tomato fruit growth and ripening. *J. Plant Physiol.* **166,** 489–498.

Mintz-Oron, S., Mandel, T., Rogachev, I., Feldberg, L., Lotan, O., Yativ, M., Wang, Z., Jetter, R., Venger, I., Adato, A., Aharoni, A. (2008) Gene expression and metabolism in tomato fruit surface tissues. Plant Physiol. **147**, 823–851.

Mohand A.F., Farkas V. (2006) Screening for hetero-transglycosylating activities in extracts from nasturtium (*Tropaeolum majus*). *Carbohydr. Res.* **341,** 577–581.

Molgaard, A., Kauppinen, S., Larsen, S. (2000) Rhamnogalacturonan acetylesterase elucidates the structure and function of a new family of hydrolases. *Structure*. **8**(4), 373-383.

Molina-hidalgo, F.J., Franco, A.R., Villatoro, C., Medina-puche, L., Mercado, A., Hidalgo, M.A., Monfort, A., Caballero, J.L., Muñoz-blanco,

J. (2013) Enzyme involved in the degradation of cell-wall middle lamellae. *J Exp Bot.* **64**(6), 1471-1483.

Montella, I.R., Schama, R., Valle, D. (2012) The classification of esterases: An important gene family involved in insecticide resistance- A Review. *Mem Inst Oswaldo Cruz*. **107**, 437-449.

Naranjo, M.A., Forment, J., Roldán, M., Serrano, R., Vicente, O. (2006) Overexpression of Arabidopsis thaliana LTL1, a salt-induced gene encoding a GDSL-motif lipase, increases salt tolerance in yeast and transgenic plants. *Plant Cell Environ.* **29**, 1890–1900.

Ndamukong, I., Chetram, A., Saleh, A., Avramova, Z. (2009) Wall-modifying genes regulated by the Arabidopsis homolog of trithorax, ATX1: repression of the XTH33 gene as a test case. *Plant J*. **58**, 541–553.

Neal, G.E. (1965) Changes occurring in the cell walls of strawberries during ripening. *J Sci Food Agric.* **16**, 604-611.

Nishikubo, N., Takahashi, J., Roos, A.A., Derba-Maceluch, M., Piens, K., Brumer, H., Teeri, T.T., Stålbrand, H., Mellerowicz, E.J. (2011) Xyloglucan *endo*-transglycosylase-mediated xyloglucan rearrangements in developing wood of hybrid aspen. *Plant Physiol.* **155,** 399–413.

Nishitani, K., Masuda, Y. (1982) Acid pH-induced structural changes in cell wall xyloglucans in *Vigna angularis* epicotyl segments. *Plant Sci. Lett.* **28**, 87–94.

Nishitani, K., Masuda, Y. (1983) Auxin-induced changes in the cell wall xyloglucans: Effects of auxin on the two different subfractions of xyloglucans in the epicotyls cell wall of *Vigna angularis*. *Plant Cell Physiol.* **24**, 345–355.

Nishitani, K., Tominaga, R. (1992) Endo-xyloglucan transferase, a novel class of glycosyltransferase that catalyses transfer of a segment of xyloglucan molecule to another xyloglucan molecule. *J. Biol. Chem.* **267**, 21058–21064.

Nitsch, J.P. (1950) Growth and morphogenesis of the strawberry as related to auxin. *Ann J Bot.* **37**, 211-215.

Nogata, Y., Yoza, K., Kusumoto, K., Ohta, H. (1996) Changes in molecular weight and carbohydrate composition of cell wall polyuronide and hemicellulose during ripening in strawberry fruit. In : Visser J Voragen AGJ, eds. *Pectins and pectinases*. Amsterdam: Elsevier Science pp 591–596.

Oh, M.H., Romanow, W.G., Smith, R.C., Zamski, E., Sasse, J., Clouse, S.D. (1998) Soybean *Bru1* encodes a functional xyloglucan endotransglycosylase that is highly expressed in inner epicotyl tissues during brassinosteroid promoted elongation. *Plant Cell Physiol.* **39**, 124-130.

Oh, I.S., Park, A.R., Bae, M.S., Kwon, S.J., Kim, Y.S., Lee, J.E., Kang, N.Y., Lee, S., Cheong, H., Park, O.K. (2005) Secretome analysis reveals an Arabidopsis lipase involved in defense against *Alternaria brassicicola*. *Plant Cell.* **17**, 2832-2847.

O'Neill, M.A., Albersheim, P., Darvill, A.G. (1990) The pectic polysaccharides of primary cell walls. *Methods in Plant Biochemistry*. **2**, 415-441.

Oosumi, T., Gruszewski, H., Blischak, L., Baxter, A., Wadl, P., Shuman, J., Veilleux, R.E., Shulaev, V. (2006) High effciency transformation of the diploid strawberry (*Fragaria vesca*) for functional genomics. *Planta.* **223**,1219-1230.

Opazo, M.C., Figueroa, C.R., Henríquez, J., Herrera, R., Brunob, C., Valenzuela, P.D.T., Moya-Leóna, M.A. (2010) Characterization of two divergent cDNAs encoding xyloglucan endotransglycosylase/hydrolase (XTH) expressed in *Fragaria chiloensis* fruit. *Plant Sci*. **179**, 479–488.

Osato, Y., Yokoyama, R., Nishitani, K. (2006) A principal role for *AtXTH18* in *Arabidopsis thaliana* root growth: a functional analysis using RNAi plants. *J. Plant Res.* **119**, 153-162.

Palomer, X., Llop-Tous, I., Vendrell, M., Krens, F.A., Schaart, J.G., Boone, M.J., van der Valk, E., Salentijn, E.M.J. (2006) Antisense down-regulation of strawberry endo-β-(1,4)-glucanase genes does not prevent fruit softening during ripening. *Plant Sci.* **171**, 640–646.

Paniagua, C., Blanco-Portales, R., Barceló-Muñoz, M., García-Gago, J.A., Waldron, K.W., Quesada, M.A., Muñoz-Blanco, J., Mercado, J.A. (2016) Antisense down-regulation of the strawberry β-galactosidase gene FaβGal4 increases cell wall galactose levels and reduces fruit softening. *J Exp Bot.* **67**(3), 619–631

Paniagua, C., Santiago-Doménech, N., Kirby, A.R., Gunning, A.P., Morris, V.J., Quesada, M.A., Matas, A.J., Mercado, J.A. (2017) Structural changes in cell wall pectins during strawberry fruit development. *Plant Physiol Biochem*. **118**, 55-63.

Pena, M.J., Darvill, A.G., Eberhard, S., York, W.S., O'Neill, M.A. (2008) Moss and liverwort xyloglucans contain galacturonic acid and are structurally

distinct from the xyloglucans synthesized by hornworts and vascular plants. *Glycobiology*. **18**, 891-904.

Perkins-Veazie, P. (1995) Growth and ripening of strawberry fruit. *Hortic Rev.* **17**, 267–297.

Planas, A. (2000) Bacterial 1,3-1,4-beta-glucanases: structure, function and protein engineering. *Biochim. Biophys. Acta.* **1543**, 361-382.

Posé, S., Kirby, A.R., Mercado, J.A., Morris, V.J., Quesada, M.A. (2010) Structural characterization of cell wall pectin fractions in ripe strawberry fruits using AFM. *Carbohydr Polym.* **88**, 882–890.

Posé, S., Paniagua, C., Cifuentes, M., Blanco-Portales, R., Quesada, M.A., Mercado, J.A. (2013) Insights into the effects of polygalacturonase FaPG1 gene silencing on pectin matrix disassembly, enhanced tissue integrity, and firmness in ripe strawberry fruits. *J Exp Bot.* **64**, 3803–3815.

Prasanna, V., Prabha, T.N., Tharanathan, R.N. (2007) Fruit ripening phenomena-an overview. *Crit Rev Food Sci Nutr.* **47**(1), 1-19.

Pringle, D., Dickstein, R. (2004) Purification of ENOD8 proteins from Medicago sativa root nodules and their characterization as esterases, *Plant Physiol. Biochem.* **42**, 73-79.

Purugganan, M.M., Braam, J., Fry, S.C. (1997) The Arabidopsis TCH4 xyloglucan endotransglycosylase: substrate specificity, pH optimum, and cold tolerance. *Plant Physiol.* **115**, 181–190.

Qin, Y., Teixeira da Silva, J.A., Zhang, L., Zhang, S. (2008) Transgenic strawberry: state of the art for improved traits. *Biotechnol Adv.* **26**, 219-232.

Okazawa, K., Sato, Y., Nakagawa, T., Asada, K., Kato, I., Tomita, E., Nishitani, K. (1993) Molecular cloning and cDNA sequencing of endoxyloglucan transferase, a novel class of glycosyltransferase that mediates molecular grafting between matrix polysaccharides in plant cell walls. *J. Biol. Chem.* **268**, 25364–25368.

Ouyang, S., Zhu, W., Hamilton, J., Lin, H., Campbell, M., Childs, K., Thibaud-Nissen, F., Malek, R.L., Lee, Y., Zheng, L. (2007) The TIGR Rice Genome Annotation Resource: improvements and new features. *Nucleic Acids Res.* **35**, 883–887.

Quesada, M.A., Blanco-Portales, R., Posé, S., García-Gago, J.A., Jiménez-Bermúdez, S., Muñoz-Serrano, A., Caballero, J.L., Pliego-Alfaro, F., Mercado, J.A., Muñoz-Blanco, J. (2009) Antisense down-regulation of the *FaPG1* gene reveals an unexpected central role for

polygalacturonase in strawberry fruit softening. *Plant Physiol.* **150**, 1022–1032.

Redgwell, R.J. and Fry, S.C. (1993) Xyloglucan endotransglycosylase activity increases during kiwifruit (*Actinidia deliciosa*) ripening: implications for fruit softening, *Plant Physiol.* **103**, 1399-1406.

Reina, J.J., Guerrero, C., Heredia, A. (2007) Isolation, characterization, and localization of AgaSGNH cDNA: a new SGNH-motif plant hydrolase specific to *Agave americana L.* leaf epidermis. *J Exp Bot.* **58**(11), 2717–2731.

Reiter, W. (2002) Biosynthesis and Properties of the Plant Cell Wall. *Curr. Opin. Plant Biol*. **5**, 536–542.

Renard, Lemeunier, C., Thibault, J.F., (1995) Alkaline extraction of xyloglucan from depectinised apple pomace: optimisation and characterisation C.M.G.C. *Carbohydr Polym.* **28**, 209-216.

Ridley, B.L., O'Neill, M.A., Mohnen, D. (2001) Pectins: structure, biosynthesis, and oligogalacturonide-related signaling. *Phytochemistry.* **57**, 929-967.

Rose, J.K.C., Bennett, A.B. (1999) Cooperative disassembly of the cellulose-xyloglucan network of plant cell walls: parallels between cell expansion and fruit ripening. *Trends Plant Sci.* **4**,176-183.

Rose, J.K.C., Braam, J., Fry, S.C., Nishitani, K. (2002) The XTH family of enzymes involved in xyloglucan endotransglucosylation and endohydrolysis: current perspectives and a new unifying nomenclature. *Plant Cell Physiol.* **43**, 1421–1435.

Rosli, H.G., Civello, P.M., Martinez, G.A. (2004) Changes in cell wall composition of three *Fragaria* × *ananassa* cultivars with different softening rate during ripening. *Plant Physiol Biochem.* **42**, 823–831.

Rousseau-Gueutin, M., Lerceteau-Köhler, E., Barrot, L., Sargent, D.J., Monfort, A., Simpson, D., Arús, P., Guérin, G., Denoyes-Rothan, B. (2008) Comparative genetic mapping between octoploid and diploid *Fragaria* species reveals a high level of colinearity between their genomes and the essential disomic behavior of the cultivated octoploid strawberry. *Genetics.* **179**, 2045-2060.

Saab, I., Sachs, M. (1996) A flooding-induced xyloglucan endotransglucosyl-ase homologue in maize is responsive to ethylene and associated with aerenchyma. *Plant Physiol.* **112**, 385–391.

Saladie´, M., Rose, J.K.C., Cosgrove, D.J., Catala´, C. (2006) Characterization of a new xyloglucan endotransglucosylase/hydrolase (XTH) from ripening tomato fruit and implications for the diverse modes of enzymatic action. *Plant J.* **47**, 282–295.

Santiago-Doménech, N., Jiménez-Bermúdez, S., Matas, A.J., Rose, J.K.C., Muñoz-Blanco, J., Mercado, J.A., Quesada, M.A. (2008) Antisense inhibition of a pectate lyase gene supports a role for pectin depolymerization in strawberry fruit softening. *J Exp Bot.* **59**, 2769–2779.

Schröder, R., Atkinson, R.G., Langenkämper, G., Redgwell, R.J. (1998) Biochemical and molecular characterisation of xyloglucan endotransglycosylase from ripe kiwifruit. *Planta*. **204**, 242–251.

Shi, J.X., Malitsky, S., De Oliveira, S., Branigan, C., Franke, R.B., Schreiber, L., Aharoni, A. (2011) SHINE transcription factors act redundantly to pattern the archetypal surface of Arabidopsis flower organs. *PLoS Genet*. **7**. (5), e1001388.

Shi, Y.Z., Zhu, X.F., Miller, J.G., Gregson, T., Zheng, S.J., Fry, S.C. (2015) Distinct catalytic capacities of two aluminium-repressed *Arabidopsis thaliana* xyloglucan endotransglucosylase/hydrolases, XTH15 and XTH31, heterologously produced in Pichia. *Phytochemistry.* **112**(1), 160–169.

Shulaev, V., Sargent, D.J., Crowhurst, R.N., Mockler, T.C., Folkerts, O., Delcher, A.L., Jaiswal, P., Mockaitis, K., Liston, A., Mane, S.P., Burns, P., Davis, T.M., Slovin, J.P., Bassil, N., Hellens, R.P., Evans, C., Harkins, T., Kodira, C., Desany, B., Crasta, O.R., Jensen, R.V., Allan, A.C., Michael, T.P., Setubal, J.C., Celton, J.M., Rees, D.J., Williams K.P., Holt, S.H., Ruiz Rojas, J.J., Chatterjee, M., Liu, B., Silva, H., Meisel, L., Adato, A., Filich-kin, S.A., Troggio, M., Viola, R., Ashman, T.L., Wang, H., Dharmawardhana, P., Elser, J., Raja, R., Priest, H.D., Bryant, D.W., Fox, S.E., Givan, S.A., Wilhelm, L.J., Naithani, S., ChristoVels, A., Salama, D.Y., Carter, J., Lopez Girona, E., Zdepski, A., Wang, W., Kerstetter, R.A., Schwab, W., Korban, S.S., Davik, J., Monfort, A., Denoyes-Rothan, B., Arus, P., Mittler, R., Flinn, B., Aharoni, A., Bennetzen, J.L., Salzberg, S.L., Dickerman, A.W., Velasco, R., Borodovsky, M., Veilleux, R.E., Folta, K.M. (2011) The genome of woodland strawberry (*Fragaria vesca*). *Nat Genet.* **43**, 109–116.

Singh, A.P., Tripathi, S.K., Nath, P., Sane, A.P. (2011) Petal abscission in rose is associated with the differential expression of two ethylene-responsive xyloglucan endotransglucosylase/hydrolase genes, *RbXTH1* and *RbXTH2*. *J Exp Bot.* **62,** 5091–5103.

Slovin, J.P., Schmitt, K., Folta, K.M. (2009) An inbred line of the diploid strawberry *Fragaria vesca* f. semper Xorens for genomic and molecular genetic studies in the Rosaceae. *Plant Methods*. **5** (15).

Slovin, J., Michael, T. (2011) Strawberry. Structural and functional genomics. Folta K, Kole C (eds) Genetics, genomics and breeding of berries. Science Publishers, EnWeld, 162–193.

Smith, R.C. and Fry, S.C. (1991) Endotransglycosylation of xyloglucan in plant cell suspension cultures. *Biochem. J.* **279**, 529-535.

Soni, S., Sathe, S.S., Odaneth, A. A., Lali, A.M. (2017) SGNH hydrolase-type esterase domain containing Cbes-AcXE2: a novel and thermostable acetyl xylan esterase from *Caldicellulosiruptor bescii*. *Extremophiles.* **21**(4), 687-679

Sood, S., Sharma, A., Sharma, N., Kanwar S.S. (2016) Carboxylesterases: Sources, Characterization and Broader Applications. *iMedPub J*. **1**(1), 1-11.

Sorensen, I., Pettolino, F.A., Wilson, S.M., Doblin, M.S., Johansen, B., Bacic, A., Willats, W.G. (2008) Mixed-linkage (1→ 3), (1→4)-b-D-glucan is not unique to the Poales and is an abundant component of Equisetum arvense cell walls. *Plant J.* **54**, 510– 521.

Spolaore, S., Trainotti, L., Casadoro, G. (2001) A simple protocol for transient gene expression in ripe fleshy fruit mediated by *Agrobacterium*. *J Exp Bot.* **52**, 845–850.

Steele, N.M., Fry, S.C. (1999) Purification of xyloglucan endotransglycosylases (XETs): a generally applicable and simple method based on reversible formation of an enzyme-substrate complex. *Biochem. J.* **340**, 207–211.

Steele, N.M., Fry, S.C. (2000) Differences in catalytic properties between native isoenzymes of xyloglucan endotransglycosylase (XET). *Phytochemistry.* **54,** 667–680.

Strohmeier, M., Hrmova, M., Fischer, M., Harvey, A.J., Fincher, G.B., Pleiss, J. (2004) Molecular modelling of family GH16 glycoside hydrolases: potential roles for xyloglucan transglucosylases/hydrolases in cell wall modification in the Poaceae. *Protein Sci.* **13**, 3200–3213.

Tabuchi, A., Mori, H., Kamisaka, S., Hoson, T. (2001) A new type of endo-xyloglucan transferase devoted to xyloglucan hydrolysis in the cell wall of azuki bean epicotyls. *Plant Cell Physiol*. **42**,154-161.

Takeda, T., Mitsuishi, Y., Sakai, F., Hayashi, T. (1996) Xyloglucan endotransglycosylation in suspension-cultured poplar cells. *Biosci. Biotech. Biochem.* **60**, 1950–1955.

Taiz, L., Zeiger, E. (2010) Plant physiology. Sinauer Associates,Inc., Publishers, Sunderland.

Thompson, J.E., and Fry, S.C. (2001) Restructuring of wall-bound xyloglucan by transglycosylation in living plant cells. *Plant J.* **26**, 23–34.

Trethewey, J.A.K., Campbell, L.M., Harris, P.J. (2005) (1→3),(1→4)-β-D-Glucans in the cell walls of the Poales (*sensu lato*): An immunogold labeling study using a monoclonal antibody. *Am J Bot.* **92**, 1660-1674.

Tyukhtenko, S.I., Litvinchuk, A.V., Chang, C.F., Lo, Y.C., Lee, S.J., Shaw, J.F., Liaw, Y.C., Huang, T.H. (2003) Sequential structural changes of Escherichia coli thioesterase/ protease I in the serial formation of Michaelis and tetrahedral complexes with diethyl p-nitrophenyl phosphate. *Biochemistry*. **42**(27), 8289–8297.

Updegraff, E.P., Zhao, F., Preuss, D. (2009) The extracellular lipase EXL4 is required for efficient hydration of Arabidopsis pollen. *Sex. Plant Reprod.* **22**, 197–204.

Upton, C., Buckley, J.T. (1995) A new family of lipolytic enzymes?. *Biochem Sci.* **20**(5),178–179.

Van Sandt, V., Guisez, Y., Verbelen, J-P., Vissenberg, K. (2006) Analysis of a xyloglucan endotransglycosylase/hydrolase (XTH) from the lycopodiophyte Selaginella kraussiana suggests that XTH sequence characteristics and function are highly conserved during the evolution of vascular plants. *J Exp Bot.* **57**, 2909–2922.

Van Sandt, V.S.T., Suslov, D., Verbelen, J.P., Vissenberg, K. (2007) Xyloglucan endotransglucosylase activity loosens a plant cell wall. *Ann Bot*. **100**, 1467-1473.

Van Larebeke, N., Engler, G., Holsters, M., Van den Elsacker, S., Zaenen, J., Schilperoort, R.A., Schell, J. (1974) Large plasmid in *Agrobacterium tumefaciens* essential for crown gall-inducing ability. *Nature*. **252**, 169–170.

Vicente, A.R., Saladié, M., Rose, J.K.C., Labavitch, J.M. (2007) The linkage between cell wall metabolism and fruit softening: looking to the future. *J Sci Food Agric.* **87**, 1435-1448.

Vissenberg, K., Martinez-Vilchez, I.M., Verbelen, J.P., Miller, J.G., Fry, S.C. (2000) *In vivo* colocalization of xyloglucan endotransglycosylase activity

and its donor substrate in the elongation zone of arabidopsis roots. *Plant Cell.* **12**, 1229-1237.

Visser, J., Voragen, A.G.J. (1996) Pectins and pectinases. *Progress in biotechnology.* Vol 14. Elsevier Science.

Volokita, M., Rosilio-Brami, T., Rivkin, N., Zik, M. (2010) Combining comparative sequence and genomic data to ascertain phylogenetic relationships and explore the evolution of the large GDSL-lipase family in land-plants. *Mol Biol Evol.* **28**(1), 551–565.

Wada, S., Ray, P.M. (1978) Matrix polysaccharides of oat coleoptile cell walls. *Phytochemistry.* **17**, 923-931.

West, R. W. J., Yocum, R. R., Ptashne, M. (1984) *Saccharomyces cerevisiae GAL1-GAL10* divergent promoter region: location and function of the upstream activator sequence UASG*. Mol. Cell. Biol.* **4**, 2467-2478.

Wingfield, P.T., (2001) Protein precipitation using ammonium sulfate. *Curr Protoc Protein Sci. doi:10.1002/0471140864.psa03fs13.*

Wooley, L.C., James, D.J., Manning, K. (2001) Purification and properties of an endo-β-1,4-glucanase from strawberry and down-regulation of the corresponding gene *cel1. Planta.* **214**,11–21.

Wu, Y., Jeong, B.R., Fry, S.C., Boyer, J.S. (2005) Change in XET activities, cell wall extensibility and hypocotyl elongation of soybean seedlings at low water potential. *Planta.* **220**, 593–601.

Xu, W., Purugganan, M.M., Polisensky, D.H., Antosiewicz, D.M., Fry, S.C., Braam, J. (1995) Arabidopsis TCH4, regulated by hormones and the environment, encodes a xyloglucan endotransglucosylase. *Plant Cell*. **7**, 1555–1567.

Yeats, T.H., Howe, K.J., Matas, A.J., Buda, G.J., Thannhauser, T.W., Rose, J.K. (2010) Mining the surface proteome of tomato (*Solanum lycopersicum*) fruit for proteins associated with cuticle biogenesis. *J Exp Bot.* **61**, 3759–3771.

Yokoyama, R., and Nishitani, K. (2000) Functional diversity of xyloglucan-related proteins and its implications in the cell wall dynamics in plants. *Plant Biology.* **2**, 598–604.

Yokoyama, R., and Nishitani, K. (2001) A comprehensive expression analysis of all members of a gene family encoding cell-wall enzymes allowed us to predict cis-regulatory regions involved in cell-wall construction in specific organs of Arabidopsis. *Plant Cell Physiol.* **42**, 1025–1033.

Yokoyama, R., Rose, J.K.C., Nishitani, K. (2004) A surprising diversity of and abundance of xyloglucan endotransglucosylase/hydrolases in rice. Classification and expression analysis. *Plant Physiol.* **134**, 1088–1099.

Yokoyama, R., Uwagaki, Y., Sasaki, H., Harada, T., Hiwatashi, Y., Hasebe, M., Nishitani, K. (2010) Biological implications of the occurrence of 32 members of the XTH (xyloglucan endotransglucosylase/hydrolase) family of proteins in the bryophyte Physcomitrella patens. *Plant J.* **64,** 645-656.

Youens-Clark, K., Buckler, E., Casstevens, T., Chen, C., Declerck, G., Derwent, P., Dharmawardhana, P., Jaiswal, P., Kersey, P., Karthikeyan, A.S. (2010) Gramene database in 2010: updates and extensions. *Nucleic Acids Res.* **39**,1085–1094.

Youssef, S.M., Jiménez-Bermúdez, S., Luz Bellido, M.,Martín-Pizarro, C., Barceló, M., Abdal-Aziz, S.A., Caballero, J.L., López-Aranda, J.M., Pliego-Alfaro, F., Mu˜ noz, J., Quesada, M.A., Mercado, J.A. (2009) Fruit yield and quality of strawberry plants transformed with a fruit specific strawberry pectate lyase gene. *Sci. Hortic.* **119**, 120–125.

Zhu, X.F., Shi, Y.Z., Lei, G.J., Fry, S.C., Zhang, B.C., Zhou, Y.H., Braam, J., Jiang, T., Xu, X.Y., Mao, C.Z., Pan, Y.J., Yang, J.L., Wu, P. & Zheng, S.J. (2012) XTH31, Encoding an *in vitro* XEH/XET-active enzyme, regulates aluminum sensitivity by modulating *in Vivo* XET action, cell wall xyloglucan content, and aluminum binding capacity in Arabidopsis. *The Plant Cell*. **24**(11), 4731–4747.

Zhang, J., Wang, X., Yu, O., Tang, J., Gu, X., Wan, X., Fang, C. (2011) Metabolic profiling of strawberry (*Fragaria* x *ananassa* Duch.) during fruit development and maturation, *J Exp Bot*. **62**(3), 1103–1118.

Zhou, S., Sauvé, R., Thannhauser, T.W. (2009) Proteome changes induced by aluminium stress in tomato roots. *J Exp Bot.* **60**, 1849–1857.

APPENDIX

a.

Compute pI/Mw

Theoretical pI/Mw (average) for the user-entered sequence:

```
        10         20         30         40         50         60
MASASLFLSV ILGLSLFLGP VSSAKFDELF QPYWASDHFT YEGELLHMKL DNYSGAGFSS

        70         80         90        100        110        120
KNKYMFGKVT VQIKLVEGDS AGTVTAFYMS SDGPLHNEFD FEFLGNTTGE PYSVQTNLYI

       130        140        150        160        170        180
NGVGNREQRL DLWFDPTTDF HSYSIFWNQR QVVFLVDETP IRVHTNMESK GLPFPKDQAM

       190        200        210        220        230        240
GVYSSIWNAD DWATQGGRVK TDWSHGPFVA SYKGFDINAC ECPASVAGAE NAKKCSSSNG

       250        260        270        280        290
DKKYWWDEPV LSELNVHQNH QLVWVKNHHM VYDYCTDSAR FPVTPVECVH HRH
```

Theoretical pI/Mw: 5.46 / 33159.04

b.

Compute pI/Mw

Theoretical pI/Mw (average) for the user-entered sequence:

```
        10         20         30         40         50         60
MYPSLRSGSV IASISLCFLS LFSLSAFARP ATFLQDFQVT WSDSHIRQID GGRAIQLVLD

        70         80         90        100        110        120
QNSGCGFSSK HKYLFGRVSM KIKLIPGDSA GTVTAFYMNS DTDAVRDELD FEFLGNRTGQ

       130        140        150        160        170        180
PYTVQTNIYA HGQGNREERV NLWFDPAADF HTYTILWNHH HIVFYVDDVP IRLYKNNEAK

       190        200        210        220        230        240
GIPYPKLQPM GVFSTLWEAD DWATRGGLEK INWSKAPFYA YYKDFDIEGC SVPGPANCAS

       250        260        270        280        290
SAQNWWEGTA YQALNALEYR RYKWVRMNHM IYDYCSDRSR YPKPPPECVA GL
```

Theoretical pI/Mw: 6.44 / 33347.59

Appendix 1. Molecular weight and isoelectric point prediction of FvXTH9 (a) and FvXTH6 (b). Theoretical pI/MW was performed using Compute pI/MW tool (http://www.expasy.ch/tools/pi_tool.html)

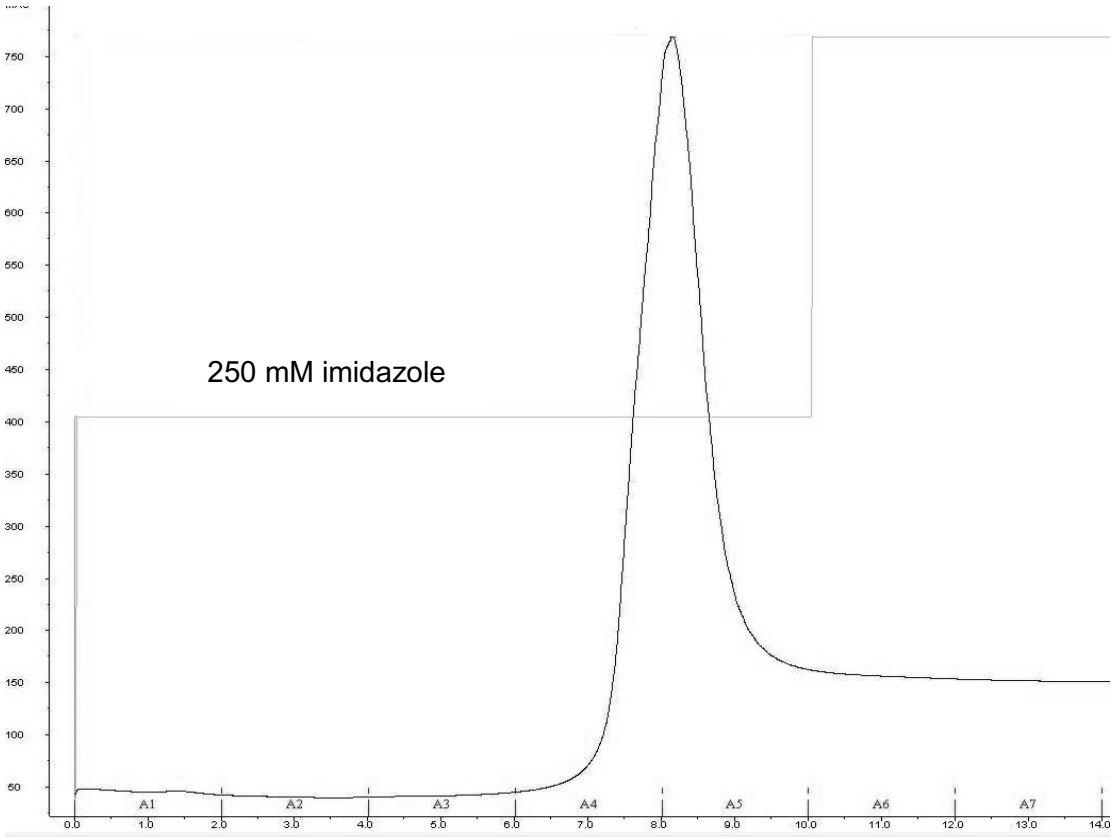

Appendix 2. Purification of FvXTH9His using HisTrap FF column

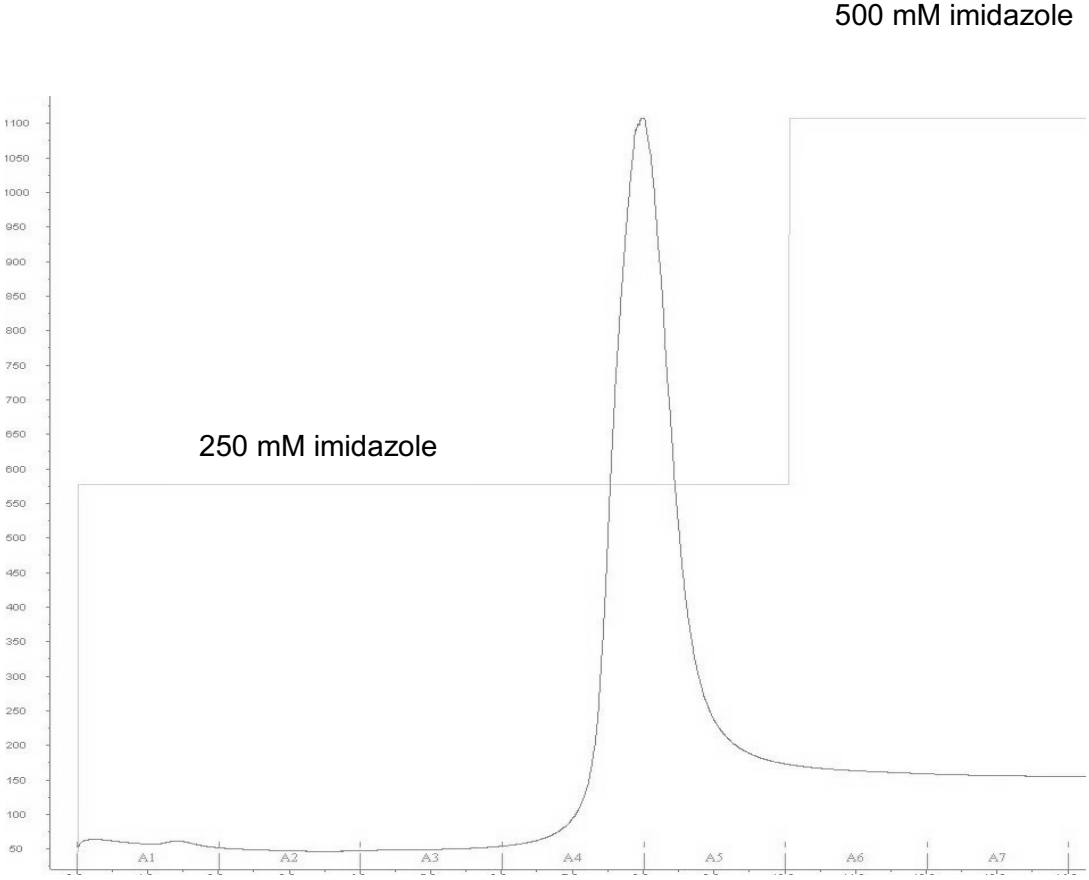

Appendix 3. Purification of FvXTH6His using HisTrap FF column

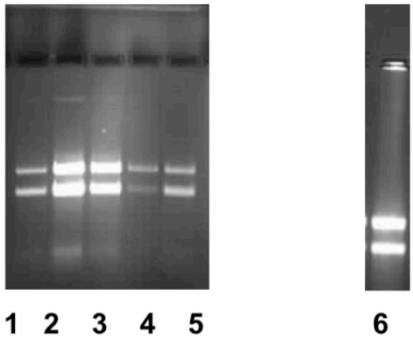

Appendix 4. mRNA of *F.* × *ananassa* (1-5) *and F. vesca* (6) fruit. The first-strand cDNAs were synthesized from 1 µg of total RNA using M-MLV Reverse Transcriptase and random primer (5'-NNNNNN-3'). 1, small green; 2, large green; 3, white; 4, tuning; 5, red fruit of *F.* × *ananassa*; 6, large green fruit of *F. vesca.*

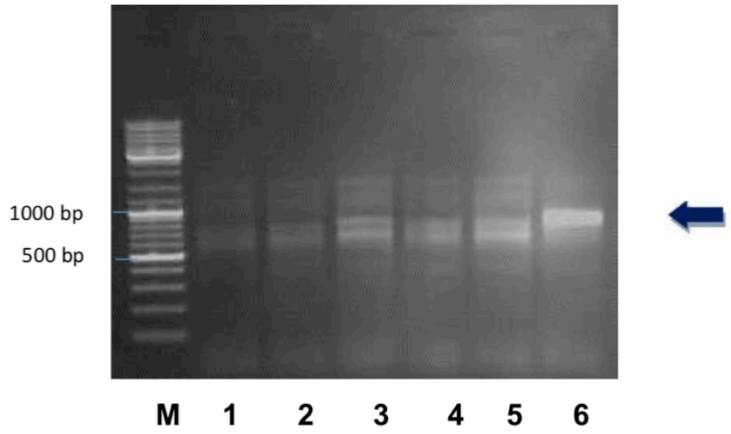

Appendix 5. Amplification of *FvXTH6* using cDNA from *F.* × *ananassa* (1-5) *and F. vesca* (6) fruit. M, DNA marker; 1, small green; 2, large green; 3, white; 4, tuning; 5, red; 6, ripe fruit.

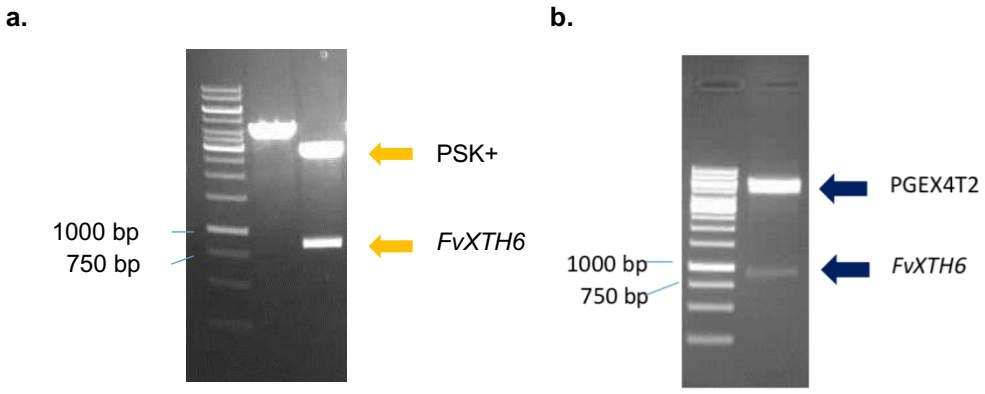

Appendix 6. Restriction enzyme analysis of recombinant (a) *FvXTH6*-PSK+ using Sma I and (b) *FvXTH6*-pGEX-4T-2 using BamHI and SmaI

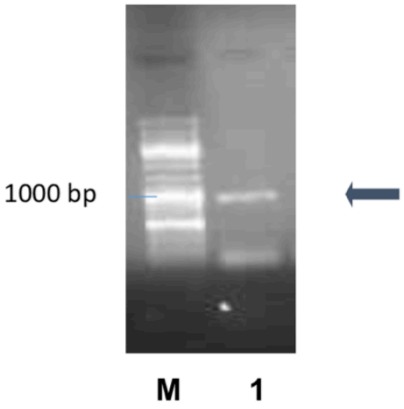

Appendix 7. Amplification of *FvXTH9* using cDNA from *F. vesca* fruit. M, DNA marker; 1, *FvXTH9*

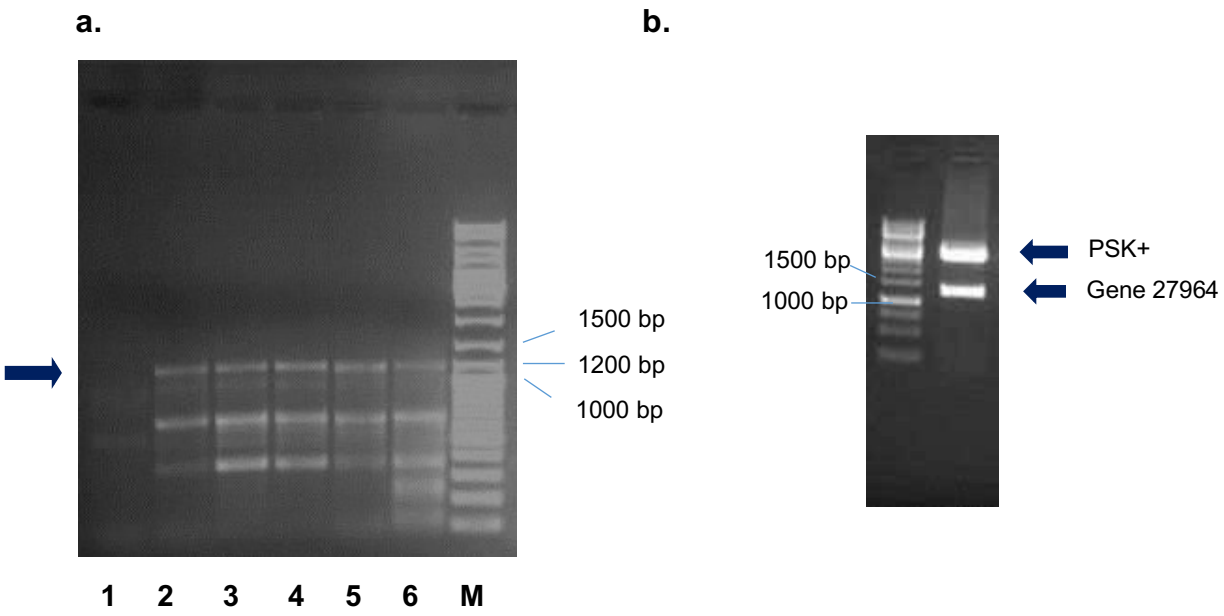

Appendix 8. (a) Amplification of gene27964 using cDNA from *F.* × *ananassa* (1-5) *and F. vesca* (6) fruit. PCR bands amplified from cDNA of 1, small green; 2, large green; 3, white; 4, tuning; 5, red fruit of *F.* × *ananassa*; 6, ripe fruit of *F. vesca*; M, DNA marker. Target gene27964 (1.161 bp) bands were shown in arrow. (b) Restriction enzyme analysis of recombinant *FvGDSL esterase* using SmaI and XhoI. M, DNA marker; 1, gene27964 and PSK+ plasmid bands

	gene287...	gene286...	gene286...	gene197...	gene052...	gene197...	gene052...	gene052...	gene122...	gene197...	gene052...	gene051...	gene248...	gene248...	gene092...	gene017...	gene002...	gene055...	gene019...	gene195...	gene175...	gene175...	gene246...	gene096...	gene006...	gene006...	gene137...	gene188...
gene28700 translation		54.2%	52.8%	46.4%	42.1%	47.8%	36.9%	47.6%	44.6%	44.1%	36.1%	35.5%	43.2%	23.2%	37.4%	35.4%	35.6%	37.2%	36.0%	32.9%	31.7%	29.3%	20.5%	26.5%	24.3%	28.2%	25.6%	20.2%
gene28699 translation	54.2%		60.2%	50.9%	43.6%	51.6%	39.9%	52.3%	51.8%	48.4%	43.0%	39.3%	52.4%	23.0%	40.7%	38.8%	38.9%	38.2%	37.5%	35.8%	34.6%	34.8%	22.4%	30.4%	24.3%	28.7%	30.7%	19.7%
gene28698 translation	52.8%	60.2%		58.6%	57.9%	61.0%	47.3%	58.4%	59.5%	57.9%	41.0%	44.8%	57.7%	29.2%	43.2%	41.5%	47.8%	40.9%	42.2%	38.8%	36.5%	36.0%	21.0%	32.2%	26.2%	28.6%	31.0%	20.5%
gene19782 translation	46.4%	50.9%	58.6%		99.0%	86.9%	68.1%	77.2%	72.9%	71.4%	78.0%	51.5%	59.3%	28.6%	44.4%	44.4%	45.5%	44.2%	44.6%	42.6%	39.4%	32.9%	21.8%	29.9%	25.2%	27.3%	30.0%	21.0%
gene05205 translation	42.1%	43.6%	57.9%	99.0%		79.4%	79.4%	68.2%	71.0%	69.9%	0%	50.0%	51.8%	34.0%	48.1%	39.8%	43.2%	40.5%	41.2%	42.3%	32.4%	32.4%	26.0%	32.7%	25.2%	25.2%	24.5%	12.5%
gene19781 translation	47.8%	51.6%	61.0%	86.9%	79.4%		76.2%	75.0%	71.3%	70.0%	69.5%	50.6%	58.0%	26.7%	44.8%	44.4%	45.5%	43.5%	46.0%	42.6%	39.0%	34.3%	22.5%	31.0%	26.2%	27.7%	31.3%	21.4%
gene05220 translation	36.9%	39.9%	47.3%	68.1%	79.4%	76.2%		59.7%	57.2%	55.1%	66.9%	40.4%	45.9%	18.8%	34.6%	34.5%	36.6%	34.2%	35.3%	34.0%	29.7%	26.0%	18.6%	24.9%	25.2%	22.1%	24.5%	16.6%
gene05204 translation	47.6%	52.3%	58.4%	77.2%	68.2%	75.0%	59.7%		73.3%	69.6%	61.9%	49.7%	60.7%	30.0%	43.4%	43.4%	50.0%	44.9%	47.0%	43.3%	38.7%	34.0%	22.1%	31.4%	27.8%	28.8%	32.2%	22.0%
gene12291 translation	44.6%	51.8%	59.5%	72.9%	71.0%	71.3%	57.2%	73.3%		69.8%	53.4%	49.6%	59.5%	28.7%	46.0%	42.9%	46.0%	44.7%	44.8%	41.8%	38.3%	33.4%	23.4%	34.3%	29.9%	28.9%	29.5%	22.7%
gene19783 translation	44.1%	48.4%	57.9%	71.4%	69.9%	70.0%	55.1%	69.6%	69.8%		54.2%	46.9%	59.6%	31.6%	45.5%	41.4%	46.0%	42.1%	44.0%	42.9%	38.0%	33.0%	22.5%	31.9%	22.4%	26.7%	29.1%	21.4%
gene05221 translation	36.1%	43.0%	41.0%	78.0%	0%	69.5%	66.9%	61.9%	53.4%	54.2%		38.7%	50.0%	6.7%	21.9%	33.1%	32.0%	31.5%	30.5%	28.9%	26.5%	16.5%	9.6%	15.7%	0%	19.1%	20.9%	10.9%
gene05197 translation	35.5%	39.3%	44.8%	51.5%	50.0%	50.6%	40.4%	49.7%	49.6%	46.9%	38.7%		44.4%	22.0%	38.7%	34.9%	38.7%	36.3%	35.9%	33.4%	34.1%	27.0%	19.6%	26.8%	20.8%	22.8%	26.4%	19.1%
gene24871 translation	43.2%	52.4%	57.7%	59.3%	51.8%	58.0%	45.9%	60.7%	59.5%	59.6%	50.0%	44.4%		38.6%	42.5%	40.7%	48.6%	43.5%	43.8%	40.8%	37.4%	35.0%	22.5%	31.4%	21.4%	26.1%	29.6%	22.5%
gene24869 translation	23.2%	23.0%	29.2%	28.6%	34.0%	26.7%	18.8%	30.0%	28.7%	31.6%	6.7%	22.0%	38.6%		23.8%	21.5%	28.4%	25.1%	25.9%	24.2%	19.5%	21.2%	16.7%	16.0%	14.0%	14.6%	18.0%	13.0%
gene09279 translation	37.4%	40.7%	43.2%	44.4%	48.1%	44.8%	34.6%	43.4%	46.0%	45.5%	21.9%	38.7%	42.5%	23.8%		44.8%	37.5%	41.0%	38.2%	34.8%	35.0%	37.4%	21.5%	27.2%	27.1%	27.4%	27.8%	21.0%
gene01781 translation	35.4%	38.8%	41.5%	44.4%	39.8%	44.4%	34.5%	43.4%	42.9%	41.4%	33.1%	34.9%	40.7%	21.5%	44.8%		42.1%	45.3%	40.2%	40.9%	39.4%	38.0%	20.4%	29.4%	28.0%	27.2%	29.7%	19.1%
gene00216 translation	35.6%	38.9%	47.8%	45.5%	43.2%	45.5%	36.6%	50.0%	46.0%	46.0%	32.0%	38.7%	48.6%	28.4%	37.5%	42.1%		46.0%	43.2%	44.0%	43.9%	36.9%	21.5%	27.9%	22.9%	26.6%	31.9%	24.1%
gene05591 translation	37.2%	38.2%	40.9%	44.2%	40.5%	43.5%	34.2%	44.9%	44.7%	42.1%	31.5%	36.3%	43.5%	25.1%	41.0%	45.3%	46.0%		48.5%	44.7%	41.6%	36.5%	21.5%	31.1%	28.4%	28.8%	33.1%	21.8%
gene01986 translation	36.0%	37.5%	42.2%	44.6%	41.2%	46.0%	35.3%	47.0%	44.8%	44.0%	30.5%	35.9%	43.8%	25.9%	38.2%	40.2%	43.2%	48.5%		43.4%	40.4%	34.5%	22.6%	30.2%	26.8%	27.6%	31.5%	20.9%
gene19553 translation	32.9%	35.8%	38.8%	42.6%	42.3%	42.6%	34.0%	43.3%	41.8%	42.9%	28.9%	33.4%	40.8%	24.2%	34.8%	40.9%	44.0%	44.7%	43.4%		35.8%	33.8%	22.2%	29.6%	25.7%	27.2%	31.1%	24.3%
gene17598 translation	31.7%	34.6%	36.5%	39.4%	32.4%	39.0%	29.7%	38.7%	38.3%	38.0%	26.5%	34.1%	37.4%	19.5%	35.0%	39.4%	43.9%	41.6%	40.4%	35.8%		42.2%	22.0%	29.9%	29.0%	31.1%	32.2%	19.2%
gene17597 translation	29.3%	34.8%	36.0%	32.9%	32.4%	34.3%	26.0%	34.0%	33.4%	33.0%	16.5%	27.0%	35.0%	21.2%	37.4%	38.0%	36.9%	36.5%	34.5%	33.8%	42.2%		23.0%	28.1%	28.0%	25.7%	30.7%	16.3%
gene24600 translation	20.5%	22.4%	21.0%	21.8%	26.0%	22.5%	18.6%	22.1%	23.4%	22.5%	9.6%	19.6%	22.5%	16.7%	21.5%	20.4%	21.5%	21.5%	22.6%	22.2%	22.0%	23.0%		45.7%	29.5%	24.9%	27.8%	16.2%
gene09672 translation	26.5%	30.4%	32.2%	29.9%	32.7%	31.0%	24.9%	31.4%	34.3%	31.9%	15.7%	26.8%	31.4%	16.0%	27.2%	29.4%	27.9%	31.1%	30.2%	29.6%	29.9%	28.1%	45.7%		33.0%	30.6%	35.9%	23.0%
gene00663 translation	24.3%	24.3%	26.2%	25.2%	25.2%	26.2%	25.2%	27.8%	29.9%	22.4%	0%	20.8%	21.4%	14.0%	27.1%	28.0%	22.9%	28.4%	26.8%	25.7%	29.0%	28.0%	29.5%	33.0%		98.1%	40.6%	9.1%
gene00661 translation	28.2%	28.7%	28.6%	27.3%	25.2%	27.7%	22.1%	28.8%	28.9%	26.7%	19.1%	22.8%	26.1%	14.6%	27.4%	27.2%	26.6%	28.8%	27.6%	27.2%	31.1%	25.7%	24.9%	30.6%	98.1%		38.8%	17.7%
gene13718 translation	25.6%	30.7%	31.0%	30.0%	24.5%	31.3%	24.5%	32.2%	29.5%	29.1%	20.9%	26.4%	29.6%	18.0%	27.8%	29.7%	31.9%	33.1%	31.5%	31.1%	32.2%	30.7%	27.8%	35.9%	40.6%	38.8%		23.9%
gene18893 translation	20.2%	19.7%	20.5%	21.0%	12.5%	21.4%	16.6%	22.0%	22.7%	21.4%	10.9%	19.1%	22.5%	13.0%	21.0%	19.1%	24.1%	21.8%	20.9%	24.3%	19.2%	16.3%	16.2%	23.0%	9.1%	17.7%	23.9%	

Appendix 9. Amino acid homology (percent identity) of XTHs candidates from *F. vesca*